REVIEW ARTICLE

New bonding modes of carbon and heavier group 14 atoms Si–Pb

Gernot Frenking,*[a] Ralf Tonner,[a] Susanne Klein,[a] Nozomi Takagi,[b]
Takayazu Shimizu,[a] Andreas Krapp,[a] Krishna K. Pandey[c] and Pattiyil Parameswaran[d]

Recent theoretical studies are reviewed which show that the naked group 14 atoms E = C–Pb in the singlet ^1D state behave as bidentate Lewis acids that strongly bind two σ donor ligands L in the donor–acceptor complexes $L \rightarrow E \leftarrow L$. Tetrylones EL_2 are divalent E(0) compounds which possess two lone pairs at E. The unique electronic structure of tetrylones (carbones, silylones, germylones, stannylones, plumbylones) clearly distinguishes them from tetrylenes ER_2 (carbenes, silylenes, germylenes, stannylenes, plumbylenes) which have electron-sharing bonds R–E–R and only one lone pair at atom E. The different electronic structures of tetrylones and tetrylenes are revealed by charge- and energy decomposition analyses and they become obvious experimentally by a distinctively different chemical reactivity. The unusual structures and chemical behaviour of tetrylones EL_2 can be understood in terms of the donor–acceptor interactions $L \rightarrow E \leftarrow L$. Tetrylones are potential donor ligands in main group compounds and transition metal complexes which are experimentally not yet known. The review also introduces theoretical studies of transition metal complexes [TM]–E which carry naked tetrele atoms E = C–Sn as ligands. The bonding analyses suggest that the group-14 atoms bind in the ^3P reference state to the transition metal in a combination of σ and $\pi_\parallel$ electron-sharing bonds TM–E and $\pi_\perp$ back-donation TM→E. The unique bonding situation of the tetrele complexes [TM]–E makes them suitable ligands in adducts with Lewis acids. Theoretical studies of [TM]–E→W(CO)$_5$ predict that such species may becomes synthesized.

1. Introduction

This review summarizes recent theoretical work which deals with molecules where novel types of chemical bonds of group 14 atoms C–Pb in main group compounds and transition metal complexes were found. Experimental and theoretical evidence suggest that there are carbon compounds such as carbodiphosphorane C(PPh$_3$)$_2$ – known since 1961[1] – which are best described in terms of donor–acceptor interactions $L \rightarrow C \leftarrow L$ between a bare carbon atom in the excited ^1D state and two strong σ donors L, namely divalent carbon(0) compounds CL$_2$. The term carbone has been suggested for these molecules which exhibit a chemical reactivity that is clearly different from carbenes CR$_2$. The same bonding situation may also be found in the heavier tetrylone homologues EL$_2$ (E = Si–Pb). Stable silylones SiL$_2$ and germylones GeL$_2$ could become synthesized after theoretical studies suggested that they might exist.

We also review theoretical studies of transition metal complexes [TM]–C which have a bare carbon atom as ligand. Examples of such carbon complexes have been synthesized in 2002 where the ruthenium species [(PCy$_3$)$_2$Cl$_2$Ru(C)] could become isolated.[2] A formal electron count which takes the carbon atom as two-electron donor suggests that the molecule is a 16 valence-electron complex. The bonding analysis shows that the bare carbon atom which is isolobal to CO binds through its ^3P ground state to the transition metal which yields two electron-sharing bonds and one donor–acceptor bond. This makes carbon a formal four-electron donor which indicates that [(PCy$_3$)$_2$Cl$_2$Ru(C)] is actually a Ru(ɪᴠ) compound. Theoretical studies of carbon complexes [TM]–C and heavier group 14 homologues [TM]–E (E = Si–Pb) which are experimentally not known are discussed here.

2. Divalent carbon(0) compounds (carbones)

The vast majority of organic compounds which until 1988 were known as stable species in condensed phase exhibit carbon atoms that use all four valence electrons in single, double or triple bonds with other elements across the periodic table

[a] Fachbereich Chemie, Philipps-Universität Marburg, Hans-Meerwein-Strasse, D-35032 Marburg, Germany. E-mail: frenking@chemie.uni-marburg.de
[b] Fukui Institute of Fundamental Chemistry, Kyoto University, Japan
[c] School of Chemical Sciences, Devi Ahilya University Indore, Indore-452017, India
[d] Department of Chemistry, National Institute of Technology Calicut, NIT Campus P.O., Calicut - 673 601, India

5106 | Chem. Soc. Rev., 2014, 43, 5106–5139

This journal is © The Royal Society of Chemistry 2014

(Scheme 1a). Except for a very few special cases such as the notorious CO,[3] carbon appears nearly always as tetravalent C(IV)[4] in stable organic compounds. The situation changed when Bertrand[5] in 1988 and Arduengo[6] in 1991 isolated compounds which are now recognized[7] as stable carbenes CR$_2$. In carbenes, carbon uses only two of its valence electrons while the remaining two retain as a lone electron pair (Scheme 1b). The chemistry of N-heterocyclic carbenes (NHCs) has become a particular focus of synthetic chemistry because NHCs are versatile ligands in transition metal complexes which were found very useful as powerful catalysts.[8] The carbene chemistry of divalent carbon(II) compounds is now well established in organic synthesis.[9]

It has recently been recognized that there are organic compounds in which carbon exhibits yet another bonding situation. Divalent carbon(0) compounds CL$_2$ possess a carbon atom which retains all four valence electrons as two lone pairs and where the bonding to the σ donor ligands L occurs through donor–acceptor interactions L→C←L (Scheme 1c). The electronic reference state of carbon in CL$_2$ is the excited ^{1}D singlet state with the electron configuration $1s^2 2s^2 2p_x^0 2p_y^0 2p_z^2$ which is 29.1 kcal mol^{-1} higher in energy than the ^{3}P ground state (Fig. 1).[10] The donation from the lone-pair electrons of the ligands takes place from the in-phase (+,+) combination of the donor orbitals into the vacant $2p_x$ orbital (σ symmetry) and

Gernot Frenking

Gernot Frenking studied chemistry at the universities Aachen, Kyoto and TU Berlin where he received his PhD in 1979. After obtaining his habilitation in theoretical organic chemistry at the TU Berlin in 1984 he moved to the USA where he worked one year at UC Berkeley followed by four years at SRI International in Menlo Park, California. In 1989 he returned to Germany as Associate Professor for Computational Chemistry at the Philipps University Marburg where he was appointed Full Professor for Theoretical Chemistry in 1998. His research interests are the nature of the chemical bond, molecules with unusual bonding situations and reaction mechanisms of chemical reactions.

Ralf Tonner

Ralf Tonner studied chemistry at the universities Marburg and Auckland/New Zealand. He obtained his doctoral degree in chemistry in 2007 at the Philipps University Marburg. With the support of the DAAD (Deutscher Akademischer Austauschdienst) and then with a Feodor Lynen scholarship of the Alexander von Humboldt Foundation, he carried out postdoctoral work from 2007–2010 with Peter Schwerdtfeger at Massey University, New Zealand. In 2010 he was appointed Nachwuchsgruppenleiter at the Philipps University Marburg. His current research interests are in the field of chemical bonding and reactivity on surfaces.

Susanne Klein

Susanne Klein, born in 1984, studied chemistry at the Philipps University in Marburg from 2003 to 2008. She did her diploma thesis and her PhD with Prof. Dr Gernot Frenking about carbones and related compounds from 2008 to 2011. Afterwards she went to the Max-Planck-Institute for chemical energy conversion in Mülheim and joined the group of Prof. Dr Frank Neese to study reduction potentials and the nature of the manganese–oxo bonds. Since 2014 she is working at the Institut Heidger in Osann-Monzel doing food analytics – actually with the focus on quantitative NMR analytics of wine.

Nozomi Takagi

Nozomi Takagi finished his BSc in Rikkyo University and received his PhD from Tokyo Metropolitan University. After that, he joined the group of Prof. Shigeru Nagase at the Institute for Molecular Science (IMS) as a Research Fellowship for Young Scientists of JSPS. Then, he joined the group of Prof. Gernot Frenking at the Philipps University Marburg as a postdoctoral fellow. Then, he joined the group of Prof. Shigeyoshi Sakaki at the Fukui Institute for Fundamental Chemistry (FIFC) of Kyoto University. He is now at the Elements Strategy Initiative for Catalysts and Batteries (ESICB) of Kyoto University as a Program-Specific Researcher. His research filed is theoretical and computational chemistry for the joint area of heavier main group elements and transition metals.

This journal is © The Royal Society of Chemistry 2014

Chem. Soc. Rev., 2014, **43**, 5106–5139 | **5107**
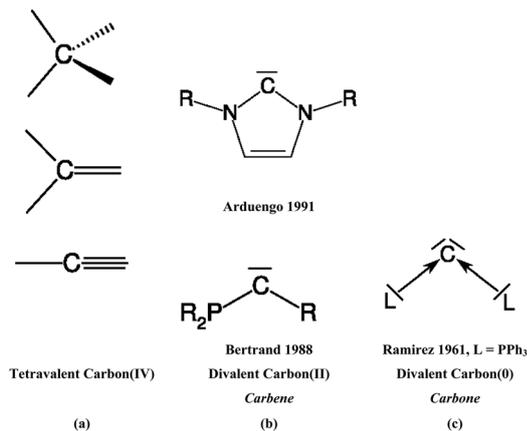
Scheme 1 Schematic representation of (a) tetravalent carbon(IV) compounds; (b) divalent carbon(II) compounds (carbenes), (c) divalent carbon(0) compounds (carbones).

Fig. 1 Schematic presentation of the orbital interactions between carbon atom in the $(1s^2 2s^2 2p_x^0 2p_y^0 2p_z^2)$ ^1D state and two σ donor ligands L. The $+,+$ sign indicates the in-phase combination of the donor orbitals into the vacant $2p_x$ orbital (σ symmetry) while the $+,-$ sign denotes the out-of-phase combination of the donor orbitals into the vacant $2p_y$ orbital (in-plane $\pi_\parallel$ symmetry).

from the out-of-phase $(+,-)$ combination of the donor orbitals into the vacant $2p_y$ orbital (in-plane $\pi_\parallel$ symmetry). The orientation of the carbon $2p_z^2$ orbital is orthogonal to the CL_2 plane, *i.e.* it becomes the out-of-plane $p(\pi_\perp)$ lone pair orbital. The excitation energy $^3P \rightarrow {}^1D$ is compensated by the strong donor–acceptor bonding between the Lewis base L and the (double) Lewis acid (^1D) carbon. The name carbone has been suggested[11] for the latter divalent carbon(0) compounds in analogy to the name carbene for divalent carbon(II) compounds CR_2 which have only one lone pair and two electron-sharing bonds C–R.
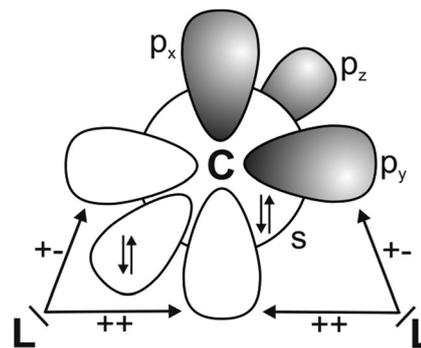
Another important difference between carbones and carbenes is that the former compounds are π donors while the latter are usually weak π acceptors.

The first carbone was already synthesized in 1961 when Ramirez reported about the isolation of the carbodiphosphorane $C(PPh_3)_2$.[1] The chemistry of carbodiphosphoranes was systematically explored in experimental work in the following years.[12] A critical examination of the bonding description in the past literature shows that the carbon–phosphorous bond in carbodiphosphoranes is usually classified as diylide which is sketched

Krishna K. Pandey

Krishna K. Pandey born in Kanpur in 1951. He obtained his PhD Degree in 1981 from Indian Institute of Technology Kanpur, India. He worked with Herbert Roesky, Goettingen, Germany; Gernot Frenking, Marburg, Germany; Holger Braunschweig, Wurzburg, Germany; Simon Aldridge, Oxford; Dennis Liotta, Emory, Atlanta and Cameron Jones, Monash, Australia. He has been appointed as full-Professor in 1990 in D. A. University Indore, India. The main research area of Dr Pandey focuses on quantum-chemical calculations of transition metal complexes with Group 13, Group 14 and Group 15 ligands using different density functionals and ONIOM, CCSD(T) calculations.

Pattiyil Parameswaran

Pattiyil Parameswaran was born in Kerala, India, in 1978. After completing MSc degree in chemistry from St. Thomas' College, Thrissur (University of Calicut), Kerala, in 2000, he joined University of Hyderabad for doctoral studies under the guidance of Prof. Eluvathingal D. Jemmis. During his PhD period, he spent two years at Indian Institute Science, Bangalore and also worked with Prof. Uwe Rosenthal at University of Rostock as a DST-DAAD exchange programme fellow. After receiving doctoral degree in 2007, he moved to Germany and worked with Prof. Gernot Frenking at the Fachbereich Chemie, Philipps-University Marburg as Alexander von Humboldt Research Fellow (2007–2009). He also worked with Prof. Keiji Morokuma at Fukui Institute for Fundamental Chemistry, Kyoto University as Japan Science and Technology-Postdoctoral Research Fellow (2009–2010). He is currently working as Assistant Professor at National Institute of Technology Calicut since 2010. His main research focus is the detailed understanding of structure, bonding, reactivity and reaction mechanism by computational quantum mechanical calculations.
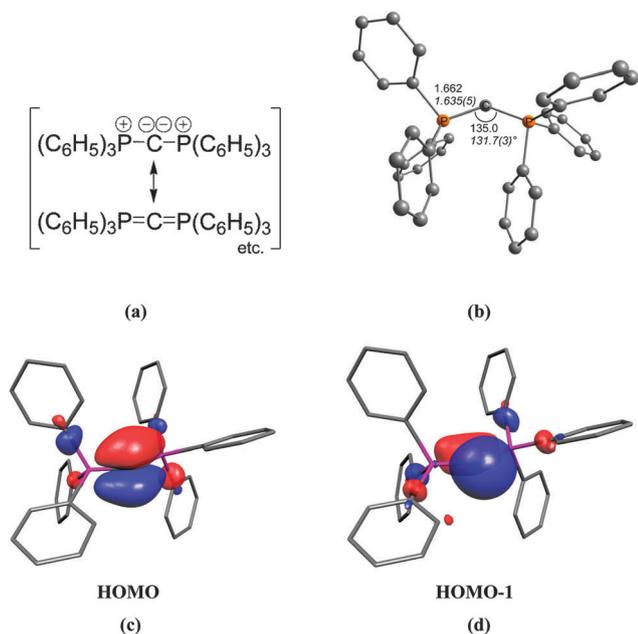
5108 | *Chem. Soc. Rev.*, 2014, **43**, 5106–5139

This journal is © The Royal Society of Chemistry 2014

Fig. 2 (a) Sketch of the bonding situation in hexaphenylcarbodiphosphorane as suggested by Ramirez.[1] (b) Calculated (BP86/SVP) and experimental (in *italics*) geometry of C(PPh$_3$)$_2$. Frontier orbitals (c) HOMO and (d) HOMO−1 of C(PPh$_3$)$_2$.[16]

Fig. 3 Calculated (BP86/SVP) and (in italics) experimental bond lengths and angles of O$_2$C−C(PPh$_3$)$_2$.[18,31]

with mesomeric structures as shown in Fig. 2a. This picture was already suggested by Ramirez in his 1961 publication[1] when the structure of hexaphenylcarbodiphosphorane was not known yet. It was not until 1978 when the first X-ray structural analysis revealed that C(PPh$_3$)$_2$ has a strongly bent P–C–P angle of 131.7°.[13] Recent DFT calculations gave a geometry which is in very good agreement with the experimental data (Fig. 2b).[14] Inspection of the frontier orbitals of C(PPh$_3$)$_2$ showed that the HOMO is a π-type lone pair orbital while the HOMO−1 is a σ-type lone pair orbital (Fig. 2c and d).[15]

The description of the bonding situation in carbodiphosphoranes in terms of donor–acceptor interactions Ph$_3$P→C←PPh$_3$ was put forward in 2006 in a combined theoretical and experimental study by Tonner *et al.*[16] providing crucial support for the postulated Lewis structure by Kaska *et al.* from 1973.[17] The authors had analyzed in a preceding study the nature of the carbon–carbon bond between carbodiphosphorane and CO$_2$ as well as CS$_2$ yielding the adducts X$_2$C−C(PPh$_3$)$_2$ (X = O, S) which were isolated and characterized through an X-ray structure analysis (Fig. 3).[18] The complexes possess rather short carbon–carbon bonds which are shorter than a standard single bond. With the help of charge- and energy decomposition analyses, they identified a donor–acceptor bond X$_2$C←C(PPh$_3$)$_2$ which has a dominant σ component and a weaker π component. It was concluded that *carbodiphosphoranes C(PR$_3$)$_2$ are double electron pair donors having σ- and π-carbon lone-pair orbitals.*[18] The latter finding was elaborated in the 2006 theoretical study where the twofold donor strength of carbodiphosphoranes C(PR$_3$)$_2$ with different substituents R with respect to H$^+$ and the Lewis acids BH$_3$, BCl$_3$ and AlCl$_3$ was estimated and analyzed using *ab initio* and DFT methods.[16] The calculations showed that
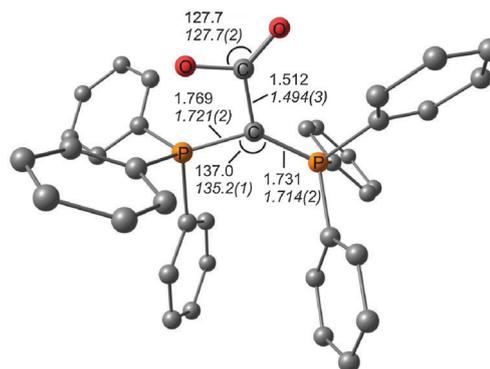
carbodiphosphoranes have not only a very large first proton affinity (PA) which classifies them as very strong bases. They also have a very large second PA which agrees with the notion of two lone pairs. A subsequent theoretical study of the first and second proton affinities of carbon bases showed that the first PA of carbodiphosphoranes C(PR$_3$)$_2$ has a similar strength as the first PA of NHCs but that C(PR$_3$)$_2$ exhibit a significantly higher second PA than NHCs.[19] Pertinent examples are shown in Table 1. The calculations also predicted that the double Lewis base C(PPh$_3$)$_2$ is capable of binding two BH$_3$ molecules at the carbon lone pairs in the stable complex (H$_3$B)$_2$–C(PPh$_3$)$_2$ while NHC binds only one BH$_3$ at the carbon atom.[16] The theoretical finding about the carbodiphosphorane adduct was verified by the isolation of the complex [{(μ-H)H$_4$B$_2$}C{PPh$_3$}$_2$](B$_2$H$_7$) where the (H$_3$B)$_2$ moiety of (H$_3$B)$_2$–C(PPh$_3$)$_2$ releases one H$^-$ to excess B$_2$H$_6$ yielding the hydrogen bridged B$_2$H$_5^+$ complex of carbodiphosphorane (Fig. 4a).[20] Calculations of the model complex [{(μ-H)H$_4$B$_2$}-C{PH$_3$}$_2$]$^+$ showed that the carbon–borane bonding can be understood in terms of σ- and π-donation from the double donor C{PH$_3$}$_2$ to the B$_2$H$_5^+$ acceptor (Fig. 4b).

The double donor ability of the carbodiphosphoranes C(PPh$_3$)$_2$ and the contrast to the carbene NHC was convincingly demonstrated in a joint experimental/theoretical work by Alcarazo, Thiel and co-workers.[21] The authors realized that the σ and π lone

Table 1 First and second proton affinities (MP2/TZVPP//BP86/SVP) of N-heterocyclic carbenes and carbodiphosphoranes. All energy values are given in kcal mol^{-1}[19]

R	NHC$^{R\ a}$		C(PR$_3$)$_2$	
	1st PA	2nd PA	1st PA	2nd PA
H	254.2	47.7^b	255.7	114.4
Me	262.3	71.8	278.4	156.2
Ph	264.7	100.1	280.0	185.6
NH$_2$	253.9	76.7	280.0	153.5
NMe$_2$	259.8	106.5	279.9	174.9
^{t}Bu	270.6	92.3		
Mesityl	270.4	105.3	280.7	201.1
Adamantyl	274.9	105.7		
Cyclohexyl			280.5	184.0

^{a} Substituent at the nitrogen atom of NHC. ^{b} Second protonation at an olefinic carbon atom of the ring is ∼1 kcal mol^{-1} more favorable.
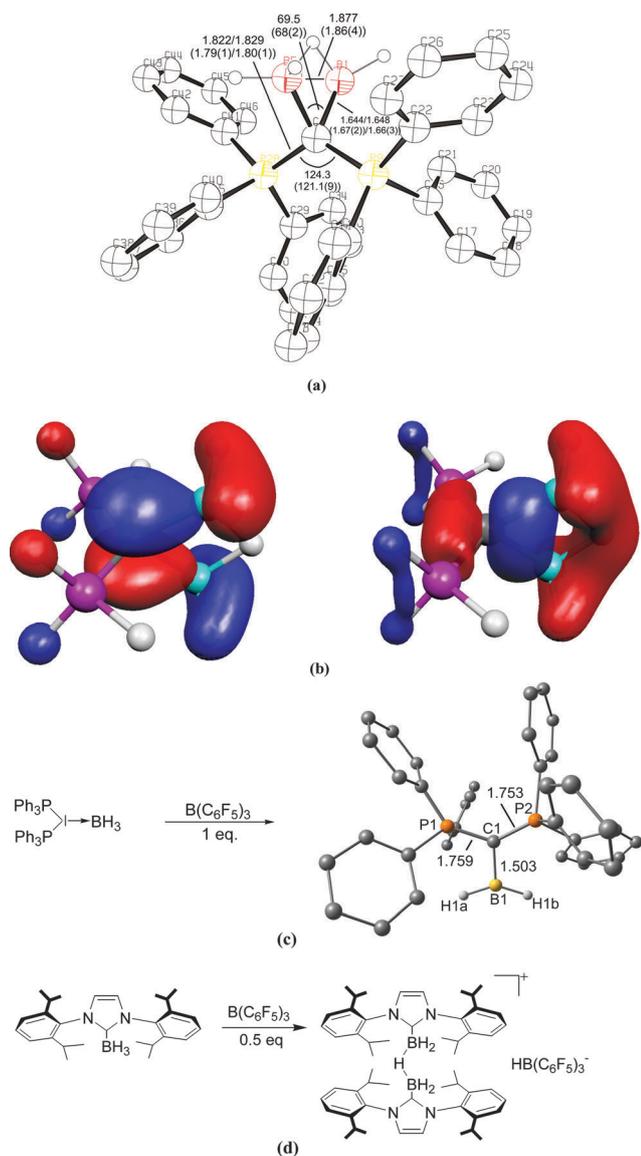
This journal is © The Royal Society of Chemistry 2014

Chem. Soc. Rev., 2014, 43, 5106–5139 | **5109**

Fig. 4 (a) Calculated at BP86/SVP and (in parentheses) experimental bond lengths and angles of $[\{(\mu\text{-H})H_4B_2\}C\{PH_3\}_2]^+$.[20] (b) Plot of the HOMO and HOMO−1 of $[\{(\mu\text{-H})H_4B_2\}C\{PH_3\}_2]^+$. (c) Reaction of $(H_3B)\leftarrow C(PPh_3)_2$ with $B(C_6F_5)_3$ yielding the complex $[(H_2B)\Leftarrow C(PPh_3)_2]^+$. (d) Reaction of $(H_3B)\leftarrow NHC$ with $B(C_6F_5)_3$ yielding the bridged complex $[NHC\rightarrow\{(\mu\text{-H})H_4B_2\}\leftarrow NHC]^+$.[21]

pairs of a carbone could be utilized to bind a double Lewis acid such as BH_2^+ which has vacant σ and π orbitals (Fig. 4c). They reacted the complex $(H_3B)\leftarrow C(PPh_3)_2$ with the strong Lewis acid $B(C_6F_5)_3$ and obtained in good yields the complex $[(H_2B)\Leftarrow C(PPh_3)_2]^+$ which has σ and π donor–acceptor bonds. The reaction of the carbene complex $(H_3B)\leftarrow NHC$ with $B(C_6F_5)_3$ gave the bridged adduct $[NHC\rightarrow\{(\mu\text{-H})H_4B_2\}\leftarrow NHC]^+$ which is a striking example for the different chemical behaviour between a carbone and a carbene (Fig. 4d).

The calculations of carbodiphosphoranes $C(PR_3)_2$ were the starting point for further theoretical studies of divalent carbon(0) compounds CL_2 with other ligands than phosphanes. Inspection of the literature revealed that the carbonyl

homologues $C(PPh_3)(CO)^{22}$ and $C(CO)_2^{23}$ which is usually described as carbon suboxide O=C=C=C=O are experimentally known for a long time. The bonding model in terms of donor–acceptor interactions $L\rightarrow C\leftarrow L$ easily explains the finding that the divalent C(0) compounds with the better π acceptor ligands CO have larger bending angles τ for $C(PPh_3)(CO)$ (τ = 145.5°)[22] and $C(CO)_2$ (τ = 156.0°).[24] There is a correlation between the π-acceptor strength of ligand L and the bending angle L–C–L in carbones CL_2. Stronger π-acceptor ligands L induce more obtuse bending angles in CL_2. The deviation from linearity and the very shallow bending potential of carbon suboxide is difficult to explain with the standard bonding model of a cumulene O=C=C=C=O while it becomes plausible when the donor–acceptor model $L\rightarrow C\leftarrow L$ is employed.

The litmus test for the predictive power of the donor–acceptor model $L\rightarrow C\leftarrow L$ was provided by the theoretical study of the hitherto unknown class of carbodicarbenes $C(NHC)_2$ which were suggested by Tonner and Frenking as stable molecules.[25] Chemical experience has shown that NHCs have comparable donor properties as phosphanes which initiated a theoretical study of CL_2 with NHC ligands L. The optimized geometry of $C(NHC^{Me})_2$ (Fig. 5) shows a bending angle at the central carbon atom of 131.8°, which is similar to the value that is calculated for $C(PPh_3)_2$. The experimental verification of the theoretical work followed shortly after. Bertrand and co-workers isolated the benzoannelated carbodicarbene $C(NHC^{Bz})_2$ which is also shown in Fig. 5.[26] The bending angle in $C(NHC^{Bz})_2$ is 134.8° which is close to the calculated value for $C(NHC^{Me})_2$. Fürstner et al. reported at the same time about protonated carbon complexes which carry $C(NHC)_2$ as ligands.[27] The latter group recently synthesized a series of mixed carbones with one phosphane and various other ligands $C(PPh_3)(L)$ where L is CO, CNPh, PPh_3 or a carbene CR_2 with different substituent R.[28] The authors investigated experimentally and theoretically the monoaurated and diaurated complexes $(ClAu)_2-C(PPh_3)(L)$. It was suggested that the binding strength toward a second AuCl molecule should be used as measure of the carbone character of a compound CL_2.

Fig. 5 shows also the optimized geometry of $C[C(NMe_2)_2]_2$ which has a nearly linear C–C–C structure and a geometry where the $C(NMe_2)_2$ moieties are orthogonal to each other. The molecule may thus become identified as tetraaminoallene (TAA) $(NMe_2)_2C=C=C(NMe_2)_2$. However, the calculations predict that not only the first but also the second PA of the TAA which are very large have values similar to carbodicarbenes. The analogous TAA with ethyl groups instead of methyl has even a second PA of 175.8 kcal mol^{-1}.[19] Protonation at the central carbon atom is in both cases favoured over protonation at nitrogen. It has therefore been suggested that TAAs have "hidden carbone character" and that the bonding situation may also be described in terms of donor–acceptor interactions $(NMe_2)_2C\rightarrow C\leftarrow C(NMe_2)_2$.[14] The chemical reactivity of TAAs supports the suggestion. The X-ray structure of doubly protonated TAAs where both protons bind to the central carbon atom has been reported.[29] Even more convincing evidence for the "hidden carbone character" comes from the work of Viehe et al.

5110 | Chem. Soc. Rev., 2014, 43, 5106–5139

This journal is © The Royal Society of Chemistry 2014

(a)

1. PA: 294.3 kcal/mol

2. PA: 168.4 kcal/mol

(b)

1. PA: 284.7 kcal/mol

2. PA: 167.8 kcal/mol

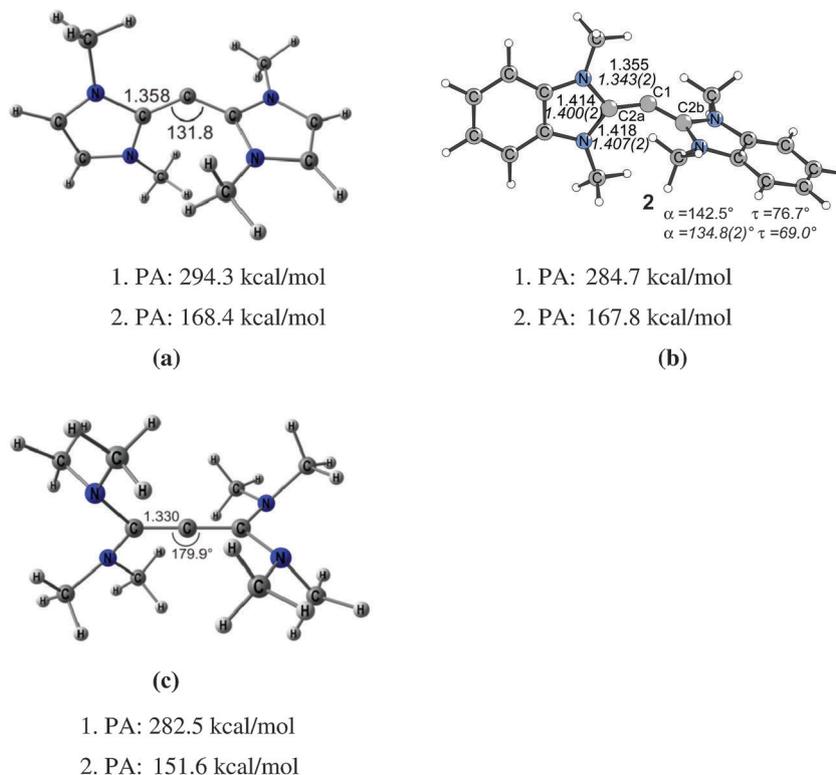**(c)**

1. PA: 282.5 kcal/mol

2. PA: 151.6 kcal/mol

Fig. 5 Calculated (BP86/TZ2P) geometries and first and second proton affinities PA (MP2/TZVPP) of (a) carbodicarbene $C(NHC^{Me})_2$. (b) Benzoannelated carbodicarbene $C(NHC^{Bz})_2$ (BP86/SVP). (c) Tetraaminoallene $(NMe_2)_2C\!\!=\!\!C\!\!=\!\!C(NMe_2)_2$. Bond lengths are given in Å, angles in degree. Experimental data for $C(NHC^{Bz})_2$ are given in *italics*.[26,32]

who found that methyl and ethyl substituted TAAs react "extremely readily and in good yields with carbon dioxide" to give adducts which are analogous to the CO_2 adduct of $C(PPh_3)_2$ which is shown in Fig. 3.[30]

It becomes obvious that the nature of the ligand L has a very strong influence on the structure and reactivity of carbon compounds CL_2. The methylene group L = CH_2 has a triplet ground state which binds a carbon atom in its (^3P) triplet ground state yielding the parent allene $H_2C\!\!=\!\!C\!\!=\!\!CH_2$. The first PA (182.4 kcal mol^{-1}) and particularly the second PA (-5.2 kcal mol^{-1}) are strikingly different to the first and second PA of TAAs.[25a] Diaminocarbenes $C(NR_2)_2$ have a singlet ground state and a very large singlet–triplet gap which supports donor–acceptor binding with a carbon atom in the (^1D) excited state. The correlation between singlet–triplet gap and donor–acceptor bond will be further discussed in the section about the heavy group 14 homologues EL_2 which is given below. TAAs have a very shallow bending mode like $C(CO)_2$ and other compounds CL_2 where L is a σ donor. Table 2 gives the calculated energies that are necessary to stretch the bending angle of various compounds CL_2 from the equilibrium structure to the linear form or to the value of 136.9° which is the energy minimum value for $C(PPh_3)_2$. The calculated data indicate that very little energy is required for bending the molecules over a wide range.

The structures and bonding situation in divalent carbon(0) parent compounds CL_2 where L = PH_3, PMe_3, PPh_3, CO, $C(NHC)_2$, $C(NHC^{Me})_2$, $C(NMe_2)_2$ and the first and second proton affinities and bond strengths of complexes of CL_2 with main

group Lewis acids BH_3, CO_2 and transition metal species $W(CO)_5$ and $Ni(CO)_n$ (n = 2, 3) have been investigated in a series of theoretical studies by our group.[14,31,32] The results show that carbones possess characteristic properties as double Lewis base which distinguishes them from carbenes. This was recognized in a comment article by Bertrand entitled "Rethinking carbon" where the author expressed his belief that the new concept may lead to "new chemistry and applications for carbon, the basic element for all known life."[33] Very recently, another set of carbones has been investigated with quantum chemical methods which show that there are not only new examples of the class of compounds that may become synthesized, but that molecules which have been isolated in the past were not recognized as

Table 2 Calculated relative energies (BP86/TZ2P) of carbones CL_1L_2 with different bending angles α. All energy values in kcal mol^{-1} [14]

L_1	L_2	Equilibrium structure	α = 180°	α = 136.9°
PH_3	PH_3	0.0 (125.1°)	2.0	0.3
PMe_3	PMe_3	0.0 (136.9°)	0.9	0.0
PPh_3	PPh_3	0.0 (136.9°)	3.1	0.0
PPh_3	CO	0.0 (144.6°)	0.3	0.5
CO	CO	0.0 (180.0°)	0.0	1.9
NHC^H	NHC^H	0.0 (125.8°)	3.6	0.6
NHC^{Me}	NHC^{Me}	0.0 (131.8°)	3.2	0.1
$C(NMe_2)_2$	$C(NMe_2)_2$	0.0 (180.0°)	0.0	5.3

This journal is © The Royal Society of Chemistry 2014

Chem. Soc. Rev., 2014, **43**, 5106–5139 | **5111**

carbones. Fig. 6 shows the calculated geometries of compounds **1–10** which have been studied.

Compound **1** is the saturated homologue of the unsaturated carbodicarbene C(NHC^{Me})$_2$ which is discussed above while **2** is the benzoannelated carbodicarbene that was synthesized by Bertrand *et al.*[26] Compounds **3** and **4** may be considered as "bent allenes" or alternatively as cyclic carbones where the dicoordinated C(0) atom binds to two diaminocarbene ligands (**3a** and **3b**) or to two aminooxocarbene ligands (**4a** and **4b**). The molecules have recently become synthesized.[34] Because amino groups are better donors than oxo groups it can be expected that the carbone character of **3a** and **3b** is stronger than that of **4a** and **4b**. Compounds **5–10** exhibit various combinations of CL$_1$L$_2$ where L$_1$, L$_2$ are CO, N$_2$, NHC or phosphane. Substituted homologues of compound **9** have been synthesized more than 20 years ago but they were introduced as phosphacumulenes.[35]

Fig. 7 shows the frontier orbitals HOMO and HOMO−1 of **1–10**. It becomes obvious that the two highest lying MOs of all molecules appear like σ- and π-type lone-pair orbitals which suggest that the compounds may have chemical properties of carbones. Table 3 gives the calculated first and second PAs and the bond dissociation energy of complexes of **1–10** with one and with two BH$_3$ ligands. The second PA of all compounds is rather high except for complexes CL$_1$L$_2$ where L$_1$ is N$_2$ or CO. However, all molecules **1–10** bind two Lewis acids BH$_3$ in adducts, which – except for **4a** and **4b** – may be stable enough to become isolated in condensed phase. We are convinced that carbone chemistry is a very fruitful area of chemical research that waits to be explored.

The nature of the donor–acceptor interaction in carbones L→ C←L can be analyzed in great detail with the EDA (Energy Decomposition Analysis) method that was developed independently by Morokuma[36] and by Ziegler and Rauk.[37] The EDA analyzes the instantaneous interactions in a chemical bond A–B *via* a breakdown of the total interaction energy ΔE_{int} between the frozen fragments A and B in the electronic reference state in three major terms: (a) the electrostatic interactions ΔE_{elstat} between the frozen electronic charges and nuclei of the fragments; (b) the Pauli repulsion (exchange repulsion) ΔE_{Pauli} between electrons having the same spin; (c) the attractive orbital interactions ΔE_{orb} which arise from the mixing of the occupied and vacant orbitals between and within the fragments.

$$\Delta E_{int} = \Delta E_{elstat} + \Delta E_{Pauli} + \Delta E_{orb} \qquad (1)$$

$$\Delta E(-D_e) = \Delta E_{int} + \Delta E_{prep} \qquad (2)$$

The orbital term ΔE_{orb} can be further partitioned into contributions from orbitals which belong to different irreducible representations of the point group. The combination of the EDA with the NOCV (Natural Orbitals for Chemical Valence)[38] charge partitioning method makes it possible to separate ΔE_{orb} into pairwise contributions of the orbitals of the interacting fragments.[39] The energy difference between the frozen fragments A and B in the electronic reference state and their equilibrium structures in the ground state gives the preparation energy ΔE_{prep}. The sign converted sum of ΔE_{int} + ΔE_{prep} gives the bond dissociation energy D_e. Further details
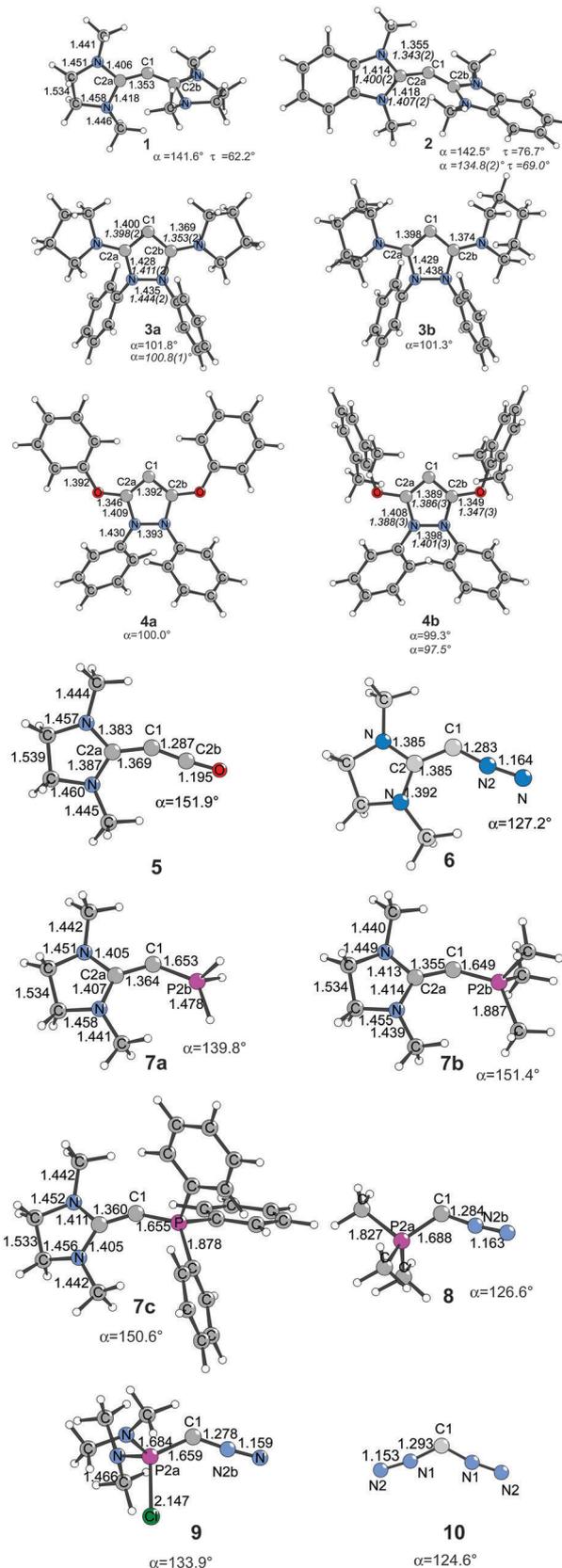

Fig. 6 Calculated (BP86/SVP) geometries of some carbones CL$_1$L$_2$.[32] Bond lengths are given in Å, angles in degree. Experimental data are given in *italics*.[26,34] The figure has been adapted from ref. 32.
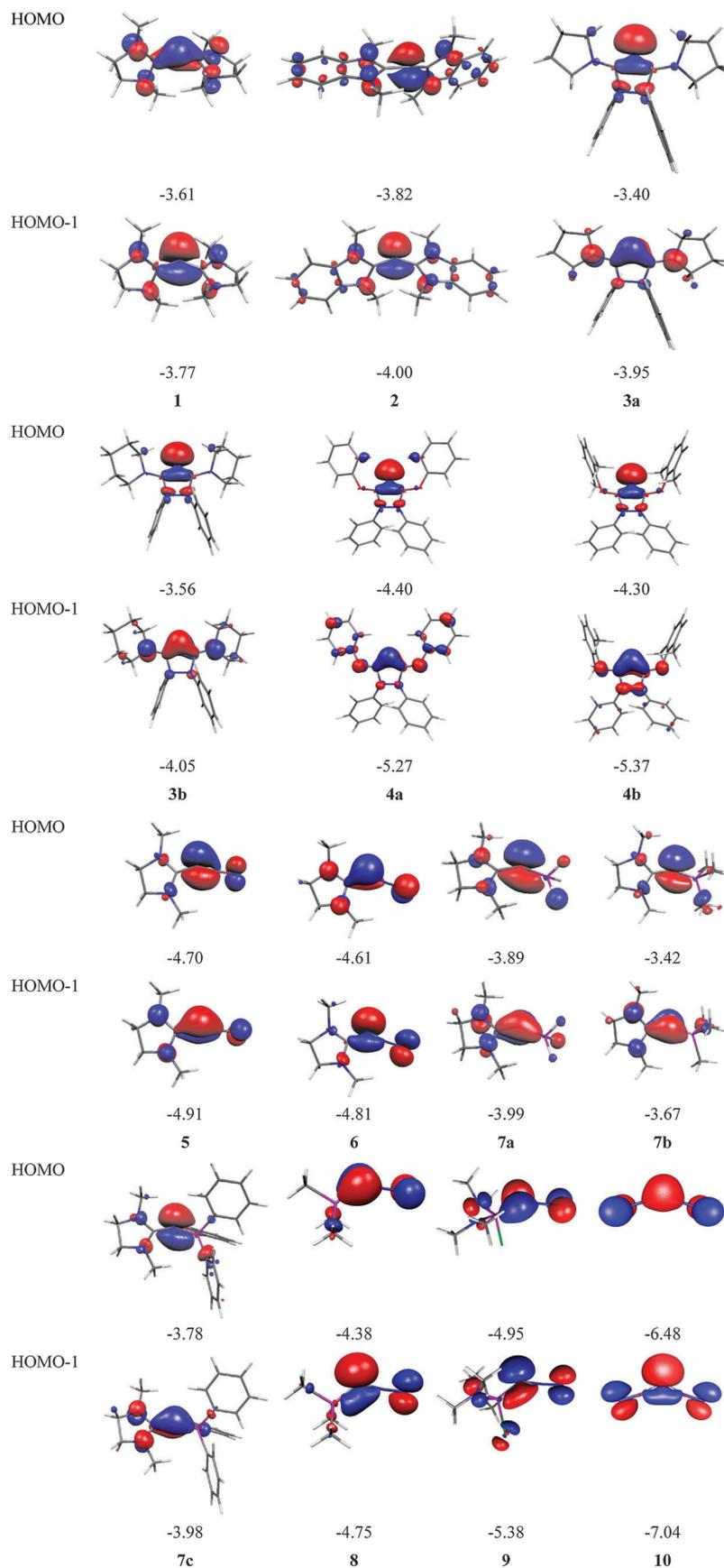
Fig. 7   Shape and energy values [eV] of the frontier orbitals (BP86/TZVPP) of the carbones **1–10** which are shown in Fig. 6.

Table 3 First and second proton affinities PA and bond dissociation energies D_e of complexes $(L_1L_2)C–BH_3$ and $(L_1L_2)C–(BH_3)_2$ at the MP2/TZVPP//BP86/SVP level of theory. All energies are given in kcal mol^{-1} [32]

			$(L_1L_2)C–(H^+)_n$		$(L_1L_2)C–(BH_3)_n$	
$C(L_1L_2)^a$	L_1	L_2	1. PA	2. PA	D_e ($n = 1$)	D_e ($n = 2$)
1	NHC^{Me}	NHC^{Me}	282.2	157.5	42.1	29.0
2	NHC^{Bz}	NHC^{Bz}	284.7	167.8	49.3	27.0
3a	Cyclo-bisdiaminocarbene		296.5	158.7	58.4	20.0
3b	Cyclo-bisdiaminocarbene		293.5	158.0	57.6	16.9
4a	Cyclo-aminooxocarbene		285.2	131.0	53.9	5.7
4b	Cyclo-aminooxocarbene		284.3	133.3	53.0	9.5
5	NHC^{Me}	CO	243.3	99.0	30.7	17.4
6	NHC^{Me}	N_2	244.1	111.5	31.9	20.7
7a	NHC^{Me}	PH$_3$	273.3	140.2	46.9	33.8
7b	NHC^{Me}	PMe$_3$	284.2	160.4	51.7	26.4
7c	NHC^{Me}	PPh$_3$	287.1	176.4	48.0	23.6
8	PMe$_3$	N_2	243.5	108.4	35.9	30.2
9	PCl(NMe$_2$)$_2$	N_2	239.7	115.5	34.8	22.6
10	N_2	N_2	195.6	47.0	22.2	14.7

^{a} The geometries of **1**–**10** are shown in Fig. 6.

and pertinent examples for EDA and EDA-NOCV calculations are available from the literature.[14,40]

The EDA and EDA-NOCV methods can also be used to analyze the interactions between two fragments such as the carbon atom in the ^1D electronic reference state and two ligands L in carbones CL$_2$. The EDA-NOCV results for the carbodiphosphorane C(PPh$_3$)$_2$ and the carbodicarbene C(NHC^{Me})$_2$ are shown in Table 4.

Table 4 Energy decomposition analysis at BP86/TZ2P with the EDA-NOCV method of the carbon–ligand interactions in carbodiphosphorane C(PPh$_3$)$_2$ and carbodicarbene C(NHC^{Me})$_2$. All values in kcal mol^{-1}

C: $X\,^3P \rightarrow\,^1D$ 43.5 kcal mol^{-1} (BP86/TZ2P)
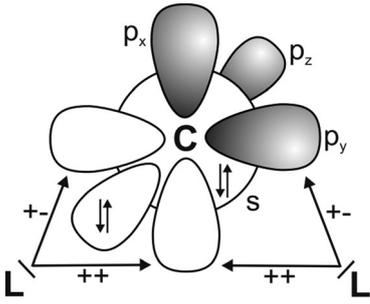
Compound	C(PPh$_3$)$_2$	C(NHC^{Me})$_2$
Interacting fragments	C (^1D) (PPh$_3$)$_2$	C (^1D) (NHC^{Me})$_2$
ΔE_{int}	−192.3	−267.3
ΔE_{Pauli}	738.4	917.6
ΔE_{elstat}^a	−284.0 (30.5%)	−354.6 (29.9%)
ΔE_{orb}^a	−646.7 (69.5%)	−830.4 (70.1%)
ΔE_σ (L→C←L (+,+) donation)^b	−384.2 (59.4%)	−517.7 (62.3%)
$\Delta E_{\pi_\parallel}$ (L→C←L (+,−) donation)^b	−190.5 (29.5%)	−196.0 (23.6%)
$\Delta E_{\pi_\perp}$ (L←C→L π backdonation)^b	−65.0 (10.1%)	−98.8 (11.9%)
ΔE_{rest}^b	−6.9 (1.1%)	−17.8 (2.1%)
ΔE_{prep}	63.6	87.3
D_e	128.6	180.0

^{a} The value in parentheses gives the percentage contribution to the total attractive interactions ($\Delta E_{elstat} + \Delta E_{orb}$). ^{b} The value in parentheses gives the percentage contribution to the total orbital interactions.

The upper part of the table shows schematically the orbital interactions between the ligands and the carbon atom which are expected to be the most important contributions to ΔE_{orb}. The in-phase (+,+) combination of the σ donor orbitals donate into the vacant p$_x$(σ) AO of C while the (+,−) out-of-phase combination donates electronic charge into the p$_y$(π$_\parallel$) orbital of carbon. Some π backdonation L←C→L from the occupied p$_z$(π$_\perp$) AO of carbon into vacant ligand orbitals may also be found. The EDA-NOCV data in Table 4 provide a quantitative estimate of the different types of orbitals interactions as well as the other energy terms which are relevant for the carbon–ligand bonding.
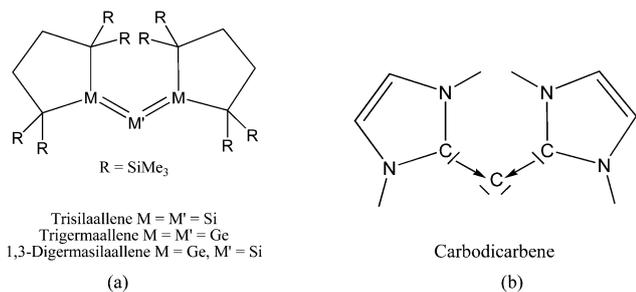
The calculations suggest that C–NHC^{Me} bonds in the carbodicarbene C(NHC^{Me})$_2$ are significantly stronger than the C–PPh$_3$ bonds in C(PPh$_3$)$_2$. This holds for both, the intrinsic interaction energies ΔE_{int} as well as for the bond dissociation energies D_e (Table 4). Inspection of the different energy terms indicate that the nature of the carbon–ligand bonding in the two complexes is very similar. Both L→C←L donor–acceptor bonds have ~70% covalent character. The breakdown of the orbital term into the pairwise interactions shows that the major contribution comes from the in-phase (+,+) σ donation which provides ~60% to ΔE_{orb} while the out-of-phase (+,−) donation provides ~30% (L = NHC^{Me}) and ~24% (L = PPh$_3$) to the attractive orbital interactions. The π$_\perp$ backdonation L←C→L is only a minor component in both complexes while the remaining orbital interactions are negligible. The EDA-NOCV results in Table 4 are a striking example for the strength of modern methods of bonding analysis to provide quantitative insight into the nature of chemical bonding which is based on accurate quantum chemical methods.

3. Divalent E(0) compounds (E = Si–Pb)

Is divalent E(0) chemistry of the group 14 elements restricted to E = C or is it also found for the heavier elements E = Si–Pb? Are there compounds EL$_2$ for the latter tetrele[41] atoms which can be described as donor–acceptor complexes L→E←L? Recent theoretical studies strongly suggest that divalent E(0) compounds EL$_2$ are stable species which have already become synthesized. Like carbodiphosphoranes which were not recognized as divalent C(0) compounds, a similar situation exists for the heavier group 14 homologues.[42]

Scheme 2a shows three recently synthesized compounds which were introduced by Kira *et al.* as the first examples of heavier group 14 homologues of allenes that are stable in a condensed phase.[43] The authors named the molecules trisilaallene, trigermaallene and 1,3-digermasilallene although the equilibrium geometries of the compounds are strongly bent with bond angles (cyc)E–E–E(cyc) between 122.6° (E = Ge) and 136.5° (E = Si). The bending angles are similar to the P–C–P angle in C(PPh$_3$)$_2$ of 131.7° and to the C–C–C angle of 131.8° which was calculated for C(NHC^{Me})$_2$ and the experimental value of 134.8° for C(NHC^{Bz})$_2$. Scheme 2a sketches the bonding situation of trisilaallene, trigermaallene and 1,3-digermasilallene as they were suggested by Kira *et al.*[43] The similar bending angle implies that the bonding of the (cyc)E–E–E(cyc) moiety might be described

5114 | *Chem. Soc. Rev.*, 2014, **43**, 5106–5139

This journal is © The Royal Society of Chemistry 2014

Scheme 2 Schematic representation of the bonding situation in (a) heavy allenes as suggested by Kira[43] and (b) carbodicarbenes C(NHC)₂.

analogous to carbodicarbenes (Scheme 2b). However, there is an important difference between the carbodicarbenes C(NHC)₂ and the "bent allenes" shown in Scheme 2. The carbene donor ligands in C(NHC)₂ have nitrogen π donor atoms at the α position of the carbon donor atom while there is no π donor atom in the cyclic moieties of the heavier homologues. The trisilaallene, trigermaallene and 1,3-digermasilallene are thus substituted homologues of the parent systems E(EH₂)₂. Quantum chemical calculations by the groups of Apeloig[44] and Veszprémi[45] have shown that the classical (D_{2d}) allene structure $H_2E\!=\!E\!=\!EH_2$ where E = Si, Ge is not a minimum on the potential energy surface (PES). Geometry optimization of the D_{2d} form **A** of E(EH₂)₂ without symmetry constraints gives a strongly bent equilibrium structure **B** for H₂E–E–EH₂ with bending angles of ~70° where the planes of the EH₂ moieties are strongly rotated from the E₃ plane (Fig. 8). The latter energy minima are ~20 kcal mol⁻¹ (E = Si) and ~25 kcal mol⁻¹ (E = Ge)[45c] lower lying than the D_{2d} form which is a second-order saddle point with a degenerate imaginary frequency. Another energy minimum of E(EH₂)₂ is the cyclic form **C** (Fig. 8) which is separated by only a small energy barrier from structure **B** which has a similar energy as **C**. Apeloig and co-workers pointed out that **B** and **C** are bond-stretch isomers on the Si₃H₄ PES.[44] It becomes obvious that the equilibrium geometry **B** bears little resemblance to a classical allene. A similar situation is found for acetylene and its heavier group 14 homologues E₂H₂ (E = Si–Pb) where the linear form HE≡EH is a second-order saddle point.[46,47] The rather unusual energy minimum structures of the latter species and the difference to the carbon systems have been explained with the doublet/quartet gap of the EH fragments which yield the E₂H₂ structures.[47]

Petrov and Veszprémi recognized the connection between the strongly bent equilibrium structure of the "trisilaallene" R₂Si–Si–SiR₂ and the carbones CL₂ and they calculated various

Table 5 Calculated Lewis structures according to the NBO analysis for some compounds SiL₂. Bending angle α[°] at the central silicon atom and Wiberg bond orders P(Si–E)[45c]

NBO structure	R	α	P(Si–E)
	CH₃	76.7	1.41
	SiH₃	131.7	1.76
	BH₂	180.0	1.55
	H	79.7	1.45
	CH₃	103.5	1.65
	SiH₃	107.1	1.63
	Si(CH₃)₃	130.2	1.68
	—	89.1	0.36
	—	88.2	0.98

systems SiL₂ where L = SiR₂, NH₃, PH₃.[45c] The latter two compounds Si(EH₃)₂ which are related to carbodiphosphoranes have strongly bent geometries where the bending angle is 89.1° (E = N) and 88.2° (E = P). The NBO[48] analysis predicts two lone-pairs at the silicon atom which let the authors suggest that the bonding situation should be written in analogy to the carbones as H₃E→Si←EH₃. The authors also calculated the structures of compounds R₂Si–Si–SiR₂ with acyclic and cyclic moieties SiR₂ which are model substituents for the real substituent of the experimental "trisilaallene" of Kira et al. Table 5 shows the most important results. It becomes obvious that the bending angle of 136.5° which was measured for the isolated compound is due to steric repulsion between the bulky substituents. The agreement between the latter value and the bending angles of C(PPh₃)₂ (131.7°) and C(NHC^{Bz})₂ (134.8°) is fortuitous.

Another experimental finding which is relevant for the present work concerns the synthesis of the first "tristannaallene" [(t-but)₃Si]₂Sn=Sn=Sn[(t-but)₃Si]₂ which was already reported by Wiberg et al. in 1999 prior to the synthesis of the trisilaallene and trigermaallene.[49] The X-ray structure analysis shows that the compound has a Sn–Sn–Sn bending angle of 156.0°. The authors noted that the ¹¹⁹Sn NMR signal of the central dicoordinated tin atom appears at a very low field which is more typical for a stannylene SnR₂. On the basis of the experimental geometry and the NMR signal it was proposed that the bonding situation in the compounds is best described by the resonance formulae shown in Fig. 9.

The bonding situation in the carbodicarbene homologues **11E** and in the "bent allenes" **12E** with E = C–Pb has been investigated in recent theoretical studies by Takagi et al. who reported also about theoretical results of the related systems **13E–15E** (Scheme 3).[50] The results strongly suggest that the
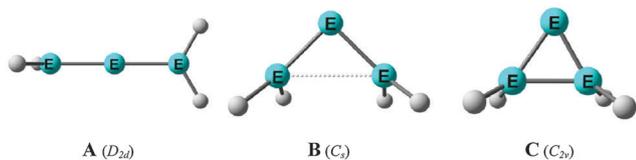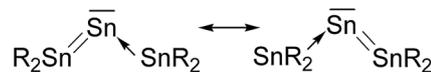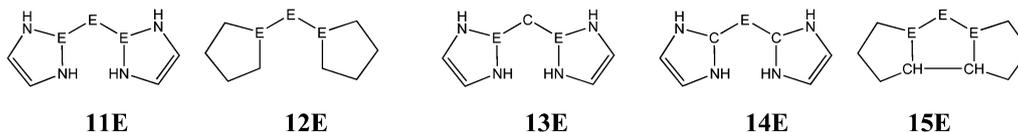
Fig. 8 Schematic representation of the three structures **A**, **B**, **C** which were found as energy minima on the E(EH₂)₂ (E = Si, Ge) potential energy surfaces by Apeloig et al.[44]

Fig. 9 Resonance structures which were suggested for Sn(SnR₂)₂ by Wiberg et al.[49]

This journal is © The Royal Society of Chemistry 2014

Chem. Soc. Rev., 2014, 43, 5106–5139 | 5115

Scheme 3 Overview of the calculated two-coordinated compounds **11E–15E** which were studied by Takagi *et al.*[50]

"allenes" which have been synthesized by Kira *et al.*[43] should rather be classified as divalent E(0) compounds.

Fig. 10 shows the optimized geometries of **11E–15E** (E = C–Sn). The carbon compounds **11C–15C** possess much wider bending angles at the dicoordinated central atom than the heavier homologues. The difference is particularly striking between **12C**, which shows the typical feature of an allene, *i.e.* a linear C=C=C moiety and an orthogonal alignment of the cyclopentyl ligands (dihedral angle of 90°/270°), and the heavier homologues **12E** (E = Si–Sn) which have very acute bending angles E–E–E between 76.4° (E = Sn) and 79.4° (E = Ge). The cyclic ligands in the latter compounds are slightly twisted with respect to each other with dihedral angles between 31.0°

(E = Ge, Sn) and 34.0° (E = Si). Inspection of the highest occupied orbitals of **11E–15E** showed that all compounds possess high-lying MOs which can be identified as σ- and π-type lone-pair orbitals.[50]

The bending angles of the experimentally observed "trisilaallene" and "trigermaallene" which carry bulky trimethylsilyl groups at α and α′ position of the cyclic ligands are much wider than in **12E**. Geometry optimizations of the compounds **12E′** (E = Si, Ge, Sn) which have trimethylsilyl groups at the α and α′ position show (Fig. 11) that the bending angles of **12E′** are much larger than those of **12E**. The calculated values for **12Si′** (135.7°) and **12Ge′** (123.8°) are in very good agreement with the experimental values for the "trisilaallene" (136.5°) and
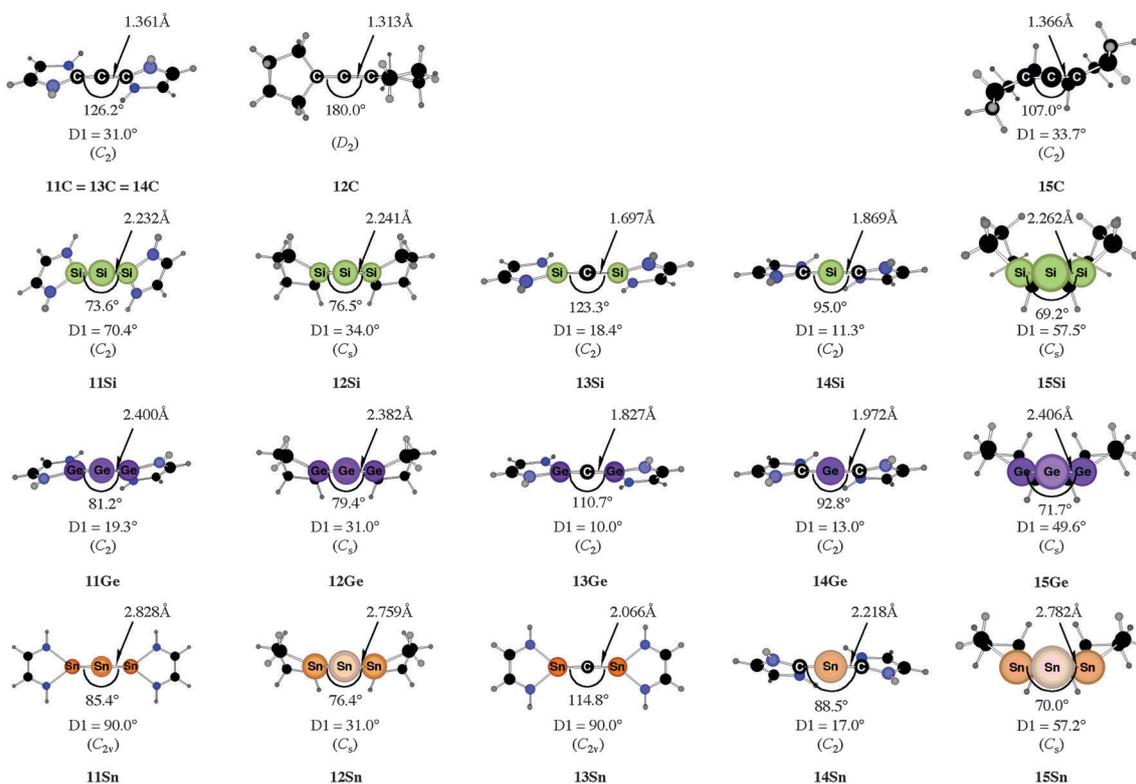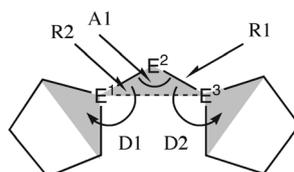

Fig. 10 Calculated geometries of tetrylones **11E–15E** (E = C, Si, Ge, Sn) showing the most important geometrical data.[50b] The figure has been adapted from ref. 50b. Distances are given in Å, angles in degree. The torsion angle D1 given below each structure is defined as the interplanar angle between the grey shaded area:
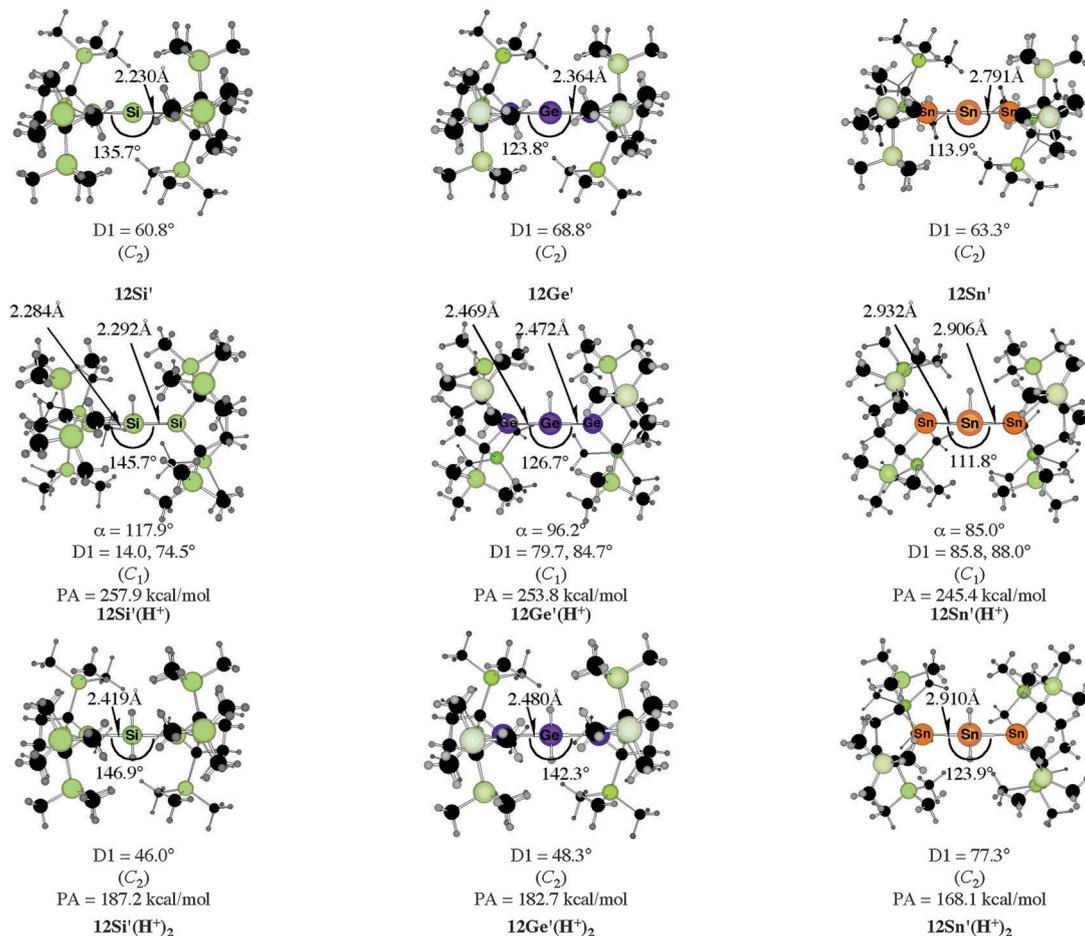
Fig. 11 Calculated geometries of the tetrylones **12E′** and the singly protonated and doubly protonated species **12E′(H⁺)** and **12E′(H⁺)₂** (E = Si, Ge, Sn) which carry bulky Si(Me)₃ substituents at the α and α′ position of the cyclic ligands of **12E**.[50b] The figure has been adapted from ref. 50b. The angle α gives the bending angle of the E–H⁺ bond with respect to the E¹–E²–E³ plane. Distances are given in Å, angles in degree. For the definition of the torsion angle D1 see Fig. 10.

"trigermaallene" (122.6°). The calculations suggest that the agreement between the experimental values for the "trisilaallene" and "trigermaallene" and the carbodicarbene and carbodiphosphoranes does not come from the similar bonding situation of the central E–E–E moiety in the carbon systems and the heavier homologues. The bonding angles in the parent systems of the heavier homologues are more acute than in the carbon species. The steric repulsion in **12E′** leads to bonding angles which are similar to those in C(NHC)₂ and C(PR₃)₂. However, the much more acute bonding angles in the parent systems **12E** (E = Si–Sn) which are <80° raise serious doubt whether these compounds should be considered as allenes. Moreover the calculations show that the molecules **11E–14E** are rather flexible with respect to the bending angles at the central dicoordinated atom and the rotation of the cyclic ligands about the central E¹–E²–E³ plane.
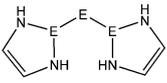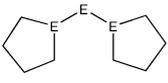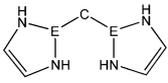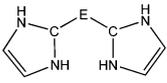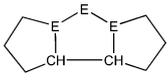
Fig. 11 shows also the calculated geometries of the singly and doubly protonated compounds **12E′(H⁺)** and **12E′(H⁺)₂** (E = Si–Sn) and the theoretically predicted first and second proton affinities. It becomes obvious that the "heteroallenes" **12E′** possess not only very large first PAs but also the second

PAs are very big. The calculated values for the second PA (168.1–187.2 kcal mol⁻¹) are similar to the second PA of C(PPh₃)₂ (185.6 kcal mol⁻¹) and for C(NHC^Me)₂ (168.4 kcal mol⁻¹). The geometries of the singly protonated compounds **12E′(H⁺)** exhibit a particular feature. The E–H⁺ bond is not coplanar to the E¹–E²–E³ plane which means that the central tetrele atom is protonated through the π-type orbital. The same situation is found in the protonated compounds of the parent systems **11E(H⁺)–15E(H⁺)** (E = Si–Sn).[50a,b] This is strikingly different to the carbone compounds where carbon is always protonated at the σ lone pair yielding a C–H⁺ bond in **11C(H⁺)**, **12C(H⁺)** and **15C(H⁺)** which is coplanar to the central E–C–E plane.

Takagi et al. reported also about complexes of **11E–15E** with one and with two Lewis acids BH₃ as ligands.[50b] They also calculated transition metal complexes (CO)₅W–D and (CO)₃Ni–D with the ligands D = **11E–15E**. Table 6 summarizes the theoretically predicted bond dissociation energies (BDEs) and proton affinities of the compounds. The calculated data suggest that the heavy-atom homologues **11E–15E** (E = Si–Sn) possess not only large values for the first and second PAs. They also yield strongly bonded complexes with one but also with two BH₃ Lewis acids.

This journal is © The Royal Society of Chemistry 2014

Chem. Soc. Rev., 2014, **43**, 5106–5139 | **5117**

Table 6 First and second proton affinities (PA) and bond dissociation energies including ZPE corrections for complexes of **11E–15E** with one and two BH$_3$ ligand and one metal carbonyl fragment at 298 K [kcal mol^{-1}][50b]

	11E	12E	13E	14E	15E
E = C					
1st PA	289.2	236.9	Same as 1C	Same as 1C	280.2
2nd PA	148.4	87.6			73.8
D_o^{298} (BH$_3$)	60.2	6.9			55.3
D_o^{298} (BH$_3$)$_2$	19.4	Diss.^{a}			Diss.^{a}
E = Si					
1st PA	249.7	237.9	261.8	275.9	228.8
2nd PA	142.9	129.3	145.3	166.7	123.9
D_o^{298} (BH$_3$)	28.3	31.6	34.6	40.8	23.2
D_o^{298} (BH$_3$)$_2$	26.2	36.3	47.8	48.1	36.6
D_o^{298} [W(CO)$_5$]	41.2	42.0	38.5	53.0	37.9
D_o^{298} [Ni(CO)$_3$]	27.8	27.5	23.0	36.1	24.6
E = Ge					
1st PA	255.0	229.9	263.9	275.7	220.3
2nd PA	141.3	127.6	173.8	154.0	120.9
D_o^{298} (BH$_3$)	27.0	20.7	39.7	39.4	26.3
D_o^{298} (BH$_3$)$_2$	27.9	29.4	30.9	43.4	16.5
D_o^{298} [W(CO)$_5$]	45.0	35.9	41.1	54.0	31.0
D_o^{298} [Ni(CO)$_3$]	28.3	20.5	25.2	36.3	17.7
E = Sn					
1st PA	260.9	226.0	276.8	277.9	225.7
2nd PA	143.6	129.6	194.8	141.5	112.4
D_o^{298} (BH$_3$)	29.4	23.3	49.1	40.6	23.8
D_o^{298} (BH$_3$)$_2$	25.1	15.2	47.4	36.0	10.6
D_o^{298} [W(CO)$_5$]	53.5	30.6	53.9	59.5	28.6
D_o^{298} [Ni(CO)$_3$]	36.7	18.1	34.4	41.1	16.3

^{a} The second BH$_3$ ligand does not bind to the divalent carbon atom. It dissociates during the geometry optimization.

Surprisingly, the BDE of the second BH$_3$ is in several complexes even higher than the BDE of the first BH$_3$! The binding of the first BH$_3$ ligand in **11E(BH$_3$)–15E(BH$_3$)** prepares the central atom E quite well for the interaction with the second borane ligand. It should be noted that the BH$_3$ ligands in some complexes are η^3 coordinated to the E$_3$ moiety while in other complexes they bind η^1 to the central atom E. A detailed discussion of the geometries of the complexes is given in the paper by Takagi et al.[50b] Finally, we note that the compounds **11E–15E** are strongly bonded ligands D in complexes (CO)$_5$W–D and (CO)$_3$Ni–D where their BDE is comparably strong as that of CO.

What is the reason for the drastically different equilibrium geometries and chemical properties of **11E–15E** which show typical features of an allene when E = C while they exhibit divalent E(0) properties when E = Si–Pb? A straightforward answer to this question can be given when the relative energies of the interacting fragments L and E in the species EL$_2$ in the lowest lying singlet and triplet states of the carbon compounds are compared with the heavier homologues. The explanation is based on the model which was introduced earlier by Trinquier and Malrieu[51a,b] and by Carter and Goddard[51c,d] who discussed the unusual structures of the heavy-atom homologues of ethylene E$_2$H$_4$ (E = Si–Pb) using the electronic singlet and triplet states of EH$_2$. Fig. 12 shows qualitatively the orbital interactions

in divalent E(0) compounds (top) and in allenes (bottom). The donor–acceptor bonds in the former species come from the interactions between singlet fragments ER$_2$ and a group 14
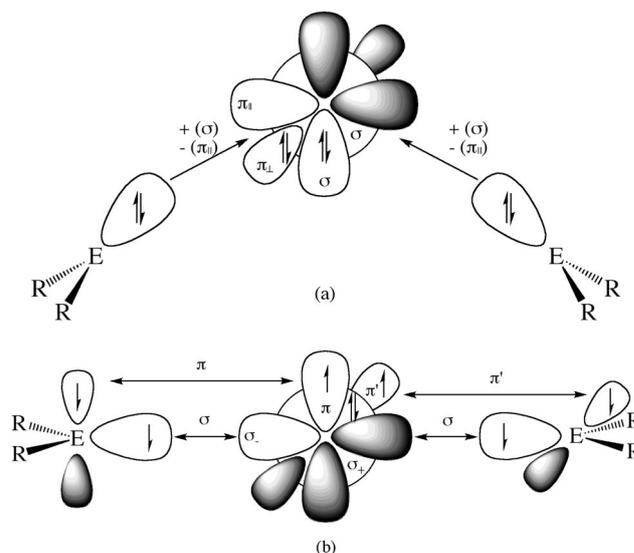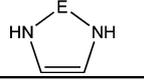

Fig. 12 Schematic representation of orbital interactions in (a) divalent E(0) compounds R$_2$E→E←ER$_2$ and (b) allenes R$_2$E=E=ER$_2$.

5118 | Chem. Soc. Rev., 2014, 43, 5106–5139

This journal is © The Royal Society of Chemistry 2014

Table 7 Energy differences (in kcal mol^{-1}) between different spin multiplicities at BP86/TZVPP

	E^a		HN⌐E⌐NH		E (cycE)	
	^{1}D	^{3}P	Singlet	Triplet	Singlet	Triplet
E = C	29.1	0.0	0.0	84.1	0.0	7.4
E = Si	18.0	0.0	0.0	60.8	0.0	27.1
E = Ge	20.4	0.0	0.0	50.5	0.0	31.0
E = Sn	24.6	0.0	0.0	37.2	0.0	31.2
E = Pb	22.4^b	0.0	0.0	30.5	0.0	33.8

^{a} Experimental excitation energies taken from: J. E. Sansonetti and W. C. Martin, *Handbook of Basic Atomic Spectroscopic Data*, National Institute of Standards and Technology, Gaithersburg, MD 20899, http://www.nist.gov/pml/data/handbook/index.cfm. ^{b} 6p$^2_{1/2}$ ← 6p$_{1/2}$6p$_{3/2}$ excitation.

atom E in the singlet (^{1}D) state. The double bonds in allenes come from the electron-sharing interactions between triplet fragments ER$_2$ and a group 14 atom E in the triplet (^{3}P) state. Table 7 gives the calculated energy differences for atoms E, for NHC and cyclopentylidene (cycC) and their heavier homologues (E = Si–Pb).

Table 7 shows that the singlet fragments in C(NHC)$_2$ are energetically favored over the triplet fragments by (2 × 84.1 kcal mol^{-1}) − 29.1 kcal mol^{-1} = 139.1 kcal mol^{-1}. This is in contrast to C(cycC)$_2$

where the triplet fragments are favored over the singlet fragments by 29.1 kcal mol^{-1} − (2 × 7.4 kcal mol^{-1}) = 14.3 kcal mol^{-1}. The situation for the heavier group 14 homologues is different because the triplet → singlet excitation energy of atom E = Si–Pb is smaller than for carbon atom and the singlet → triplet excitation energy of cycE is clearly higher than that of cycC. For example, the singlet fragments in Si(NHSi)$_2$ are favored over the triplet fragments by (2 × 60.8 kcal mol^{-1}) − 18.0 kcal mol^{-1} = 103.6 kcal mol^{-1} and they are favored in Si(cycSi)$_2$ by (2 × 27.1 kcal mol^{-1}) − 18.0 kcal mol^{-1} = 36.2 kcal mol^{-1}. A similar situation is found for the heavier homologues E = Ge–Pb. The bonding situation of a genuine allene in E(cycE)$_2$ would only be possible if stronger binding interactions between the triplet fragments than the binding interactions between the singlet fragments compensate for the differences in the excitation energies. It has been shown, however, that E→E (E = Si–Pb) donor–acceptor interactions between singlet fragments may have the same strength as E–E electron-sharing interactions between open-shell fragments.[47] The differences between the bonding situation in the heavier tetrele compounds and the carbon molecules can thus be attributed to the nature and energy levels of the electronic ground and excited states of the bonding fragments and to the strength of the interactions in the different electronic states.

The experimental work about "trisilaallene" and "trigermaallene"[43] and the theoretical studies of the parent systems
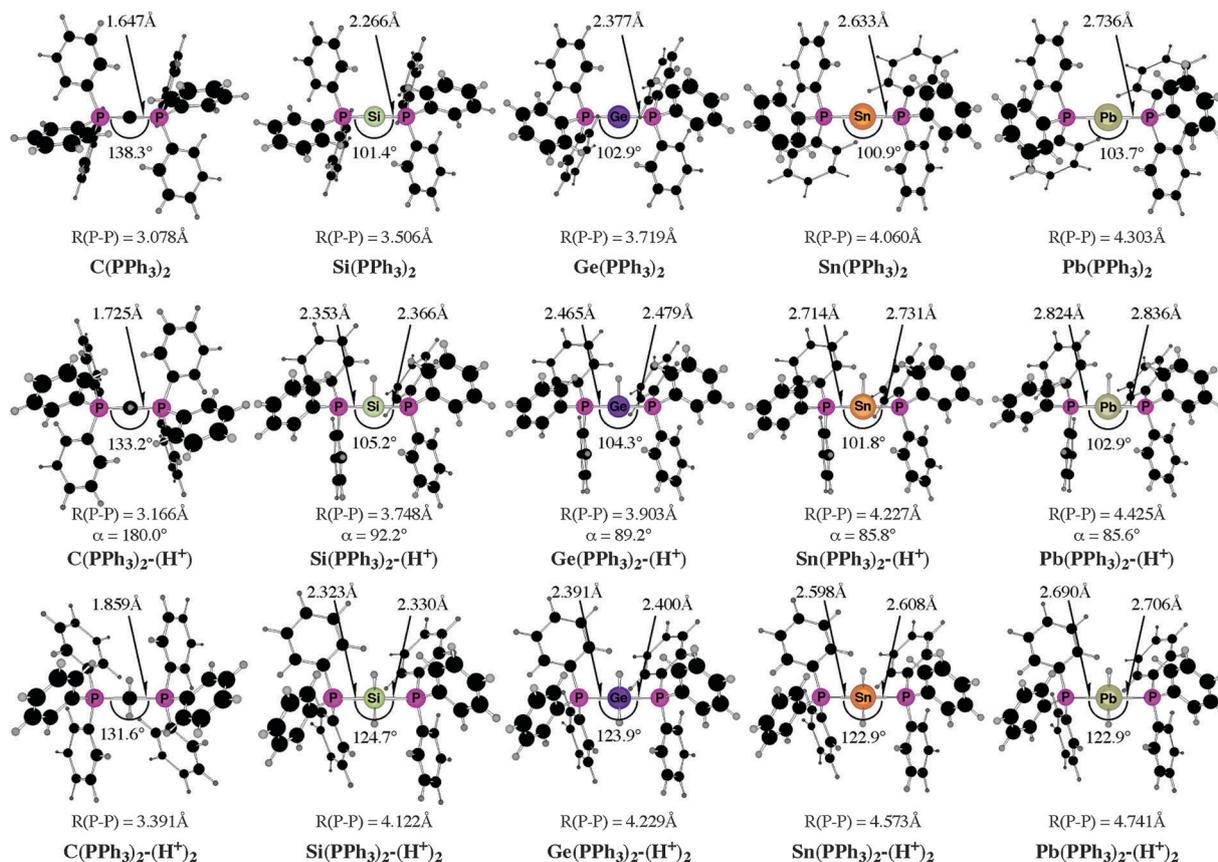

Fig. 13 Calculated geometries (BP86/TZVPP) of compounds E(PPh$_3$)$_2$ (E = C–Pb) and their mono- and di-protonated forms. The E–P bond lengths are given in Å and the P–E–P bond angle in degrees. The angle α is the bending angle of the E–H$^+$ bond with respect to the P–E–P plane.

11E–15E[50] gave rise to the question about the heavy group 14 homologues of carbodiphosphorane $E(PPh_3)_2$ (E = Si–Pb). The structures, bonding situation and double–donor properties were investigated in a theoretical study by Takagi, Tonner and Frenking.[52] The experimentally yet unknown compounds were shown to be genuine examples of tetrylones EL_2 which are predicted to have large first and second proton affinities as well as large bond dissociation energies of one and two Lewis acids BH_3 and AuCl.

Fig. 13 shows the calculated equilibrium geometries of $E(PPh_3)_2$ and the singly and doubly protonated species $E(PPh_3)_2–(H^+)$ and $E(PPh_3)_2–(H^+)_2$. The calculations predict that the bending angle P–E–P in all systems becomes more acute for the heavier group-14 complexes where E = Si–Pb than for the parent carbone. The shape of the highest lying orbitals HOMO and HOMO − 1 of the neutral parent systems $E(PPh_3)_2$ exhibits the typical features of π lone-pair (HOMO) and σ lone-pair (HOMO − 1) (Fig. 14). Table 8 gives the calculated proton affinities of $E(PPh_3)_2$ in comparison with the PA values for the homologues $E(NHC)_2$ (**14E**) and the divalent E(II) compounds NHE. It becomes obvious that the first PAs but particularly the second PAs of $E(NHC)_2$ and $E(PPh_3)_2$ are much higher than those of the NHE compounds. This clearly identifies $E(PPh_3)_2$ and $E(NHC)_2$ as divalent E(0) compounds while the NHE molecules are divalent E(II) compounds.

Further relevant information about the tetrele phosphoranes $E(PPh_3)_2$ are given in Table 9. The calculated bond dissociation energies for breaking the E-PPh_3 bonds become significantly smaller for the heavier systems C ≫ Si > Ge > Sn > Pb but protonation at atom E strongly enhances the E-PPh_3 bonds. This is a hint for possible synthesis of the neutral compounds which might becomes isolated *via* deprotonation of the cations $E(PPh_3)_2–(H^+)$ and $E(PPh_3)_2–(H^+)_2$. The calculated data also suggest that the tetrylones $E(PPh_3)_2$ are very strong donors toward one and two Lewis acids BH_3 and AuCl. Unlike

Table 8 Calculated first and second proton affinities at BP86/TZVPP for $E(PPh_3)_2$, $E(NHC)_2$ and NHE in kcal mol^{-1}
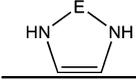
E	$E(PPh_3)_2$		$E(NHC)_2$		HN–E–NH	
	1. PA	2. PA	1. PA	2. PA	1. PA	2. PA
C	280.1	188.3	289.2	148.4	253.0	51.7
Si	279.4	186.0	275.9	166.7	208.0	82.2
Ge	276.0	174.8	275.7	154.0	199.6	82.3
Sn	272.2	164.0	277.9	141.5	201.8	80.6
Pb	270.7	147.1	273.8	114.9	205.7	66.8

the proton affinities where the carbon system has larger first and second PAs than the heavier homologues, the bond strengths of $E(PPh_3)_2$ toward one and two BH_3 and AuCl moieties are even bigger when E = Si–Pb compared with $C(PPh_3)_2$ except for the complexes $Sn(PPh_3)_2–(BH_3)$ and $Pb(PPh_3)_2–(BH_3)$. The calculated results are pointing toward a potentially fruitful and largely explored territory for experimental studies. Further theoretical information about the chemistry of tetrele phosphoranes $E(PPh_3)_2$ can be found in a recent theoretical study of transition metal complexes $[(CO)_5W–\{E(PPh_3)_2\}]$ and $[(CO)_5W–NHE]$ (E = C–Pb) where the ligand properties of tetrylenes and tetrylones are compared.[53]

There is a wealth of experimental and theoretical results which support the identification of a new class of tetrele compounds which are stable in a condensed phase where the group-14 atom has a divalent E(0) valence state. The bonding situation in the tetrylones EL_2 should be described in terms of donor–acceptor interaction L→E←L where the tetrele atom E = C–Pb retains its valence electrons as two lone pairs. The suggested nomenclature for the tetrylones EL_2 is shown in Table 10. Very recently, the first heavier homologues of carbodicarbenes $C(NHC)_2$ could become synthesized and structurally characterized by X-ray analysis. Roesky and co-workers reported

HOMO (-4.26 eV)   HOMO (-3.27 eV)   HOMO (-3.10 eV)   HOMO (-2.94 eV)   HOMO (-2.82 eV)

HOMO-1 (-4.43 eV)   HOMO-1 (-4.90 eV)   HOMO-1 (-5.14 eV)   HOMO-1 (-5.40 eV)   HOMO-1 (-5.63 eV)

$C(PPh_3)_2$ **$Si(PPh_3)_2$**   **$Ge(PPh_3)_2$**   **$Sn(PPh_3)_2$**   **$Pb(PPh_3)_2$**

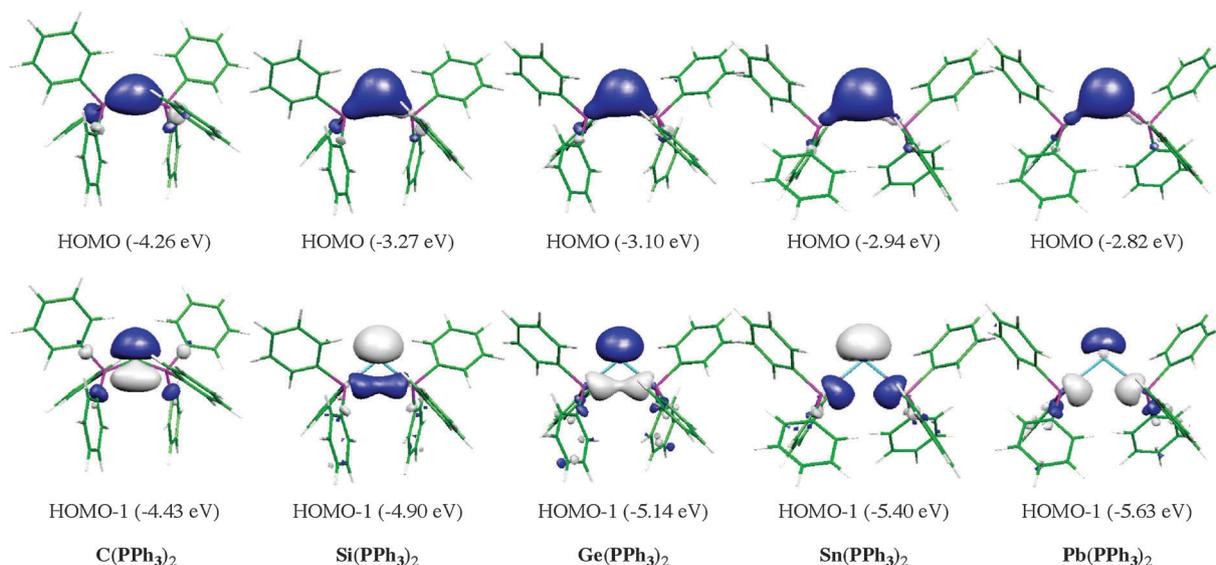**Fig. 14** Graphical representation of HOMO (top) and HOMO − 1 (bottom) of compounds $E(PPh_3)_2$. Orbital energies (BP86/TZVPP) are given in eV.

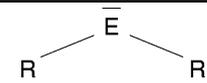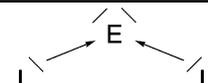5120 | *Chem. Soc. Rev.*, 2014, **43**, 5106–5139

This journal is © The Royal Society of Chemistry 2014

Table 9 Calculated energies at BP86/TZVPP of tetrelediphosphoranes $E(PPh_3)_2$ (E = C–Pb). Bond dissociation energies D_e for the $E–(PPh_3)_2$ bonds. Bond dissociation energies D_e of the complexes $E(PPh_3)_2$ with one and two Lewis acids BH_3 and AuCl. All values in kcal mol^{-1}. The ZPE corrected values D_o are shown in parentheses[52]

	D_e (D_o) $E–(PPh_3)_2$	D_e (D_o)^c $EH^+–(PPh_3)_2$	D_e (D_o)^c $E(H^+)_2–(PPh_3)_2$	D_e (D_o) $E(PPh_3)_2–BH_3$	D_e (D_o) $E(PPh_3)_2(BH_3)–BH_3$	D_e (D_o) $E(PPh_3)_2–AuCl$	D_e (D_o) $E(PPh_3)_2(AuCl)–AuCl$
$C(PPh_3)_2$	65.1^a $(63.0)^a$ 87.0^b $(84.9)^b$	136.2 (131.8)	264.9 (258.8)	35.0 (31.1)	20.8 (16.4)	63.2 (61.8)	52.5 (51.8)
$Si(PPh_3)_2$	26.7^a $(25.9)^a$ 41.0^b $(40.1)^b$	68.2 (65.8)	172.5 (169.2)	37.5 (34.8)	39.6 (37.2)	80.4 (79.2)	73.6 (72.5)
$Ge(PPh_3)_2$	22.9^a $(22.3)^a$ 36.9^b $(36.3)^b$	62.2 (60.1)	160.4 (157.7)	35.1 (32.5)	34.4 (31.9)	77.0 (76.0)	64.1 (63.0)
$Sn(PPh_3)_2$	16.7^a $(16.4)^a$ 28.8^b $(28.4)^b$	50.0 (48.3)	134.2 (132.2)	31.9 (29.7)	30.0 (27.7)	74.8 (73.7)	60.0 (59.1)
$Pb(PPh_3)_2$	13.7^a $(13.6)^a$ 25.3^b $(25.1)^b$	44.9 (43.4)	120.9 (119.4)	31.6 (29.3)	27.3 (25.2)	73.8 (72.6)	53.4 (52.6)

^{a} $E(PPh_3)_2 \rightarrow E(^3P) + 2(PPh_3)$. The values are given for one bond. ^{b} $E(PPh_3)_2 \rightarrow E(^1D) + 2(PPh_3)$. The values are given for one bond. ^{c} The values are given for one bond.

Table 10 Proposed nomenclature for divalent E(0) compounds

E	Divalent E(II): tetrylene	Divalent E(0): tetrylone
C	Carbene	Carbone
Si	Silylene	Silylone
Ge	Germylene	Germylone
Sn	Stannylene	Stannylone
Pb	Plumbylene	Plumbylone
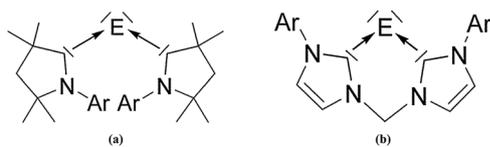
Fig. 15 Schematic representation of the silylones and germylones $E(CAAC)_2$ and E(NHC–NHC) (E = Si, Ge) which have been isolated.[54,55]

about the isolation of the silylone and germylones $E(CAAC)_2$ (E = Si, Ge) where the ligand CAAC (Cyclic Alkyl Amino Carbene) has only one nitrogen atom in the N-heterocyclic carbene moiety (Fig. 15a).[54] The silylone and germylone complexes E(NHC–NHC) where the NHC fragments are bonded to each other in a bidentate ligand have been synthesized by Driess *et al.* (Fig. 15b).[55]

4. Transition metal–carbon complexes [TM]–C

Carbones CL_2 are not the only novel class of compounds that has been introduced in chemistry in the recent past where a bare carbon atom is bonded *via* donor–acceptor interactions. Another class are transition metal (TM) compounds with a terminal carbon atom as ligand [TM]–C which can be regarded as the endpoint in the series TM–alkyl [TM]–$CR_3 \rightarrow$ TM–carbene [TM]=$CR_2 \rightarrow$ TM–carbyne [TM]≡CR complexes. Alkyl complexes of transition metals are already known since 1848 when Frankland

accidentally synthesized diethylzinc while attempting to prepare free ethyl radicals.[56] Molecules with a TM=CR_2 double bond and TM≡CR triple bond were isolated much later.[57–61] The chemical reactivity of the compounds which possess metal–carbon double and triple bonds suggests that two classes of carbene and carbyne complexes can be distinguished which exhibit different reactivities. The metal–ligand bonding in Fischer-type carbene and carbyne complexes[57,58] is best described in terms of donor–acceptor bonding using the Dewar–Chatt–Duncanson (DCD) model[62] between closed-shell fragments while the bonding in Schrock carbenes and carbynes[60,61] should be considered as electron-sharing interactions between triplet (for carbenes) and quartet (for carbynes) fragments (Fig. 16).[63]

The final member in the series of metal–carbon bonds has a naked carbon atom as ligand [TM]–C. Until recently, no such compounds were experimentally known. In 1997, Cummins and co-workers reported a structurally characterized 14 valence electron (VE) anion $[(NRAr)_3Mo(C)]^-$ (R = $C(CD_3)_2CH_3$, Ar = $C_6H_3Me_2$-3,5).[64] It was the first representative example of transition metal complex bearing a naked carbon atom as ligand.[65] The compound is isoelectronic with the nitrido complex $[(NRAr)_3Mo(N)]$.[66] The bonding situation in the anion is very similar to the neutral nitrogen homologues which indicates that the anion $[(NRAr)_3Mo(C)]^-$ should be considered as metal carbide that possesses a TM≡C$^-$ electron-sharing triple bond. It may also be viewed as the anion of Schrock-type carbynes [TM]≡CR where the positively charged substituent R$^+$ has dissociated. The bonding model for Schrock carbynes (Fig. 16d) may therefore be used for the metal–carbon bonding in the carbide anion.

Neutral complexes with bare carbon atoms were first studied with theoretical methods by Chen *et al.* in 2000.[67] The authors calculated the complex $[(CO)_4Fe(C)]$ and the related carbene and carbyne compounds $[(CO)_4Fe(CH_2)]$ and $[I(CO)_3Fe(CH)]$. The optimized geometry of $[(CO)_4Fe(C)]$ has the carbon ligand in the axial position, the equatorial form is an energetically higher lying transition state. A bonding analysis of the 18 valence electron (18VE) complex $[(CO)_4Fe(C)]$ showed that the carbon atom in the ^1D excited state which has the valence configuration $(2s)^2(2p_{z(\sigma)})^2(2p_{x(\pi)})^0(2p_{y(\pi)})^0$ is perfectly suited for donor–acceptor interactions. The $[(CO)_4Fe]$–C bond can thus be

This journal is © The Royal Society of Chemistry 2014

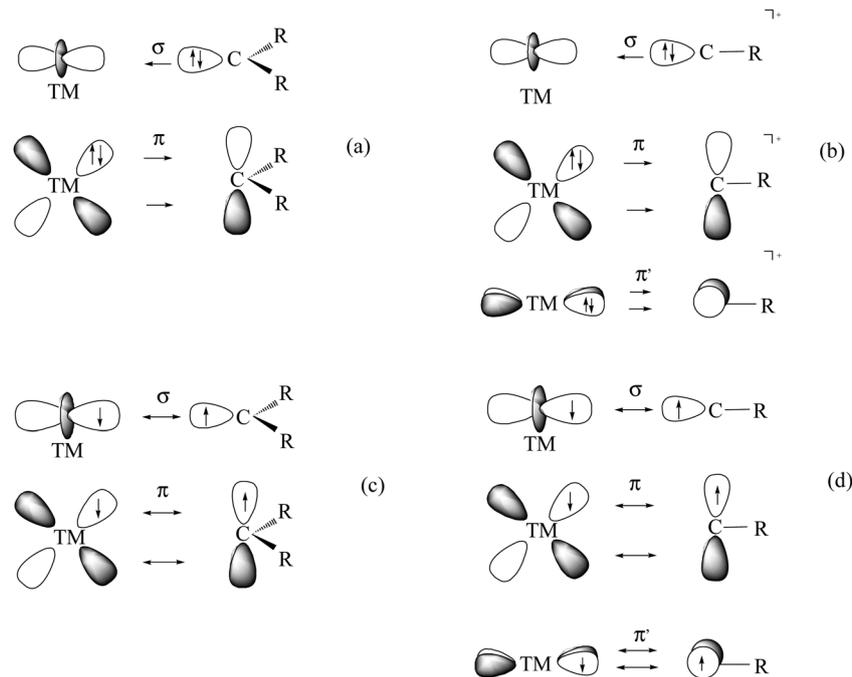*Chem. Soc. Rev.*, 2014, **43**, 5106–5139 | **5121**

Fig. 16 Pictorial representation of the bonding situation in (a) Fischer-type carbene complexes; (b) Fischer-type carbyne complexes; (c) Schrock-type carbenes (alkylidenes); (d) Schrock-type carbynes (alkylidynes).

described with the DCD model where the carbon ligand is bonded to the metal with a triple bond retaining a σ lone-pair orbital. A charge decomposition analysis showed that the singly coordinated carbon atom is a strong σ donor but also a strong π acceptor. The bond dissociation energy for the $[(CO)_4Fe]–C$ bond was calculated at CCSD(T) to be 94.5 kcal mol^{-1} which suggests that the bond is very strong.[67] The authors concluded that the molecule might be too reactive to become isolated in a condensed phase. Because of the σ lone-pair orbital at the terminal carbon atom the compound should be a strong Lewis base. Calculations of the complex $[(CO)_4FeC–BCl_3]$ showed that it is a minimum on the PES with a BDE of 25.6 kcal mol^{-1} (B3LYP).[67] The latter species might be stable enough to become isolated in a condensed phase.

The first synthesis of a neutral transition metal compound with a terminal carbon ligand which could become fully characterized by X-ray structure analysis was reported in 2002 by Heppert and co-workers.[2] They isolated the diamagnetic 16VE ruthenium complexes $[(PCy_3)_2Cl_2Ru(C)]$ (Cy = Cyclohexyl) (**A**) and $[(PCy_3)LCl_2Ru(C)]$ (L = 1,3-dimesityl-4,5-dihydroimidazol-2-ylidene) (**B**) by a metathesis facilitated reaction. A third member of the newly emerging class of stable carbon complexes that could later become isolated and structurally characterized is the related osmium compound $[(PCy_3)_2Cl_2Os(C)]$ (**C**) which was reported in 2007 by Johnson and co-workers.[68] In 2005 the same group reported about more versatile routes to the air- and moisture-stable $[(PCy_3)_2Cl_2Ru(C)]$, opening the way for broader research on the chemistry of complexes with terminal C.[69] To the best of our knowledge, no further transition metal carbon complexes could become isolated. There are reports in the literature about the synthesis of other carbon complexes but there is no X-ray structure available.[70]

The chemical reactivity of the carbon complexes was experimentally studied which sheds light on the bonding situation. Grubbs and his group reported that the complex (**A**) can act as a σ-donor towards $Mo(CO)_5$ and $Pd(SMe_2)Cl_2$ via the terminal carbon atom.[71] They isolated and structurally characterized the complexes $[(PCyc_3)_2Cl_2Ru(C)]–PdCl_2SMe_2$ and they reported about the NMR spectrum of the compound $[Cl_2(PCyc_3)_2Ru(C)]–Mo(CO)_5$ which could, however, not become isolated. Johnson and co-workers published the results of further experimental studies which show that complex (**A**) reacts with $MeO_2CC\equiv CCO_2Me$ in a formal [1+2] cycloaddition of the carbon ligand yielding the cyclopropenylidene complex $[(PCy_3)_2Cl_2Ru=CC_2(CO_2Me)_2]$.[72] It should be noted that already in 1990 Beck and co-workers reported about the crystal structure of $[(Por')Fe(C)Re(CO)_4Re(CO)_5]$[73] (Por' = 5,10,15,20-tetraphenylporhyrin), which can be described as a donor–acceptor complex between the carbon complex $[(Por')Fe(C)]$ and the Lewis acid $[Re(CO)_4Re(CO)_5]$.

The experimental finding about the stability of complexes **A**, **B** and **C** inspired theoretical work about carbon complexes. Thermodynamic aspects in TM complexes with terminal carbon atoms were calculated by Gary et al.[74] The bonding situation in the 16VE model complexes $[(PMe_3)_2Cl_2TM(C)]$ (TM = Fe, Ru) has been the subject of a detailed quantum chemical study using charge- and energy decomposition analyses by Krapp, Pandey and Frenking (KPF).[75] The authors also calculated the related carbonyl complexes $[(PMe_3)_2Cl_2TM(CO)]$ and they compared the bonding situation in the 16VE complexes with the results for the 18VE species $[(PMe_3)_2(CO)_2TM(C)]$, $[(CO)_4TM(C)]$ and $[TM(CO)_5]$ with TM = Fe, Ru. The study gives deep insight into the nature of the metal–carbon interactions.

Fig. 17 shows the optimized geometries and the most important bond distances and angles of the 16VE carbon complexes
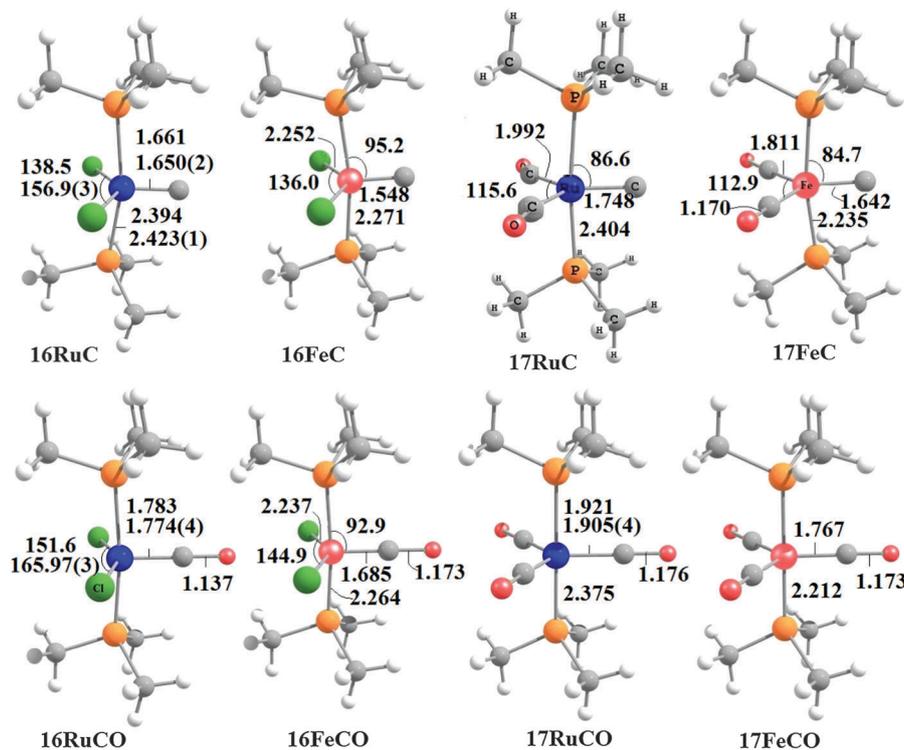
Fig. 17 Calculated geometries (BP86/TZ2P) of the carbon complexes **16TMC** and **17TMC** and the carbonyl complexes **16TMCO** and **17TMCO**. Bond lengths are given in Å, angles in degree.[75] Experimental data are given in *italics*.[2,76a,b] The figure has been adapted from ref. 75.

$[(PMe_3)_2Cl_2Ru(C)]$ (**16RuC**) and $[(PMe_3)_2Cl_2Fe(C)]$ (**16FeC**) and the 18VE species $[(PMe_3)_2(CO)_2Ru(C)]$ (**17RuC**) and $[(PMe_3)_2-(CO)_2Fe(C)]$ (**17FeC**).[75] The carbon ligand is always in the equatorial position which concurs with the experimental observations for **A–C**. The calculated interatomic distances and angles of **16RuC**, **16RuCO** and **17RuCO** are in good agreement with the experimental values of the real compounds which carry more bulky substituents.[2,76a,b] The most important difference between the 16VE complexes **16TMC** and the 18VE species **17TMC** (TM = Ru, Fe) is the TM–C bond length. The 18VE complexes have a significantly longer metal–carbon bond than the 16VE species.

The TM–C bond in the former species is also clearly weaker than in the latter compounds. Table 11 shows that the calculated

Table 11 Calculated bond dissociation energies D_e in kcal mol^{-1}. Zero-point vibrational energy corrected values D_o are given in parentheses[75]

Molecule	No.	D_e (D_o)	
		BP86/TZ2P	CCSD(T)/TZ2P^a
$Cl_2(PMe_3)Ru–C$	**16RuC**	146.5 (143.8)	—
$Cl_2(PMe_3)Fe–C$	**16FeC**	135.1 (132.3)	—
$(CO)_2(PMe_3)Ru–C$	**17RuC**	100.8 (99.6)	—
$(CO)_2(PMe_3)Fe–C$	**17FeC**	115.7 (113.6)	—
$Cl_2(PMe_3)Ru–CO$	**16RuCO**	44.6 (41.2)	—
$Cl_2(PMe_3)Fe–CO$	**16FeCO**	38.2 (34.7)	—
$(CO)_2(PMe_3)Ru–CO$	**17RuCO**	40.3 (37.6)	—
$(CO)_2(PMe_3)Fe–CO$	**17FeCO**	55.3 (51.6)	—
$(CO)_4Ru–C(ax)$	**18RuC**	88.8 (88.9)	93.3
$(CO)_4Fe–C(ax)$	**18FeC**	104.5 (102.7)	98.6
$(CO)_4Ru–CO$	**18RuCO**	32.5 (30.4)	32.2
$(CO)_4Fe–CO$	**18FeCO**	46.3 (43.1)	40.7

^{a} Small-core effective core potential were used for the metals. For details see ref. 73.
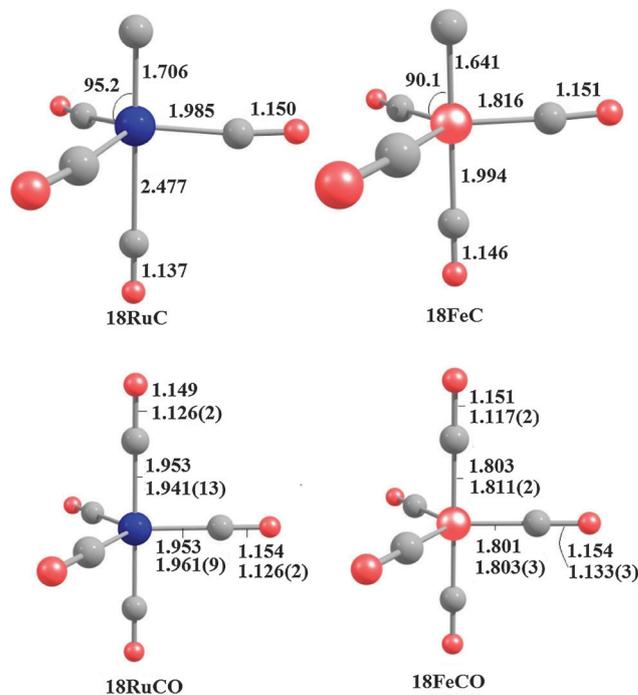
Fig. 18 Calculated geometries (BP86/TZ2P) of the carbon complexes **18RuC** and **18FeC** and the pentacarbonyls **18RuCO** and **18FeCO**.[75] Experimental data are given in *italics*.[76c–e] The figure has been adapted from ref. 75.

This journal is © The Royal Society of Chemistry 2014

Chem. Soc. Rev., 2014, **43**, 5106–5139 | **5123**
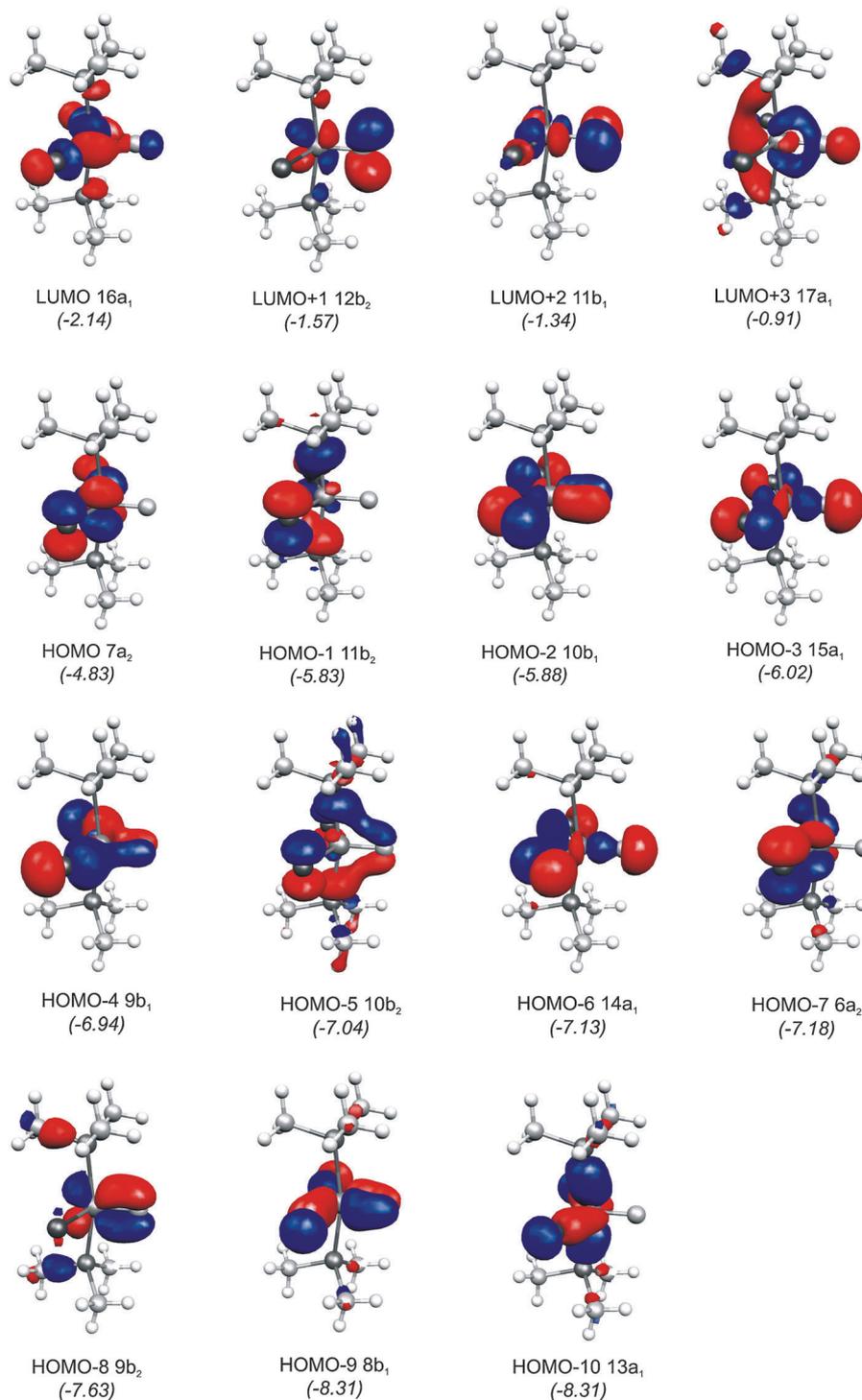
Fig. 19 Plot of the ten highest lying occupied molecular orbitals and four lowest lying vacant MOs of $[(PMe_3)_2Cl_2Ru(C)]$ (**16RuC**). The calculated eigenvalues (BP86/TZ2P) of the orbitals are given in parentheses (in eV).[75] The figure has been adapted from ref. 75.

BDEs of **16RuC** and **16FeC** are significantly higher than for **17RuC** and **17FeC**. It is interesting to note that, for the 18VE complexes **17TMC**, the Fe–C bond is stronger than the Ru–C bond while for the 16VE compounds **16TM** the Fe–C bond is weaker than the Ru–C bond. All metal–carbon bonds are very

strong. The calculations predict that the BDE in the 16VE and 18VE complexes is >100 kcal mol^{-1}.

It is interesting to compare the calculated geometries and bond energies of the carbon complexes **16TMC** and **17TMC** with the results for the corresponding carbonyl complexes **16TMCO**

and **17TMCO**. Fig. 17 gives for the latter species experimental data of the bond lengths and angles which show that the calculated values are quite accurate. The metal–CO bonds in **16TMCO** and **17TMCO** are significantly longer and weaker than the metal–C bonds in **16TMC** and **17TMC**. Table 11 shows that the calculated BDEs of the CO ligand in the former complexes are between D_e = 38.2 kcal mol^{-1} (**16FeCO**) to 55.3 kcal mol^{-1} (**17RuCO**) which is much less than the BDEs of the metal–C bonds. Note that the trend of the calculated values for the dissociation energies of the carbonyl complexes **16FeCO** < **16RuCO** and **17FeCO** > **17RuCO** is the same as for the carbon complexes **16TMC** and **17TMC**. The 16VE iron complexes have weaker bonds than the 16VE ruthenium complexes while in the 18VE complexes iron binds stronger than ruthenium. A comparison of the metal–ligand bond lengths in the carbonyl complexes **16TMCO** and **17TMCO** with the carbon complexes **16TMC** and **17TMC** indicates that the substitution of the equatorial CO ligand in the former compounds by a carbon ligand elongates the axial but particularly the other equatorial metal–ligand bonds.

Fig. 18 shows the optimized geometries of the carbon complexes [(CO)$_4$TM(C)] (**18RuC** and **18FeC**) and the pentacarbonyls [TM(CO)$_5$] (**18RuCO** and **18FeCO**).[75] As noted before, the carbon ligand in **18RuC** and **18FeC** is in the axial position. The equatorial forms of the latter compounds are not minima on the PES. The TM–C bonds in **18RuC** and **18FeC** are much shorter and possess a significantly higher BDE (Table 11) than the TM–CO bonds in **18RuCO** and **18FeCO**. The weakening effect of the carbon ligand on the other CO ligands becomes obvious by the very large trans effect in **18RuC** and **18FeC**. The calculated Fe–CO$_{ax}$ bond in **18FeC** is very long (1.994 Å) while the interatomic Ru–CO$_{ax}$ distance in **18RuC** (2.477 Å) suggests that the CO ligand is practically dissociated.

The central topic of the work by KPF[75] is the analysis of the [TM]–C bond and the comparison with the nature of the bonding in metal carbenes [TM]–CR$_2$, carbynes [TM]–CR and carbonyls [TM]–CO. Fig. 19 shows the shape of the most important occupied and vacant MOs of **16RuC** which provide via visual inspection a first impression of the nature of the ruthenium–carbon bond. Only those orbitals are displayed which have coefficients at Ru and the ligand carbon atom.

There are seven valence orbitals in **16RuC** which contribute to the [Ru]–C bond, two σ orbitals and five π orbitals. The HOMO − 3 (15a$_1$) and HOMO − 6 (14a$_1$) orbitals which come from the bonding and antibonding combination of the d$_{z^2}$ ruthenium orbital with the chlorine p(σ) lone-pair orbitals contribute to the Ru–C σ bond. Two orbitals, *i.e.* HOMO − 2 (10b$_1$) and HOMO − 9 (8b$_1$) MOs, describe the Ru–C π bonding in the Cl–Ru–Cl plane (π$_{\parallel}$). The HOMO − 8 (9b$_2$) orbital is a Ru–C π orbital in the P–Ru–P plane (π$_{\perp}$). The remaining π orbitals HOMO − 4 (9b$_1$) and HOMO − 5 (10b$_2$) have only small contributions at the carbon ligand atom. Fig. 19 shows also the three lowest lying vacant orbitals of **16RuC**. Note that the LUMO (16a$_1$), which has a small coefficient at C, is antibonding with respect to the Ru–C bond. This is important for understanding the changes in the bonding situation of the 18VE complexes where this orbital is occupied and becomes the HOMO. The π orbitals LUMO + 1

(12b$_2$) and LUMO + 2 (11b$_1$) and the occupied σ orbital HOMO − 3 (15a$_1$) are perfectly suited to serve as ligand orbitals for binding of **16RuC** to another transition metal fragment. As noted above, the complex [**16RuC**–**Mo(CO)$_5$**] where **16RuC** binds with Mo(CO)$_5$ through the carbon atom has been synthesized.[71]

It is interesting to compare the frontier orbitals of the 16VE carbon complex [(PMe$_3$)$_2$Cl$_2$Ru(C)] (**16RuC**) with the most relevant MOs of the 18VE species [(PMe$_3$)$_2$(CO)$_2$Ru(C)] (**17RuC**) and with the corresponding CO 16VE complex [(PMe$_3$)$_2$Cl$_2$Ru(CO)] (**16RuCO**) as well as the 18VE complex [(PMe$_3$)$_2$(CO)$_2$Ru(CO)] (**17RuCO**). Fig. 20 shows that the HOMO of the 18VE species **17RuC** and **17RuCO** closely resembles the LUMO of the respective 16VE complexes **16RuCO** and **16RuC** (Fig. 19). The occupation of the Ru–C and Ru–CO antibonding orbital explains why the bonds in the 18VE compounds are clearly longer than in the 16VE homologues.

Table 12 summarizes the results of a charge-partitioning analysis of the carbon and CO complexes **16TMC**–**18TMC** and **16TMCO**–**18TMCO** which shed further light on the bonding situation. The calculated values for P(TM-L) suggest that the TM–C bonds have a clearly higher bond order than the TM–CO

17RuC

HOMO 17a$_1$
(−3.56)

16RuCO

LUMO 17a$_1$
(−3.00)
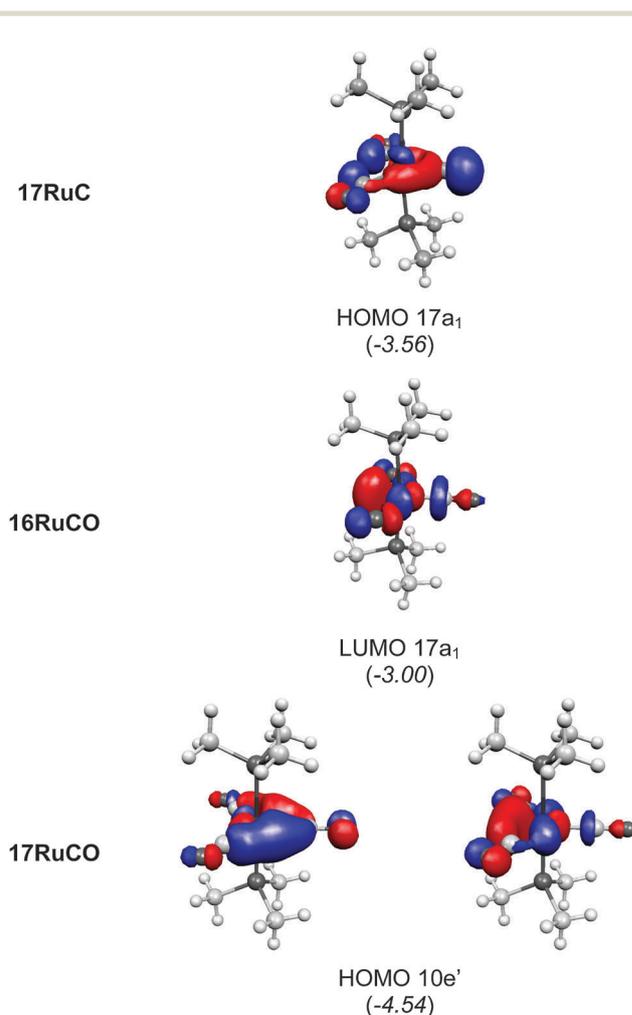
17RuCO

HOMO 10e'
(−4.54)

Fig. 20 Plot of some relevant molecular orbitals of **17RuC**, **16RuCO** and **17RuCO**. The calculated eigenvalues (BP86/TZ2P) of the orbitals are given in parentheses (in eV).[75] The figure has been adapted from ref. 75.

This journal is © The Royal Society of Chemistry 2014

Chem. Soc. Rev., 2014, **43**, 5106–5139 | **5125**

Chem Soc Rev

Review Article

Table 12 Calculated Wiberg bond orders P(TM–C) and NBO partial charges q of the complexes **16TM–21TM** at BP86/TZVPP[75]

Molecule	No.	P(TM–C)	q(TM)	q(C)	q(CO)
Cl$_2$(PMe$_3$)Ru−C	**16RuC**	2.1	−0.08	0.04	—
Cl$_2$(PMe$_3$)Fe−C	**16FeC**	2.0	−0.19	0.12	—
(CO)$_2$(PMe$_3$)Ru−C	**17RuC**	1.6	−0.38	−0.23	—
(CO)$_2$(PMe$_3$)Fe−C	**17FeC**	1.4	−0.63	−0.19	—
Cl$_2$(PMe$_3$)Ru−CO	**16RuCO**	1.4	−0.12	—	0.09
Cl$_2$(PMe$_3$)Fe−CO	**16FeCO**	1.2	−0.07	—	0.08
(CO)$_2$(PMe$_3$)Ru−CO	**17RuCO**	0.8	−0.47	—	−0.14
(CO)$_2$(PMe$_3$)Fe−CO	**17FeCO**	0.7	−0.65	—	−0.10
(CO)$_4$Ru−C	**18RuC**	1.8	−0.20	0.04	—
(CO)$_4$Fe−C	**18FeC**	1.5	−0.30	−0.02	—
(CO)$_4$Ru−CO$_{eq}$	**18RuCO**	0.7	−0.32	—	0.02
(CO)$_4$Fe−CO$_{eq}$	**18FeCO**	0.6	−0.58	—	0.08

bonds. Not surprisingly, the 16VE complexes have larger bond orders for the TM–L bonds than the 18VE species. The carbon and CO ligands carry a small positive charge in the 16VE complexes but they are negatively charged in the 18VE species. This indicates that the donor/acceptor ratio of the ligands L = C, CO in the 16VE complexes changes towards more [TM]←L net donation. The latter donation does not reside at the metal atoms. Table 12 shows that the metal atoms in the 16VE complexes are less negatively charged than in the 18VE compounds. The stronger [TM]←L net donation in the former species is conveyed to the CO ligands. We want to point out that the partial charges of the carbon and CO ligands in the 16 and 18VE compounds are not very different from each other. The question remains about the correct description of the [TM]–C

interactions. A very detailed answer to this question was given by the EDA results of KPF[75] which shall now be summarized.

What is the best description for the metal–ligand orbital interactions in the carbon complexes [(PR$_3$)$_2$Cl$_2$Ru(C)], which have been synthesized by Heppert *et al.*? Fig. 21 shows five different scenarios which are possible for the [TM]–C interactions. Model A sketches the situation which was already mentioned above for (CO)$_2$Fe–C. Here, the carbon atom in the ^{1}D excited state serves as two-electron σ donor while the empty p(π) AOs serve as π acceptors. This is the classical DCD bonding model which is valid for the bonding for metal–CO and Fischer-type metal–carbyne bonds. Model E describes the bonding in terms of three electron-sharing interactions which yield one σ-bond and two π-bonds. The latter description applies to Schrock-type metal carbynes which are better termed metal alkylidynes. Note that the two π bonds in the donor–acceptor model A and the electron-sharing model E are not the same. This is because the ligands in the two planes are different. The plane which contains the chlorine ligands is designated as π$_∥$ while the plane containing the phosphane ligands is designated as π$_⊥$ (see Fig. 21). The orbital models B, C and D describe intermediate cases where one bonding component comes from donor–acceptor interactions while the other two come from electron-sharing bonding.

The EDA results which are given in Table 13 make it possible to quantitatively estimate the strength of the different orbital interactions which are shown in Fig. 21. The EDA data refer to the instantaneous interactions between the carbon atom and the metal fragment (PMe$_3$)$_2$Cl$_2$Ru which are calculated with the frozen geometry in the complex **16RuC**. Five EDA calculations
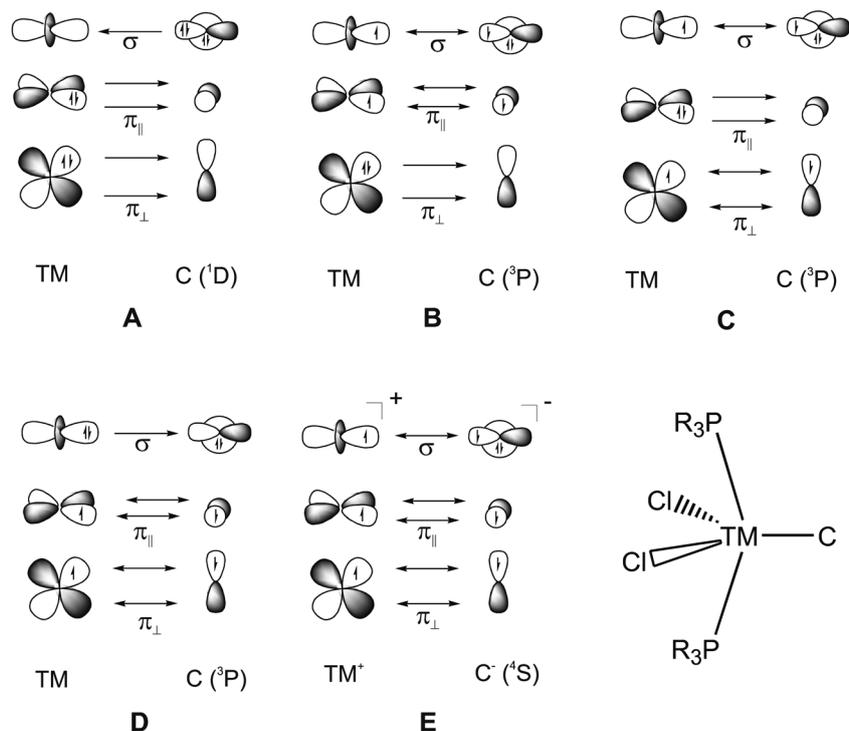

Fig. 21 Schematic representation of the electron configurations for the interacting fragments **A–E** which are used in the EDA calculations of [(PMe$_3$)$_2$Cl$_2$Ru(C)] (**16RuC**) (Table 13).

5126 | *Chem. Soc. Rev.*, 2014, **43**, 5106–5139

This journal is © The Royal Society of Chemistry 2014

Table 13 Energy decomposition analysis at BP86/TZ2P of the ruthenium–carbon bond in the complex **16RuC** using different fragment pairs A–E as shown in Fig. 21. All energies in kcal mol^{-1} [75]

Fragment	A	B	C	D	E
ΔE_{int}	−245.0	−170.4	−197.9	−183.4	−306.9
ΔE_{Pauli}	499.1	429.1	437.4	366.0	526.5
ΔE_{Elstat}[a]	−410.0 (55.1%)	−289.9 (48.4%)	−301.4 (47.4%)	−183.1 (33.3%)	−493.9 (59.3%)
ΔE_{Orb}[a]	−334.1 (44.9%)	−309.6 (51.6%)	−333.9 (52.6%)	−366.3 (66.7%)	−339.6 (40.7%)
$\Delta a_1(\sigma)$[b]	−140.1 (41.9%)	−142.0 (45.9%)	−144.9 (43.4%)	−210.5 (57.5%)	−146.6 (43.2%)
$\Delta a_2(\delta)$[b]	−0.2 (0.1%)	−0.3 (0.1%)	−0.3 (0.1%)	−0.4 (0.1%)	−1.7 (0.5%)
$\Delta b_1(\pi_\parallel)$[b]	−105.1 (31.5%)	−75.4 (24.4%)	−108.6 (32.5%)	−75.2 (20.5%)	−90.5 (26.7%)
$\Delta b_2(\pi_\perp)$[b]	−88.8 (26.6%)	−91.9 (29.7%)	−80.2 (24.0%)	−80.3 (21.9%)	−100.8 (29.7%)
ΔE_{Prep}	98.5	23.9	51.4	36.9	160.4
$-D_e$	−146.5	−146.5	−146.5	−146.5	−146.5

[a] The value in parentheses gives the percentage contribution to the total attractive interactions ($\Delta E_{Elstat} + \Delta E_{Orb}$). [b] The value in parentheses gives the percentage contribution to the total orbital interactions.

were carried out where the electron configurations of the fragments are chosen in accordance with models A–E.[75] Since **16RuC** has C_{2v} symmetry there are orbitals with $a_1(\sigma)$, $a_2(\delta)$, $b_1(\pi_\parallel)$ and $b_2(\pi_\perp)$ symmetry which directly relate the calculated values for the orbital terms with the respective orbital interactions that are shown in Fig. 21. But which of the models A–E gives the best description for the orbital interactions in **16RuC**? The answer is given by the absolute values of the total orbital interaction term ΔE_{orb}. Those fragment pairs whose orbital relaxation in the final step of the EDA gives the smallest ΔE_{orb} value provide the best description of the interacting species because their electronic structure is closest to the bonding situation in the molecule after bond formation.

Table 13 shows that the best model for the $(PMe_3)_2Cl_2Ru–C$ bond formation is given by the fragment pair B. According to this model, the metal–carbon bond in **16RuC** is a mixture of electron-sharing interactions and donor–acceptor bonding. This makes sense because **16RuC** has electron-sharing Ru–Cl bonds as well as donor–acceptor Ru–PR$_3$ bonds. Model B suggests that the Ru–C bond has about one half electrostatic character and one half covalent character. This comes from the EDA values for ΔE_{elstat} and ΔE_{orb} which contribute 48.4% and 51.6% to the total

attractive interactions. The orbital interactions ΔE_{orb} come mainly from the electron-sharing σ bond (45.9%). The electron-sharing $\pi_\parallel$ bond contributes 24.4% which is somewhat weaker than the donor–acceptor $\pi_\perp$ bond which contributes 29.7% to ΔE_{orb}. The occurrence of two electron-sharing interactions which comprise one σ and one π bond in the bonding model B (Fig. 21) suggest **16RuC** and thus, the isolated carbon complexes[2,68,69] are actually Ru(IV) and Os(IV) compounds.

The EDA calculations of the complexes **17RuC**–**18RuCO** revealed that the Ru–C and Ru–CO bonds are better described by model A than model B, because the absolute values for ΔE_{orb} were slightly lower when the former pair of interacting fragments was employed.[75] It is therefore appropriate to compare the bonding interactions between the [Ru]–C and [Ru]–CO bonds using the EDA results for model A. Since the carbon and CO ligands in **16RuC**–**17RuCO** are in the equatorial position, KPF optimized $(CO)_4RuC$ (**18RuC**) where C is equatorial (**18RuC-eq**) and analyzed the equatorial Ru–C bond with the EDA method. Structure **18RuC-eq** is a transition state but it is the appropriate species for comparison with the equatorial Ru–C and Ru–CO bonds of the other species.

Table 14 shows the EDA results using model A for the equatorial Ru–C and Ru–CO bonds of **16RuC**–**18RuCO**. Note that the

Table 14 Energy decomposition analysis at BP86/TZ2P of the equatorial Ru–C and Ru–CO bonds in the complexes **16RuC**–**18RuCO** using model A (Fig. 21). All energies in kcal mol^{-1} [75]

Molecule Bond	16RuC Ru–C	16RuCO Ru–CO	17RuC Ru–C	17RuCO Ru–CO	18RuC Ru–C	18RuCO Ru–CO
ΔE_{int}	−245.0	−98.1	−184.1	−52.4	−159.2	−42.3
ΔE_{Pauli}	499.1	211.8	461.1	207.2	421.9	181.0
ΔE_{Elstat}[a]	−410.0 (55.1%)	−154.5 (49.9%)	−378.5 (58.7%)	−144.6 (55.7%)	−342.2 (58.9%)	−127.3 (57.0%)
ΔE_{Orb}[a]	−334.1 (44.9%)	−155.4 (50.1%)	−266.7 (41.3%)	−115.0 (44.3%)	−238.9 (41.1%)	−96.0 (43.0%)
$\Delta a_1(\sigma)$[b]	−140.1 (41.9%)	−68.5 (44.1%)	−95.5 (35.8%)	−48.8 (42.4%)	−101.1 (42.3%)	−49.5 (51.6%)
$\Delta a_2(\delta)$[b]	−0.2 (0.1%)	−0.1 (0.1%)	−0.1 (0.0%)	0.0 (0.0%)	−0.1 (0.0%)	0.0 (0.0%)
$\Delta b_1(\pi_\parallel)$[b]	−105.1 (31.5%)	−46.7 (30.1%)	−105.4 (39.5%)	−39.4 (34.3%)	−91.9 (38.5%)	−29.8 (31.0%)
$\Delta b_2(\pi_\perp)$[b]	−88.8 (26.6%)	−40.1 (25.8%)	−65.7 (24.6%)	−26.8 (23.3%)	−45.8 (19.2%)	−16.7 (17.4%)
ΔE_{Prep}	98.5	53.5	83.3	12.1	75.5	9.8
$-D_e$	−146.5	−44.6	−100.8	−40.3	−83.7	−32.5

[a] The value in parentheses gives the percentage contribution to the total attractive interactions ($\Delta E_{Elstat} + \Delta E_{Orb}$). [b] The value in parentheses gives the percentage contribution to the total orbital interactions.

This journal is © The Royal Society of Chemistry 2014

Chem. Soc. Rev., 2014, 43, 5106–5139 | 5127

equatorial isomer of $(CO)_4ReC$ (**18RuC-eq**) which is 5.2 kcal mol^{-1} higher in energy than axial **16RuC-ax** is not a minimum on the potential energy surface.[75] Since the comparison is made for equatorial ligands, **18RuC-eq** must be used as the appropriate isomer. The comparison of the 16VE complex pair **16RuC–16RuCO** and the 18VE pairs **17RuC–17RuCO** as well as **18RuC–18RuCO** suggests that the interaction energies of the Ru–C bonds in the carbon complexes **16RuC**, **17RuC** and **18RuC** are much stronger than those of the Ru–CO bonds in **16RuCO**, **17RuCO** and **18RuCO**. This comes from a rather uniform increase of all attractive components of ΔE_{int}: *The carbon ligand is a much stronger σ donor as well as a better π acceptor as CO.* The σ-donor/π-acceptor ratio is shifted toward greater σ-donor strength and less π acceptor strength of C compared with CO but the overall nature of the Ru–C and Ru–CO bonds does not change dramatically. The EDA results shed light on the question why the 18VE complex **17RuC** could not become isolated while the 16VE complex **16RuC** is stable in the condensed phase. A comparison of the EDA results using the same model A for both complexes shows (Tables 10 and 11) that the [Ru]–C binding interactions in **17RuC** are much weaker than in **16RuC** mainly because the $a_1(\sigma)$ contribution which comes from the [Ru]←C donation in the 18VE species is significantly smaller than in the 16VE compound. The much weaker Ru–C

σ bonding in **17RuC** can be explained with the occupation of the σ antibonding LUMO ($16a_1$) of **16RuC** (Fig. 19) which becomes the HOMO in **17RuC** (Fig. 20).

Table 15 Calculated bond dissociation energies D_e at BP86/TZ2P of carbon and CO complexes. NBO partial charges $q(L)$ of the ligands L = [TM]C, OC. Energy values in kcal mol^{-1}[78]

Bond	D_e	$q(L)$
$(PMe_3)_2Cl_2RuC–Cr(CO)_5$	41.6	0.29
$(PMe_3)_2Cl_2RuC–Mo(CO)_5$	38.9	0.20
$(PMe_3)_2Cl_2RuC–W(CO)_5$	45.3	0.17
$(PMe_3)_2Cl_2FeC–W(CO)_5$	45.1	0.15
$(PMe_3)_2Cl_2OsC–W(CO)_5$	47.1	0.20
$(PMe_3)_2F_2RuC–W(CO)_5$	39.7	0.21
$(PMe_3)_2Br_2RuC–W(CO)_5$	44.8	0.16
$(PMe_3)_2I_2RuC–W(CO)_5$	44.3	0.15
$(Por)FeC–W(CO)_5$	52.6	0.09
$(Por)RuC–W(CO)_5$	51.6	0.14
$(Por)OsC–W(CO)_5$	53.8	0.17
$(PMe_3)_2Cl_2RuC–BH_3$	47.0	0.43
$(PMe_3)_2Cl_2RuC–BCl_3$	13.5	0.51
$OC–Cr(CO)_5$	43.2	0.28
$OC–Mo(CO)_5$	39.6	0.18
$OC–W(CO)_5$	45.7	0.13
$OC–BH_3$	42.6	0.39
$OC–BCl_3$	−6.8	0.38

(a) CO
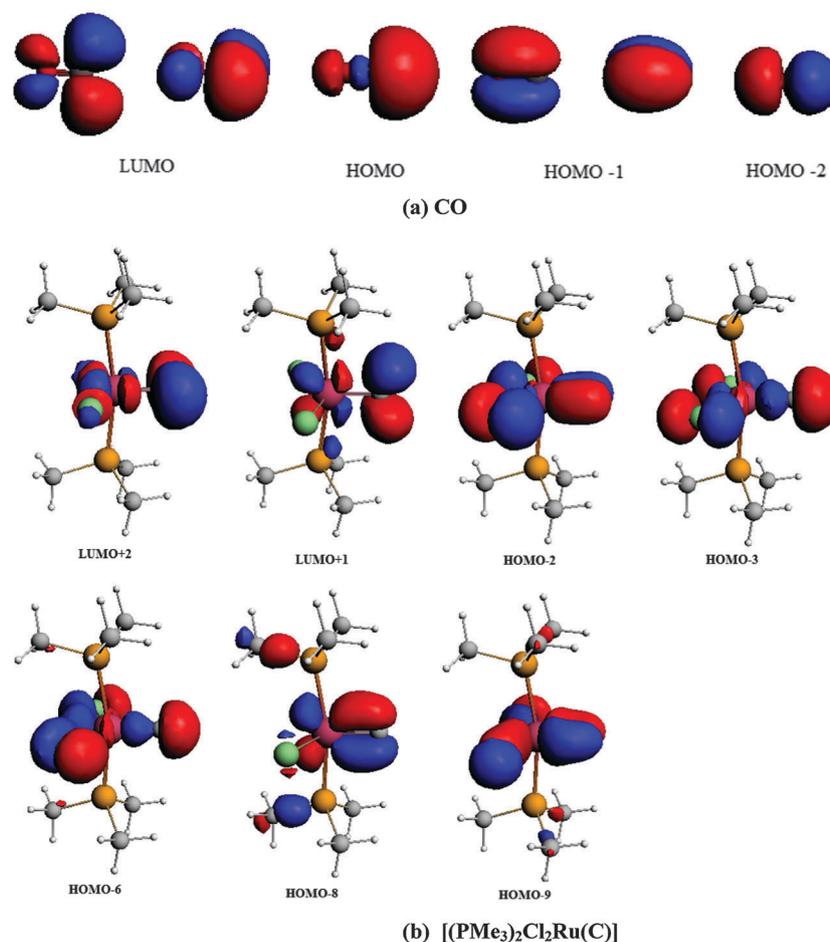
(b) [(PMe$_3$)$_2$Cl$_2$Ru(C)]

Fig. 22 Plot of the frontier orbitals of CO and [(PMe$_3$)$_2$Cl$_2$Ru(C)].

The metal–carbon bonding situation in $[(PR_3)_2Cl_2Ru(C)]$ is very similar to the bonding in CO. This finding was pointed out by KPF[75] and also by Johnson and co-workers[74] in their theoretical studies of carbon complexes. The isolobal[77] relationship between carbon complexes and carbon monoxide was the topic of a very detailed theoretical work by Krapp and Frenking (KF).[78] These workers calculated the group-8 carbon complexes $[(L)_2X_2TM(C)]$ for various combinations where L = PH$_3$, PMe$_3$, PPh$_3$, PCy$_3$, NHC and X = F, Cl, Br, I with the metals TM = Fe, Ru, Os which are related to the complexes that have been isolated so far.[2,68,69] They also investigated the iron–porphyrin complexes with carbon ligands $[(Por)TM(C)]$ (TM = Fe, Ru, Os; Por = Porphyrin) for which adducts with the Lewis acid Ru$_2$(CO)$_9$ were reported by Beck and co-workers.[73] KF calculated the carbon complexes $[(L)_2X_2TM(C)]$ and $[(Por)TM(C)]$ as well as the adducts with the Lewis acids BH$_3$, BCl$_3$, PdCl$_2$SMe$_2$ and TM(CO)$_5$ (TM = Cr, Mo, W). The latter structures were compared with the corresponding carbonyl complexes. In order to test whether the carbon complexes can also serve as bridging ligands like CO, the authors calculated the complex $[Fe_2(CO)_9]$ and the analogues molecule $[RuCl_2(PMe_3)_2(C)–Fe_2(CO)_8]$ where the carbon compound $[RuCl_2(PMe_3)_2(C)]$ binds in the η^2-coordination mode. The bonding situation in the compounds was investigated with charge- and energy decomposition methods.[78] The most important result will shortly be summarized.

Table 15 shows the calculated bond dissociation energies (BDEs) D_e of carbon and CO complexes $[L–TM(CO)_5]$ (TM = Cr, Mo, W) and the partial charges $q(L)$ of the ligands. It becomes obvious that the BDEs of $[(PMe_3)_2Cl_2Ru(C)–TM(CO)_5]$ are nearly the same as for the respective carbonyl adduct $[OC–TM(CO)_5]$ and that the partial charges of the L = and the partial charges of the ligands L = $[(PMe_3)_2Cl_2Ru(C)]$ have nearly the same values as for L = OC. The calculated values for the porphyrin substituted carbon complexes $[(Por)TM(C)–W(CO)_5]$ (TM = Fe, Ru, Os) indicate somewhat stronger bonds than the other adducts. The carbon complexes $[(PMe_3)_2Cl_2Ru(C)]$ bind a bit stronger to the main group Lewis acids BH$_3$ and BCl$_3$ than CO. The theoretical data support the suggestion that $[(PMe_3)_2Cl_2Ru(C)]$ and OC have similar ligand properties.

Fig. 22 shows the most important frontier orbitals of $[(PMe_3)_2Cl_2Ru(C)]$ and CO. The similarities in the shape of the occupied σ- and π-bonding orbitals and the vacant π* orbitals, which may serve as donor and acceptor orbitals are striking. Fig. 23 displays a selected set of complexes where $[(PMe_3)_2Cl_2Ru(C)]$ and CO are bonded as ligands to the Lewis acids (LAs) W(CO)$_5$, PdCl$_2$SMe$_2$, Fe$_2$(CO)$_8$, BH$_3$ and BCl$_3$. The structures of the complexes are very similar. The complex $[(PMe_3)_2Cl_2RuC–Fe_2(CO)_8]$ is a minimum on the PES which shows that the carbon complex like CO may bind in an η^2-fashion to the Fe$_2$(CO)$_8$. A closer examination of the donor–acceptor bonds in $[(PMe_3)_2Cl_2RuC–LA]$ and $[OC–LA]$ reveals that the carbon complexes exhibit slightly longer C–LA bonds than CO (Fig. 23).

The strongly isolobal relationship between CO and the carbon complexes $[TM]C$ becomes clearly apparent by comparing the EDA results for transition metal complexes which carry CO and $[TM]C$ as ligands. Table 16 shows the EDA results for
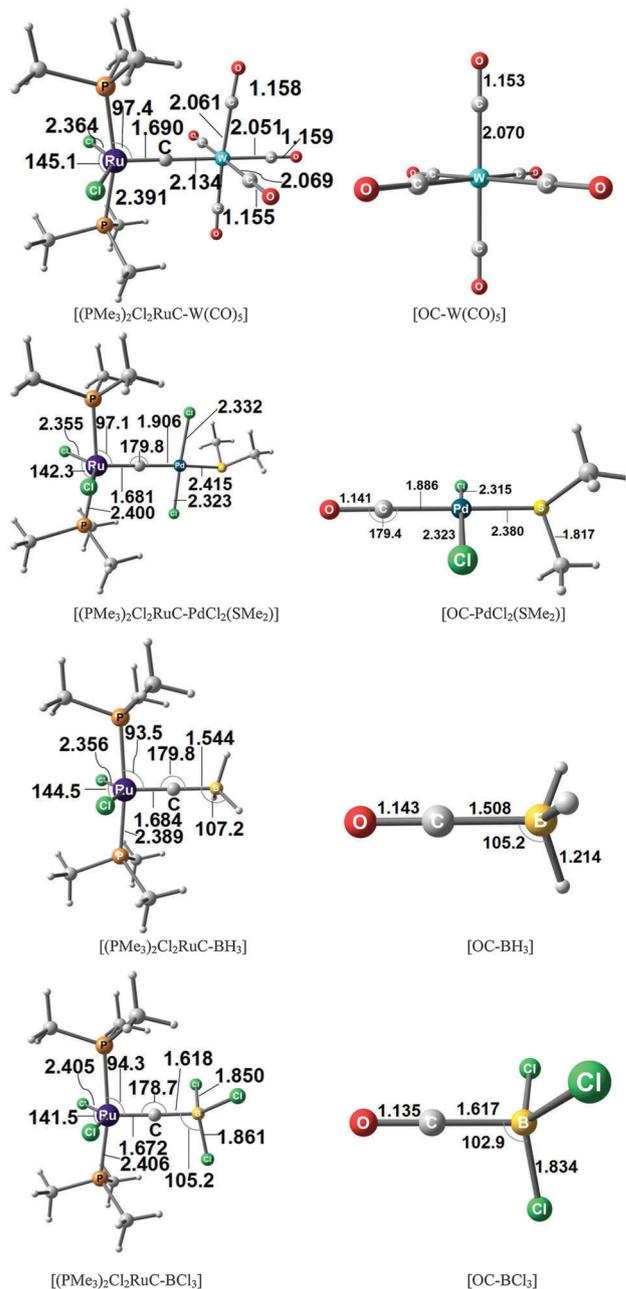
Fig. 23 Optimized geometries (BP86/TZVPP) of some carbon and carbonyl complexes. Bond lengths are given in Å, angles in degree.[78] The figure has been adapted from ref. 78.

complexes L–W(CO)$_5$ where L = $[TM]C$ and CO. Four different ligands $[TM]C$ have been chosen, namely $[(PMe_3)_2Cl_2Fe(C)]$, $[(PMe_3)_2Cl_2Ru(C)]$, $[(PMe_3)_2Cl_2Os(C)]$ and the porphyrin species $[(Por)RuC]$. The calculated data for the different energy terms show the great similarity between $[TM]C$ and CO. The calculated values for the total interaction energy ΔE_{int} between the ligands L and the metal fragment W(CO)$_5$ are very similar. In particular the ΔE_{int} values for the model phosphane ligand (PMe$_3$)$_2$TMCl$_2$ differ by only ∼1 kcal mol^{-1} from the data for CO. The percentage contributions of electrostatic attraction ΔE_{elstat} and orbital

Table 16 Energy decomposition analysis of complexes L−W(CO)$_5$ where L = [TM]C and CO at BP86/TZ2P//BP86/TZVPP. Energies in kcal mol^{-1}[78]

	(PMe$_3$)$_2$Cl$_2$FeC−W(CO)$_5$	(PMe$_3$)$_2$Cl$_2$RuC−W(CO)$_5$	(PMe$_3$)$_2$Cl$_2$OsC−W(CO)$_5$	(Por)RuC−W(CO)$_5$	OC−W(CO)$_5$
ΔE_{int}	−50.9	−49.7	−51.1	−56.2	−49.7
ΔE_{Pauli}	116.8	110.0	112.2	128.7	118.6
$\Delta E_{Elstat}{}^a$	−89.1 (53.1%)	−85.8 (53.7%)	−92.2 (56.5%)	−99.2 (53.7%)	−89.7 (53.3%)
$\Delta E_{Orb}{}^a$	−78.6 (46.9%)	−73.9 (46.3%)	−71.1 (43.5%)	−85.6 (46.3%)	−78.6 (46.7%)
$\Delta E(\sigma)^b$	−49.2 (62.6%)	−45.8 (62.0%)	−45.5 (63.9%)	−49.3 (57.5%)	−36.3 (46.1%)
$\Delta E(\pi)^b$	−29.4 (37.4%)	−28.1 (38.0%)	−25.7 (36.1%)	−36.4 (42.5%)	−42.3 (53.9%)

^{a} Values in parentheses give the percentage contribution to the total attractive interaction ($\Delta E_{Elstat} + \Delta E_{Orb}$). ^{b} Values in parentheses give the percentage contribution to the total orbital interaction (ΔE_{Orb}).

(covalent) interactions ΔE_{orb} to the total attraction of the metal–carbon ligands are also quite similar to the results for CO. The most significant difference concerns the ratio of σ-donation/π-backdonation. The EDA results suggest that $(CO)_5W \rightarrow CO$ π-backdonation is a bit stronger than $(CO)_5W \leftarrow CO$ σ-donation. The opposite trend is calculated for the metal–carbon complexes where the $(CO)_5W \leftarrow C[TM]$ σ-donation is clearly stronger than $(CO)_5W \rightarrow C[TM]$ π-backdonation.[78]

5. Transition metal–tetrele complexes [TM]−E (E = Si, Ge, Sn)

The first purposeful synthesis of a transition metal carbene complex in 1964 by Fischer[57,58] was soon followed by experimental research with the aim to isolate the heavier group-14 homologues [TM]=ER$_2$ (E = Si–Pb).[79] The first examples of stannylene and plumbylene complexes were reported in 1976 by Lappert and co-workers.[80] One year later, the first transition metal complex with a germylene ligand could become isolated by the same group.[81] The first (unsupported)[82] silylene complex which was structurally characterized by X-ray analysis was reported in 1990 by Tilley.[83] Table 17 shows an overview of the first syntheses of transition metal carbene and carbyne complexes and heavier group-14 homologues. We want to point

out that unlike the lighter homologues, until today no X-ray structure for a plumbylene complex has been reported.

A similar time-delayed history exists for the experimental attempts to synthesis the heavy group-14 homologues of transition metal carbyne complexes.[84] Following the first synthesis of a carbyne complex by Fischer in 1973,[59] the next member in the series which could become characterized by X-ray analysis was a germylyne complex which was reported by Power in 1996.[85] The other three members of the group of heavier carbyne homologues for which X-ray structure analyses have been synthesized by Filippou. The first isolation of a stannylene complex in 2003[86] was followed by the first synthesis of a plumbylyne complex in 2004.[87] Very recently, the first X-ray structure analysis of a silylyne complex was reported by Filippou.[88] It is foreseeable that the first synthesis of a carbon complex by Heppert[2] in 2002 also triggers intensive efforts to isolate the heavier group-14 homologues [TM]–E. Until today, all attempts have not been successful. This is not surprising when one looks at the history of carbyne homologues where it took 23 years after the work of Fischer before the first heavier homologue could be isolated (Table 17).

Theoretical studies have been published which could be helpful as a guideline for further experimental work. The geometries and bonding situation of the heavier homologues of the model carbon complex [(PMe$_3$)$_2$Cl$_2$TM(E)] (**16TME**) with TM = Fe, Ru, Os and E = Si, Ge, Sn has been the topic of a

Table 17 Transition metal complexes with multiply bonded terminal group-14 ligands [TM]=ER$_2$, [TM]≡ER and [TM]≡E (E = C–Pb). Literature survey of the first examples of neutral species which – except for the plumbylene complex – were structurally characterized by X-ray analysis

E	[TM]=ER$_2$	[TM]≡ER	[TM]≡E
C	E. O. Fischer and A. Maasböl, *Angew. Chem.*, 1964, **76**, 645; *Angew. Chem., Int. Ed. Engl.*, 1964, **3**, 580.	E. O. Fischer, G. Kreis, C. G. Kreiter, J. Müller, G. Huttner and H. Lorenz, *Angew. Chem.*, 1973, **85**, 618; *Angew. Chem., Int. Ed.*, 1973, **12**, 564.	R. G. Carlson, M. A. Gile, J. A. Heppert, M. H. Mason, D. R. Powell, D. V. Velde and J. M. Vilain, *J. Am. Chem. Soc.*, 2002, **124**, 1580.
Si	D. A. Straus, S. D. Grumbine, T. D. Tilley, *J. Am. Chem. Soc.*, 1990, **112**, 7801.	A. C. Filippou, O. Chernov, K. W. Stumpf and G. Schnakenburg, *Angew. Chem.*, 2010, **122**, 3368; *Angew. Chem., Int. Ed.*, 2010, **49**, 3296.	Unknown
Ge	M. F. Lappert, S. J. Miles, P. P. Power, A. J. Carty, N. J. Taylor, *J. Chem. Soc., Chem. Commun.*, 1977, 458.	R. S. Simons and P. P. Power, *J. Am. Chem. Soc.*, 1996, **118**, 11966.	Unknown
Sn	J. D. Cotton, P. J. Davidson and M. F. Lappert, *J. Chem. Soc., Dalton Trans.*, 1976, 2275.	A. C. Filippou, P. Portius, A. I. Philippopoulos and Rohde, H. *Angew. Chem.*, 2003, **115**, 461; *Angew. Chem., Int. Ed.*, 2003, **42**, 445	Unknown
Pb	J. D. Cotton, P. J. Davidson and M. F. Lappert, *J. Chem. Soc., Dalton Trans.*, 1976, 2275.^{a}	A. C. Filippou, H. Rohde and G. Schnakenburg, *Angew. Chem.*, 2004, **116**, 2293; *Angew. Chem., Int. Ed.*, 2004, **43**, 2243.	Unknown

^{a} No X-ray structure available.

16FeC
$D_e = 135.1$

16FeSi
$D_e = 77.1$

16FeGe
$D_e = 69.6$

16FeSn
$D_e = 53.4$

16RuC
$D_e = 146.5$

16RuSi
$D_e = 91.8$

16RuGe
$D_e = 82.4$

16RuSn
$D_e = 65.4$

16OsC
$D_e = 159.3$

16OsSi
$D_e = 102.1$

16OsGe
$D_e = 91.8$

16OsSn
$D_e = 73.3$

Fig. 24 Optimized geometries and TM–E bond dissociation energies D_e (BP86/TZ2P) of the 16VE tetrele complexes **16TME**. Bond lengths are given in Å, angles in degree, energies in kcal mol^{-1}.[89] The figure has been adapted from ref. 89.

quantum chemical investigation by Parameswaran and Frenking (PF1).[89] The most important results will shortly be summarized.

Fig. 24 shows the optimized geometries of the 16-electron tetrele complexes **16TME** and the calculated BDEs for the $(PMe_3)_2Cl_2TM$–E bonds with E = C–Sn. The carbon complexes are shown for comparison with the heavier homologues. It becomes obvious that the heavier tetrele complexes have weaker bonds than the lighter ones but even the stannylene complexes have BDEs which are >50 kcal mol^{-1} which indicates that the TM–Sn bonds are quite strong. The bond orders drops from 2.2 for the Os–C bond to 1.4 for the Fe–Sn

bond which suggests a sizeable multiple-bond character. PF1 calculated also the 18-electron complexes $[(PR_3)_2(CO)_2TM(E)]$ (**17TME**) which exhibit interesting differences compared with the 16-electron species **16TME**.[89] The optimized geometries and the calculated BDEs for the compounds **17TME** are shown in Fig. 25.

A comparison of the theoretically predicted TM-E bond lengths and bond orders of the 18-electron complexes **17TME** with the 16-electron species **16TME** reveals that the former molecules have always longer bonds and smaller bond orders than the latter species. The two series of complexes exhibit distinctively different trends for the bond dissociation energy of
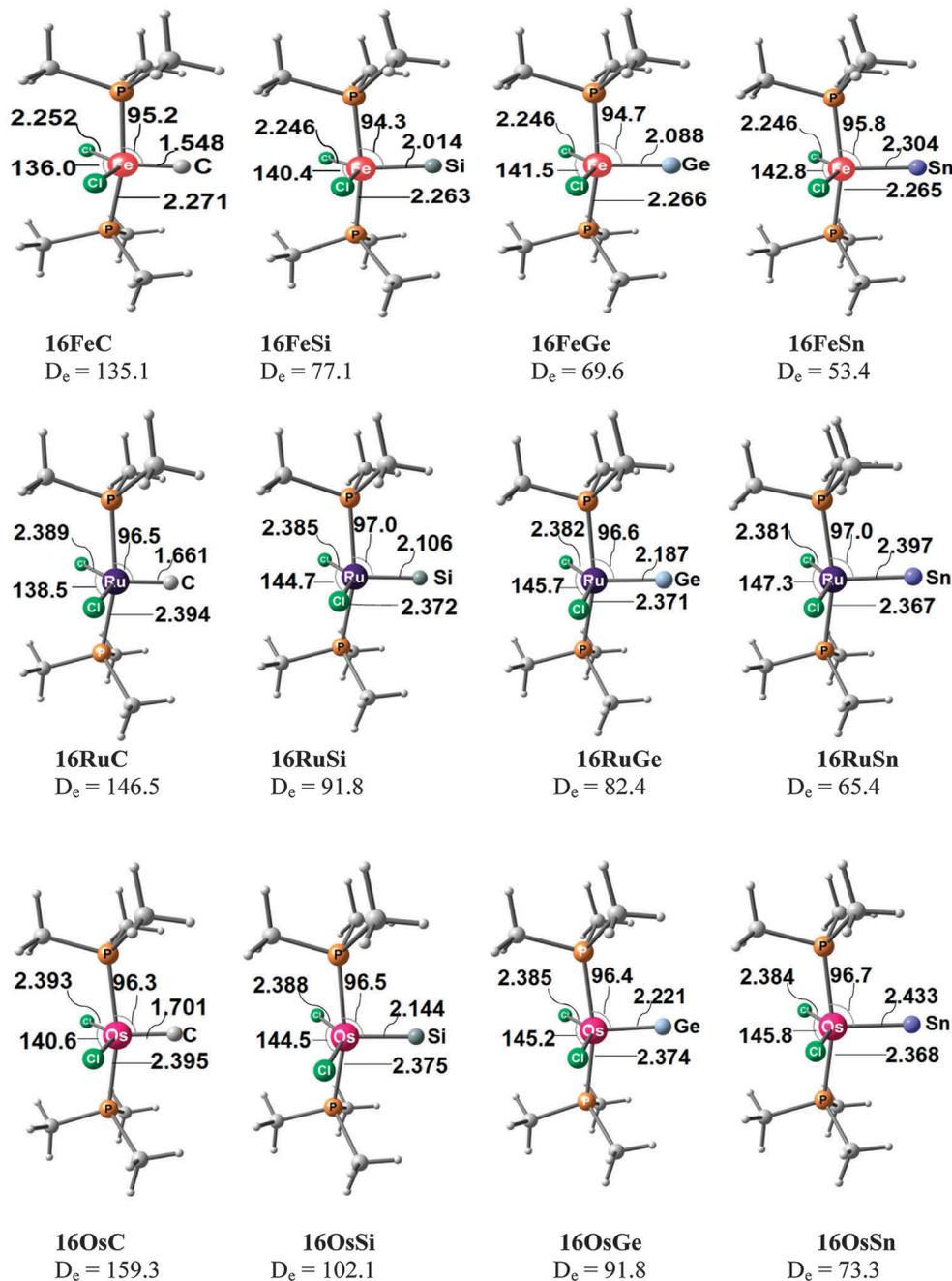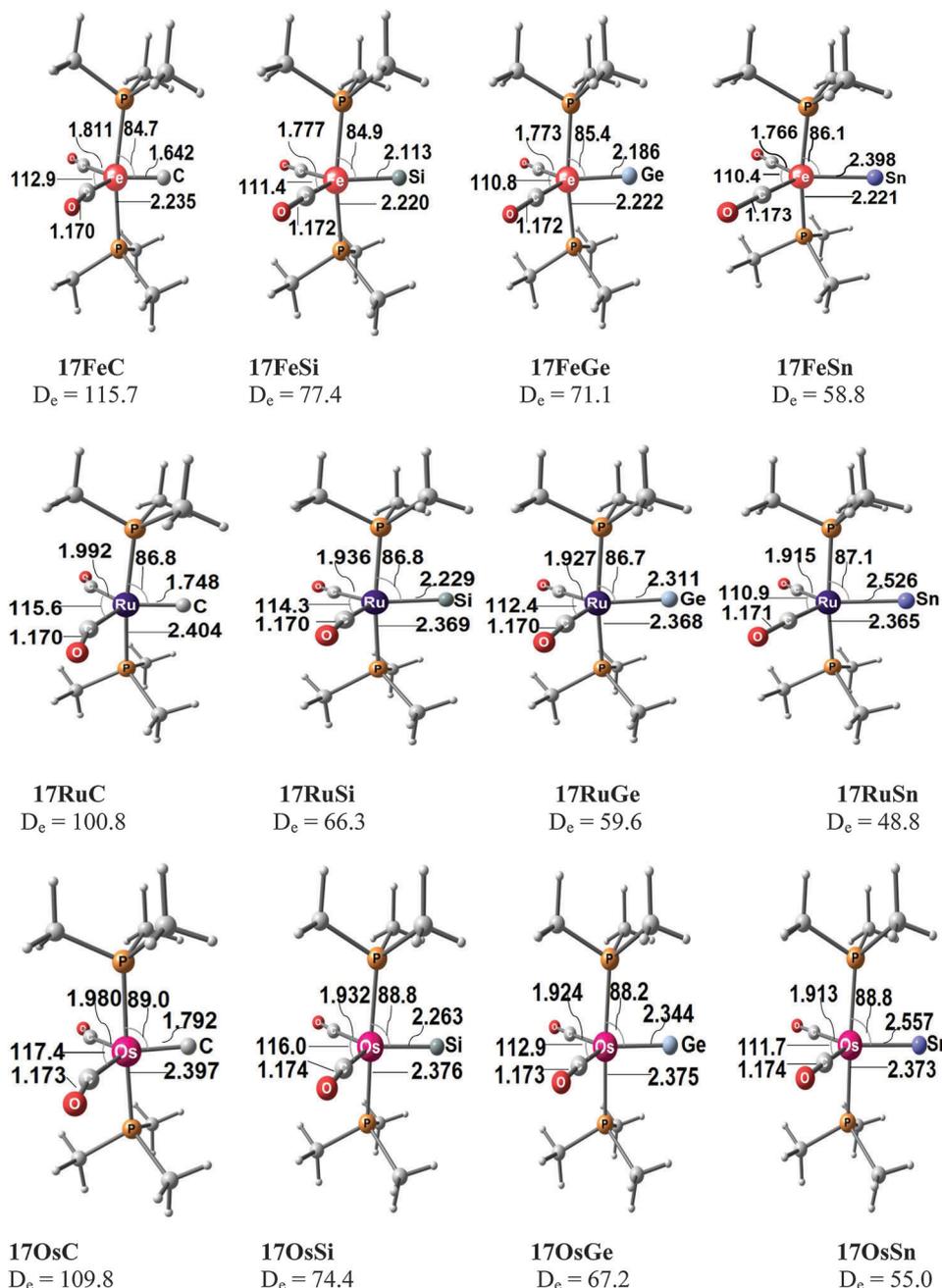
Fig. 25 Optimized geometries and TM–E bond dissociation energies D_e (BP86/TZ2P) of the 18VE tetrele complexes **17TME**. Bond lengths are given in Å, angles in degree, energies in kcal mol^{-1}.[89] The figure has been adapted from ref. 89.

the TM–E bond which are shown in Fig. 26. The BDEs of the 16-electron complexes **16TME** increase for the heavier transition metals in the order Fe < Ru < Os while the trend for the ligand atoms E is C ≫ Si > Ge > Sn. The latter trend is also calculated for the 18-electron complexes **17TME** but the transition metals exhibit the order Ru < Os < Fe. This is the well-known V-shaped sequence for the bond strength of the first, second and third row of transition metals.[63b] The calculations suggest that iron has the strongest TM–E bond in **17TME** while it has the weakest bond in **16TME**. This is an important result for experimental studies aiming at the synthesis of 18-electron complexes **17TME**.

The nature of the TM–E bond in **16TME** and **17TME** has been analyzed by PF1[89] with the EDA method in order to investigate the changes in the metal–ligand interactions when the tetrele atom becomes heavier. Table 18 shows the results for the ruthenium complexes. The data for the iron and osmium species which were reported by PF1 are not very different from the ruthenium complexes. EDA calculations using the interacting fragments according to bonding models A–E (Fig. 21) showed that the bonding situation in all 16-electron species **16TME** is best described by model B while the TM–E bond in the 18-electron complexes **17TME** can be described by the classical DCD model which is given by the fragment pair A.[75]
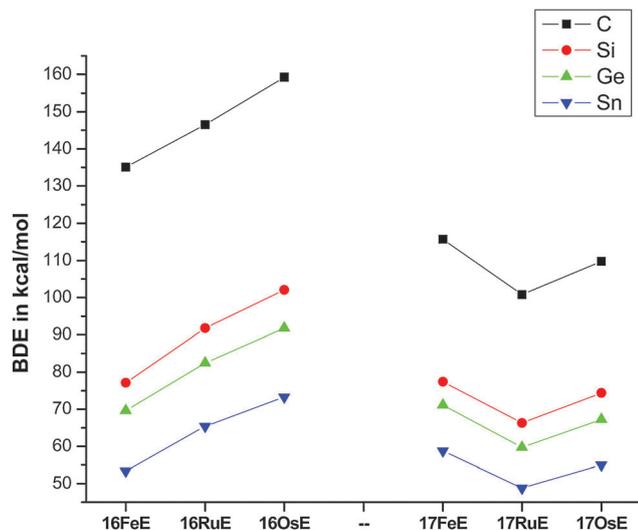
5132 | Chem. Soc. Rev., 2014, 43, 5106–5139

This journal is © The Royal Society of Chemistry 2014

Fig. 26 Trend of the calculated bond dissociation energies D_e (BP86/TZ2P) of the tetrele complexes **16TME** and **17TME**.[89]

The results in Table 18 indicate that the Ru–E bond in **16RuE** and **17RuE** is less covalent and has a higher electrostatic character when E = Si, Ge, Sn compared with the carbon complexes. The percentage π-backbonding [Ru]←E of the heavier atoms Si–Sn in the 18-electron complexes **17RuE** becomes smaller compared with **17RuC** which means that the heavier tetrele atoms Si, Ge, Sn are weaker π-acceptors than C. There is an interesting change in the weight of the two components $\Delta b_1(\pi_\parallel)$ and $\Delta b_2(\pi_\perp)$ to the π-backbonding [Ru]←E for **16RuE** and **17RuE**. Table 18 shows that the contribution of $\Delta b_1(\pi_\parallel)$ increases from **16RuE** to **17RuE** for each atoms E while the strength of $\Delta b_2(\pi_\perp)$ clearly decreases. The $\Delta b_1(\pi_\parallel)$ orbital interactions in **16RuE** come from the electron-sharing π bonds (see Fig. 21, model B) while the $\Delta b_1(\pi_\parallel)$ term in **17RuE** comes from the donor–acceptor π bonds (see Fig. 21, model A). The TM–C $\pi_\parallel$ interactions in **16RuE** compete with the strongly electron withdrawing TM–chlorine bonds while the TM–C $\pi_\parallel$ interactions in **17RuE** compete with TM–CO

π backdonation. As noted above, the carbon ligand is a much stronger π acceptor than CO. This explains why the $\Delta b_1(\pi_\parallel)$ contribution to the TM–C bond increases from **16RuE** to **17RuE**. Note that the intrinsic interaction energies ΔE_{int} in the 18VE complexes **17RuE** are larger than in the 16VE species **16RuE** (Table 18) but the BDEs of **17RuE** are clearly smaller than for **16RuE**. This comes from the significantly higher preparation energies ΔE_{prep} in the former species, because the atoms E are in the excited ^1D state in the EDA calculations using model A (Fig. 21).

In a second paper by Parameswaran and Frenking (PF2)[90] the authors calculated the structures of the adducts **16TME–W(CO)$_5$** and **17TME–W(CO)$_5$** where the tetrele complexes **16TME** and **17TME** are two-electron donor ligands. The nature of the E–W bonds was investigated with charge- and energy decomposition analyses and the results were compared with the E–W bonds in OE–W(CO)$_5$. The theoretical study could be helpful for the synthesis of the adducts which might be easier than isolating the free tetrele complexes.

Fig. 27 shows the optimized geometries of the complexes **16TME–W(CO)$_5$** which possess a linear coordination at the two coordinated tetrele atom C. A comparison with the structures of the free molecules **16TME** (Fig. 24) shows that the TM–E bonds become mostly longer in the adducts **16TME–W(CO)$_5$** but the bond lengthening gets smaller for the heavier atoms E and they become even shorter for the tin complexes and for **16OsGe–W(CO)$_5$**. The calculations predict that the TM–PMe$_3$ bonds become always slightly longer in **16TME–W(CO)$_5$** while the TM–Cl bonds become a bit shorter. The E–W distances in **16TME–W(CO)$_5$** may be compared with the calculated E–W bond lengths in OE–W(CO)$_5$ which are shown in Fig. 28. The theoretical data suggest that the OE–W bonds in the latter complexes are clearly shorter than the E–W distances in **16TME–W(CO)$_5$**.

The calculated bond energies indicate that the E–W bonds in **16TME–W(CO)$_5$** are rather strong. The theoretically predicted BDEs of the carbon complexes **16TMC–W(CO)$_5$** (D_e = 45.1–47.3 kcal mol^{-1}) have very similar values as the BDE of W(CO)$_6$ (D_e = 45.6 kcal mol^{-1}) while the heavier homologues **16TME–W(CO)$_5$** (E = Si–Sn) possess BDEs which are clearly larger than those of the respective molecule OE–W(CO)$_5$.

Table 18 EDA results at BP86/TZ2P of the Ru–E bond in the complexes **16RuE** using fragment pair B and **17RuE** using fragment pair A (see Fig. 21). All energies in kcal mol^{-1} [75]

	16RuC	16RuSi	16RuGe	16RuSn	17RuC	17RuSi	17RuGe	17RuSn
ΔE_{int}	−170.4	−113.0	−103.1	−85.9	−184.1	−117.1	−108.9	−93.0
ΔE_{Pauli}	429.1	276.4	248.8	211.9	461.1	311.9	271.9	237.5
ΔE_{Elstat} [a]	−289.9 (48.4%)	−222.0 (57.0%)	−202.9 (57.7%)	−178.2 (59.8%)	−378.5 (58.7%)	−287.1 (66.9%)	−250.8 (65.9%)	−222.9 (67.4%)
ΔE_{Orb} [a]	−309.6 (51.6%)	−167.4 (43.0%)	−149.0 (42.4%)	−119.6 (40.2%)	−266.7 (41.3%)	−141.9 (33.1%)	−129.9 (34.1%)	−107.6 (32.6%)
$\Delta a_1(\sigma)$ [b]	−142.0 (45.9%)	−79.9 (47.7%)	−73.0 (49.0%)	−61.2 (51.2%)	−95.5 (35.8%)	−66.7 (47.0%)	−62.8 (48.3%)	−55.5 (51.6%)
$\Delta a_2(\delta)$ [b]	−0.3 (0.1%)	−0.8 (0.5%)	−0.6 (0.5%)	−0.6 (0.5%)	−0.1 (0.0%)	−0.4 (0.3%)	−0.3 (0.2%)	−0.3 (0.3%)
$\Delta b_1(\pi_\parallel)$ [b]	−75.4 (24.4%)	−49.1 (29.4%)	−42.9 (28.8%)	−34.0 (28.4%)	−105.4 (39.5%)	−50.0 (35.2%)	−46.3 (35.7%)	−37.5 (34.9%)
$\Delta b_2(\pi_\perp)$ [b]	−91.9 (29.7%)	−37.6 (22.5%)	−32.6 (21.9%)	−23.8 (19.9%)	−65.7 (24.6%)	−24.9 (17.5%)	−20.6 (15.8%)	−14.3 (13.3%)
ΔE_{Prep}	23.9	21.2	20.8	20.5	83.3	50.8	49.2	44.2
$-D_e$	−146.5	−91.8	−82.4	−65.4	−100.8	−66.3	−59.7	−48.8

[a] The value in parentheses gives the percentage contribution to the total attractive interactions ($\Delta E_{Elstat} + \Delta E_{Orb}$). [b] The value in parentheses gives the percentage contribution to the total orbital interactions.

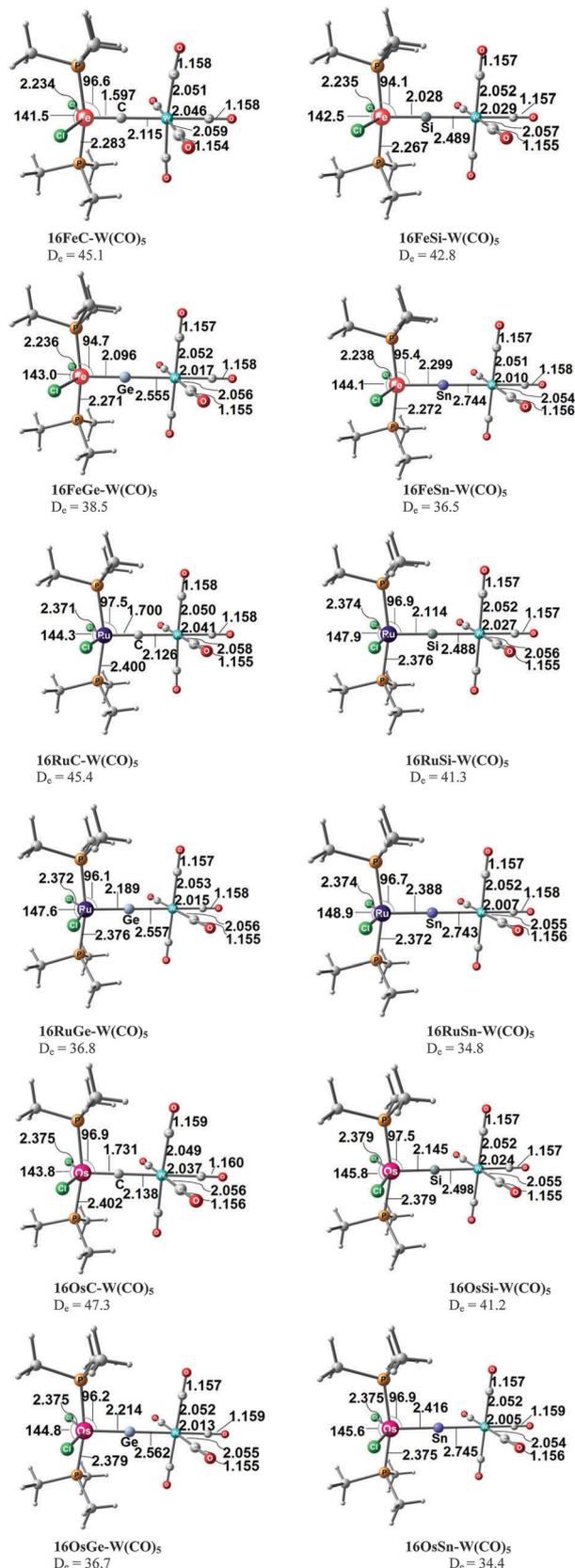This journal is © The Royal Society of Chemistry 2014

Chem. Soc. Rev., 2014, **43**, 5106–5139 | **5133**

Fig. 27 Optimized geometries and E−W bond dissociation energies D_e (BP86/TZ2P) of the tetrele complexes **16TME–W(CO)₅**. Bond lengths are given in Å, angles in degree, energies in kcal mol^{-1}.[90] The figure has been adapted from ref. 90.
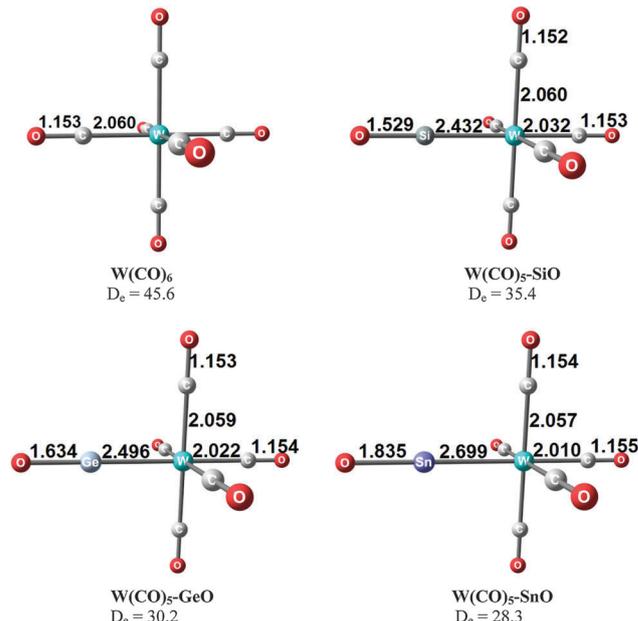

Fig. 28 Optimized geometries and E−W bond dissociation energies D_e (BP86/TZ2P) of the complexes **OE−W(CO)₅**. Bond lengths are given in Å, angles in degree, energies in kcal mol^{-1}.[90] The figure has been adapted from ref. 90.

Fig. 29 shows the optimized geometries of the complexes **17TME–W(CO)₅** which exhibit also a linear coordination mode at the tetrele atom E. There is an interesting difference in the geometry alteration of the ligand species **17TME** relative to **16TME**. The TM–C bond becomes significantly longer in **17TMC–W(CO)₅** but the TM–E bonds of the heavier homologues **17TME–W(CO)₅** where E = Si−Sn become always shorter than in **17TME**. Note that the E–W bond lengths in **17TME–W(CO)₅** are not very different from those in **16TME–W(CO)₅** but the former complexes have clearly higher BDEs (Fig. 29) than the latter (Fig. 27). It is well known that bond lengths and bond strength do not necessarily correlate.[91]

PF2[90] calculated some reaction energies which indicate the possible stabilities of the adducts **16TME–W(CO)₅** and **17TME–W(CO)₅**. The theoretical data for reactions 1 and 2 (Table 19) predict that substituting a CO ligand in W(CO)₆ by a 16VE tetrele complex **16TME** is energetically unfavourable except for **16OsC** while the substitution reaction of one CO in W(CO)₆ by **17TME** is endothermic with the trend C > Si > Ge > Sn. The heavier tetrele complexes **16TME** and **17TME** (E = Si−Sn) are always much more strongly bonded to W(CO)₅ than the diatomic species EO (reactions (3) and (4)).

The nature of the E–W bonds in **16TME–W(CO)₅** and **17TME–W(CO)₅** was analyzed by PF2[90] with the EDA method. Table 20 gives the results for the ruthenium complexes **16RuE–W(CO)₅** and **17RuE–W(CO)₅** and for **OE–W(CO)₅**. The data indicate that the nature of the bonding is not very different from each other. The covalent character of the bonds which is given by the percentage values of ΔE_{orb} in the tetrele complexes **16TME–W(CO)₅** is nearly the same as in **OE–W(CO)₅** while it is somewhat smaller in **17TME–W(CO)₅**. All ligands **16RuE**,
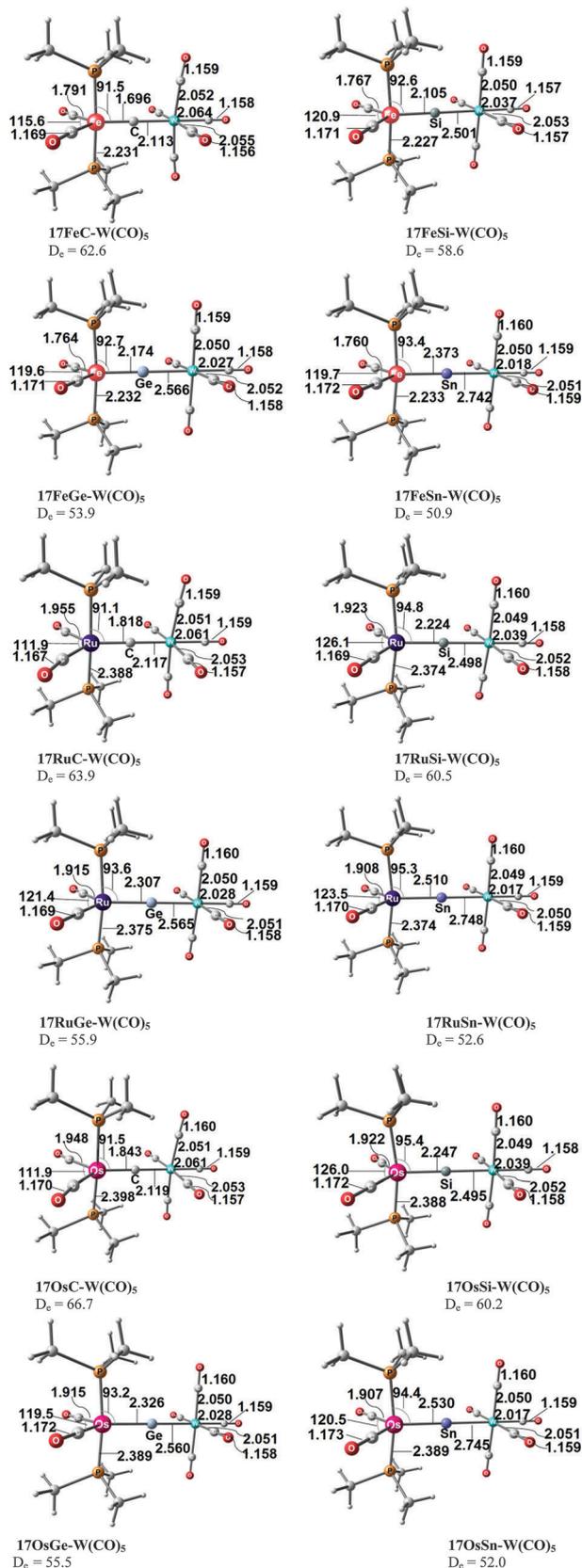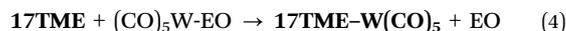
Fig. 29 Optimized geometries and E–W bond dissociation energies D_e (BP86/TZ2P) of the tetrele complexes **17TME–W(CO)$_5$**. Bond lengths are given in Å, angles in degree, energies in kcal mol^{-1}.[90]

Table 19 Calculated reaction energies ΔE (kcal mol^{-1}) at BP86/TZ2P of the reactions (1) to (4) which are shown below[90]

TM	E	$\Delta E(1)$	$\Delta E(2)$	$\Delta E(3)$	$\Delta E(4)$
Fe	C	0.7	−16.7	0.7	−16.7
	Si	2.8	−13.0	−7.4	−23.2
	Ge	7.0	−8.4	−8.3	−23.7
	Sn	9.0	−5.4	−8.2	−22.6
Ru	C	0.4	−18.0	0.4	−18.0
	Si	4.2	−15.0	−6.0	−25.2
	Ge	8.7	−10.4	−6.6	−25.7
	Sn	10.8	−7.1	−6.5	−24.3
Os	C	−1.5	−20.9	−1.5	−20.9
	Si	4.3	−14.7	−5.9	−24.9
	Ge	8.8	−10.0	−6.5	−25.3
	Sn	11.1	−6.5	−6.1	−23.7

$$\textbf{16TME} + \text{W(CO)}_6 \rightarrow \textbf{16TME–W(CO)}_5 + \text{CO} \qquad (1)$$

$$\textbf{17TME} + \text{W(CO)}_6 \rightarrow \textbf{17TME–W(CO)}_5 + \text{CO} \qquad (2)$$

$$\textbf{16TME} + \text{(CO)}_5\text{W-EO} \rightarrow \textbf{16TME–W(CO)}_5 + \text{EO} \qquad (3)$$

$$\textbf{17TME} + \text{(CO)}_5\text{W-EO} \rightarrow \textbf{17TME–W(CO)}_5 + \text{EO} \qquad (4)$$

17RuE and **OE** are stronger σ donors than π acceptors except CO which is calculated to be a stronger π acceptor.[92]

6. Summary and conclusion

The theoretical work which is reviewed here shows that the naked group-14 atoms E = C–Pb in the singlet ^1D state behave as bidentate Lewis acids which strongly bind two σ donor ligands L in the donor–acceptor complexes L→E←L. Tetrylones EL$_2$ are divalent E(0) compounds which possess two lone pairs at E. The unique electronic structure of tetrylones (carbones, silylones, germylones, stannylones, plumbylones) clearly distinguishes them from tetrylenes ER$_2$ (carbenes, silylenes, germylenes, stannylenes, plumbylenes) which have electron-sharing bonds R–E–R and only one lone pair at atom E. The different electronic structures of tetrylones and tetrylenes are revealed by charge- and energy decomposition analyses they become obvious by a distinctively different chemical reactivity. The unusual structures and chemical behaviour of tetrylones EL$_2$ can be understood in terms of the donor–acceptor interactions L→E←L. Tetrylones are potential donor ligand in main group compounds and transition metal complexes which are experimentally not yet known. The theoretical studies which are presented and discussed in this review provide an outlook over a wide area which awaits to be explored.

The second part of the review introduces theoretical studies of transition metal complexes [TM]–E which carry naked tetrele atoms E = C–Sn as ligands. The bonding analyses suggest that the group-14 atoms bind in the ^3P reference state to the

This journal is © The Royal Society of Chemistry 2014

Chem. Soc. Rev., 2014, **43**, 5106–5139 | **5135**

Table 20 Energy decomposition analysis at BP86/TZ2P of the E–W bonds in the complexes **16RuE–W(CO)₅**, **17RuE–W(CO)₅**, **17RuE–W(CO)₅** and **OE–W(CO)₅**. All energies in kcal mol⁻¹[190]

	16RuC–W(CO)₅	16RuSi–W(CO)₅	16RuGe–W(CO)₅	16RuSn–W(CO)₅	17RuC–W(CO)₅	17RuSi–W(CO)₅	17RuGe–W(CO)₅	17RuSn–W(CO)₅	OC–W(CO)₅	OSi–W(CO)₅	OGe–W(CO)₅	OSn–W(CO)₅
ΔE_{int}	−49.3	−43.4	−38.5	−36.2	−71.7	−66.9	−61.2	−58.0	−49.7	−37.7	−32.2	−29.9
ΔE_{Pauli}	113.0	103.4	87.7	77.3	163.2	153.1	130.7	120.0	118.6	94.0	79.8	72.6
$\Delta E_{Elstat}{}^a$	−87.3 (53.8%)	−78.3 (53.3%)	−67.0 (53.1%)	−59.5 (52.5%)	−146.9 (62.5%)	−137.8 (62.7%)	−118.7 (61.9%)	−109.8 (61.9%)	−89.6 (53.3%)	−63.9 (48.5%)	−54.3 (48.5%)	−52.7 (51.4%)
$\Delta E_{orb}{}^a$	−75.0 (46.2%)	−68.5 (46.7%)	−59.2 (46.9%)	−53.9 (47.5%)	−88.0 (37.5%)	−82.2 (37.4%)	−73.2 (38.1%)	−68.3 (38.1%)	−78.6 (46.7%)	−67.9 (51.5%)	−57.7 (51.5%)	−49.8 (48.6%)
$\Delta a_1(\sigma)^b$	−46.3 (61.7%)	−47.2 (68.9%)	−43.2 (72.9%)	−41.9 (77.7%)	−54.8 (62.3%)	−60.4 (73.5%)	−55.6 (76.0%)	−54.5 (79.9%)	−36.3 (46.1%)	−37.3 (54.9%)	−34.1 (59.1%)	−33.1 (66.5%)
$\Delta a_2(\delta)^b$	−0.3 (0.3%)	−0.1 (0.1%)	−0.0 (0.0%)	−0.0 (0.1%)	−0.6 (0.7%)	−0.2 (0.2%)	−0.1 (0.2%)	−0.1 (0.2%)	−0.0 (0.0%)	−0.3 (0.4%)	−0.2 (0.3%)	−0.2 (0.3%)
$\Delta b_1(\pi_\parallel)^b$	−13.4 (17.8%)	−10.0 (14.6%)	−7.4 (12.5%)	−5.5 (10.1%)	−13.5 (15.4%)	−9.9 (12.1%)	−7.8 (10.6%)	−6.1 (9.0%)	−21.2 (26.9%)	−15.2 (22.4%)	−11.7 (20.3%)	−8.3 (16.6%)
$\Delta b_2(\pi_\perp)^b$	−15.1 (20.2%)	−11.3 (16.4%)	−8.6 (14.5%)	−6.5 (12.1%)	−19.1 (21.7%)	−11.7 (14.2%)	−9.7 (13.2%)	−7.5 (11.0%)	−21.2 (26.9%)	−15.2 (22.4%)	−11.7 (20.3%)	−8.3 (16.6%)
ΔE_{Prep}	3.9	2.1	1.7	1.4	7.8	6.4	5.2	5.4	4.0	2.4	2.1	1.6
$-De$	−45.4	−41.3	−36.8	−34.8	−63.9	−60.5	−55.9	−52.6	−45.6	−35.4	−30.2	−28.3

^{a} The value in parentheses gives the percentage contribution to the total attractive interactions ($\Delta E_{Elstat} + \Delta E_{orb}$). ^{b} The value in parentheses gives the percentage contribution to the total orbital interactions.

transition metal in a combination of σ and π∥ electron-sharing bonds TM–E and π⊥ backdonation TM→E. The unique bonding situation of the tetrele complexes [TM]–E makes them suitable ligands in adducts with Lewis acids. Theoretical studies of [TM]–E→W(CO)₅ predict that such species may becomes synthesized. This is also a large field of promising experimental research which awaits to become explored.

Acknowledgements

References

1 F. Ramirez, N. B. Desai, B. Hansen and N. McKelvie, *J. Am. Chem. Soc.*, 1961, **83**, 3539.

2 R. G. Carlson, M. A. Gile, J. A. Heppert, M. H. Mason, D. R. Powell, D. V. Velde and J. M. Vilain, *J. Am. Chem. Soc.*, 2002, **124**, 1580.

3 G. Frenking, C. Loschen, A. Krapp, S. Fau and S. H. Strauss, *J. Comput. Chem.*, 2007, **28**, 117.

4 We use the term valence as indicator for the number of chemical bonds while the oxidation state which is given in parentheses gives the number of valence electrons which is used for chemical bonding. Thus, tetravalent carbon(ɪv) employs four valence electrons for four bonds, divalent carbon(ɪɪ) uses two valence electrons for two bonds while two electrons remain as lone-pair. Divalent carbon(0) compounds have two lone-pairs and two donor–acceptor bonds.

5 A. Igau, H. Grützmacher, A. Baceiredo and G. Bertrand, *J. Am. Chem. Soc.*, 1988, **110**, 6463.

6 A. J. Arduengo III, R. L. Harlow and M. Kline, *J. Am. Chem. Soc.*, 1991, **113**, 2801.

7 (*a*) W. Kirmse, *Angew. Chem.*, 2004, **116**, 1799; W. Kirmse, *Angew. Chem., Int. Ed.*, 2004, **43**, 1767; (*b*) D. Martin, M. Melaimi, M. Soleilhavoup and G. Bertrand, *Organometallics*, 2011, **30**, 5304; (*c*) O. Kaufhold and F. E. Hahn, *Angew. Chem.*, 2008, **120**, 4122; O. Kaufhold and F. E. Hahn, *Angew. Chem., Int. Ed.*, 2008, **47**, 4057; (*d*) P. L. Arnold and S. Pearson, *Coord. Chem. Rev.*, 2007, **251**, 596; (*e*) M. Albrecht, *Chem. Commun.*, 2008, 3601; (*f*) O. Schuster, L. Yang, H. G. Raubenheimer and M. Albrecht, *Chem. Rev.*, 2009, **109**, 3445; (*g*) M. Albrecht, *Chimia*, 2009, **63**, 105; (*h*) M. Iglesias and M. Albrecht, *Dalton Trans.*, 2010, **39**, 5213.

8 *N-Heterocyclic Carbenes in Transition Metal Catalysis*, ed. F. Glorius, Springer, Berlin, 2007.

9 Recent reviews: (*a*) A. J. Arduengo III, *Acc. Chem. Res.*, 1999, **32**, 913; (*b*) D. Bourissou, O. Guerret, F. P. Gabbaï and G. Bertrand, *Chem. Rev.*, 2000, **100**, 39; (*c*) W. A. Herrmann, *Angew. Chem., Int. Ed.*, 2002, **41**, 1290; (*d*) *N-Heterocyclic Carbenes in Synthesis*, ed. S. P. Nolan, Wiley-VCH, Weinheim, Germany, 2006; (*e*) E. Peris and R. H. Crabtree, *Coord. Chem. Rev.*, 2004, **248**, 2239; (*f*) C. M. Crudden and D. P. Allen, *Coord.*

Chem. Rev., 2004, **248**, 2247; (*g*) S. Díez-González and S. P. Nolan, *Coord. Chem. Rev.*, 2007, **251**, 874; (*h*) E. A. B. Kantchev, C. J. O'Brien and M. G. Organ, *Angew. Chem.*, 2007, **119**, 2824; E. A. B. Kantchev, C. J. O'Brien and M. G. Organ, *Angew. Chem., Int. Ed.*, 2007, **46**, 2768; (*i*) F. E. Hahn and M. C. Jahnke, *Angew. Chem., Int. Ed.*, 2008, **47**, 3122; (*j*) S. Würtz and F. Glorius, *Acc. Chem. Res.*, 2008, **41**, 1523; (*k*) S. Díez-González, N. Marion and S. P. Nolan, *Chem. Rev.*, 2009, **109**, 3612; (*l*) R. Wolf and W. Uhl, *Angew. Chem., Int. Ed.*, 2009, **48**, 6774; (*m*) T. Dröge and F. Glorius, *Angew. Chem., Int. Ed.*, 2010, **49**, 6940; (*n*) M. Melaimi, M. Soleilhavoup and G. Bertrand, *Angew. Chem., Int. Ed.*, 2010, **49**, 8810.

10 V. Kaufman and J. F. Ward, *J. Opt. Soc. Am.*, 1966, **56**, 1591.

11 G. Frenking and R. Tonner, *Pure Appl. Chem.*, 2009, **81**, 597.

12 (*a*) W. Petz and G. Frenking, *Top. Organomet. Chem.*, 2010, **30**, 49; (*b*) N. D. Jones and R. G. Cavell, *J. Organomet. Chem.*, 2005, **690**, 5485; (*c*) O. I. Kolodiazhnyi, *Phosphorous Ylides: Chemistry and Application in Organic Synthesis*, Wiley-VCH, Weinheim, 1999; (*d*) O. I. Kolodiazhnyi, *Tetrahedron*, 1996, **52**, 1855; (*e*) *Ylides and Imines of Phosphorus*, ed. A. W. Johnson, Wiley&Sons, New York, 1993; (*f*) H. Schmidbaur, *Angew. Chem.*, 1983, **95**, 980; H. Schmidbaur, *Angew. Chem., Int. Ed. Engl.*, 1983, **22**, 907.

13 G. E. Hardy, J. I. Zink, W. C. Kaska and J. C. Baldwin, *J. Am. Chem. Soc.*, 1978, **100**, 8002.

14 R. Tonner and G. Frenking, *Chem. – Eur. J.*, 2008, **14**, 3260.

15 There are no genuine σ and π orbitals in C(PPh₃)₂ because the molecular geometry has no mirror plane. However, the shape of the orbitals easily identifies them as σ- and π-type with respect to the local P–C–P plane.

16 R. Tonner, F. Öxler, B. Neumüller, W. Petz and G. Frenking, *Angew. Chem.*, 2006, **118**, 8206; R. Tonner, F. Öxler, B. Neumüller, W. Petz and G. Frenking, *Angew. Chem., Int. Ed.*, 2006, **45**, 8038.

17 C. Kaska, D. K. Mitchell and R. F. Reichelderfer, *J. Organomet. Chem.*, 1973, **47**, 391.

18 W. Petz, C. Kutschera, M. Heitbaum, G. Frenking, R. Tonner and B. Neumüller, *Inorg. Chem.*, 2005, **44**, 1263.

19 R. Tonner, G. Heydenrych and G. Frenking, *ChemPhysChem*, 2008, **9**, 1474.

20 W. Petz, F. Öxler, B. Neumüller, R. Tonner and G. Frenking, *Eur. J. Inorg. Chem.*, 2009, 4507.

21 B. Inés, M. Patil, J. Carreras, R. Goddard, W. Thiel and M. Alcarazo, *Angew. Chem., Int. Ed.*, 2011, **50**, 8400.

22 J. J. Daly and P. Wheatley, *J. Chem. Soc.*, 1966, 1703.

23 O. Diels and B. Wolf, *Ber. Dtsch. Chem. Ges.*, 1906, **39**, 689.

24 J. Koput, *Chem. Phys. Lett.*, 2000, **320**, 237. The value for the C–C–C bending angle stems from a high-level quantum chemical calculation at CCSD(T)/cc-pVQZ which predicts that the barrier to linearity is only 18 cm⁻¹. This is in agreement with the high-resolution infrared spectrum of C₃O₂ which suggests that the molecule is quasi-linear: J. Vander Auwera, J. W. C. Johns and O. L. Polyansky, *J. Chem. Phys.*, 1991, **95**, 2299.

25 (*a*) R. Tonner and G. Frenking, *Angew. Chem.*, 2007, **119**, 8850; R. Tonner and G. Frenking, *Angew. Chem., Int.*

Ed., 2007, **46**, 8695; (*b*) G. Frenking and R. Tonner, *Wiley Interdiscip. Rev.: Comput. Mol. Sci.*, 2011, **1**, 869; (*c*) G. Frenking and R. Tonner, in *Contemporary Carbene Chemistry*, ed. R. A. Moss and M. P. Doyle, Wiley, New Jersey, 2013, p. 167.

26 C. A. Dyker, V. Lavallo, B. Donnadieu and G. Bertrand, *Angew. Chem.*, 2008, **120**, 3250; C. A. Dyker, V. Lavallo, B. Donnadieu and G. Bertrand, *Angew. Chem., Int. Ed.*, 2008, **47**, 3206.

27 A. Fürstner, M. Alcarazo, R. Goddard and C. W. Lehmann, *Angew. Chem.*, 2008, **120**, 3254; A. Fürstner, M. Alcarazo, R. Goddard and C. W. Lehmann, *Angew. Chem., Int. Ed.*, 2008, **47**, 3210.

28 M. Alcarazo, W. Lehmann, A. Anoop, W. Thiel and A. Fürstner, *Nat. Chem.*, 2009, **1**, 295.

29 M. J. Taylor, P. W. J. Surman and G. R. Clark, *J. Chem. Soc., Chem. Commun.*, 1994, 2517.

30 H. G. Viehe, Z. Janousek, R. Gompper and D. Lach, *Angew. Chem.*, 1973, **85**, 581; H. G. Viehe, Z. Janousek, R. Gompper and D. Lach, *Angew. Chem., Int. Ed. Engl.*, 1973, **12**, 566.

31 R. Tonner and G. Frenking, *Chem. – Eur. J.*, 2008, **14**, 3273.

32 S. Klein, R. Tonner and G. Frenking, *Chem. – Eur. J.*, 2010, **16**, 10160.

33 C. A. Dyker and G. Bertrand, *Nat. Chem.*, 2009, **1**, 265.

34 (*a*) C. A. Dyker, V. Lavallo, B. Donnadieu and G. Bertrand, *Angew. Chem.*, 2008, **120**, 3250; C. A. Dyker, V. Lavallo, B. Donnadieu and G. Bertrand, *Angew. Chem., Int. Ed.*, 2008, **47**, 3206; (*b*) I. Fernandez, C. A. Dyker, A. DeHope, B. Donnadieu, G. Frenking and G. Bertrand, *J. Am. Chem. Soc.*, 2009, **131**, 11875.

35 (*a*) J.-M. Sotiropoulos, A. Baceiredo and G. Bertrand, *J. Am. Chem. Soc.*, 1987, **109**, 4711; (*b*) N. DubauAssibat, A. Baceiredo, F. Dahan and G. Bertrand, *Bull. Soc. Chim. Fr.*, 1995, **132**, 1139; (*c*) J.-M. Sotiropoulos, A. Baceiredo and G. Bertrand, *Bull. Soc. Chim. Fr.*, 1992, **129**, 367.

36 K. Morokuma, *J. Chem. Phys.*, 1971, **55**, 1236.

37 (*a*) T. Ziegler and A. Rauk, *Inorg. Chem.*, 1979, **18**, 1755; (*b*) T. Ziegler and A. Rauk, *Inorg. Chem.*, 1979, **18**, 1558.

38 M. Mitoraj and A. Michalak, *Organometallics*, 2007, **26**, 6576.

39 (*a*) A. Michalak, M. Mitoraj and T. Ziegler, *J. Phys. Chem. A*, 2008, **112**, 1933; (*b*) M. P. Mitoraj, A. Michalak and T. Ziegler, *J. Chem. Theory Comput.*, 2009, **5**, 962.

40 (*a*) F. M. Bickelhaupt and E. J. Baerends, in *Rev. Comput. Chem*, ed. K. B. Lipkowitz and D. B. Boyd, Wiley-VCH, Inc., New York, 2000, vol. 15, p. 1; (*b*) M. Lein and G. Frenking, in *Theory and Applications of Computational Chemistry: The First 40 Years*, ed. C. E. Dykstra, G. Frenking and K. S. Kim and G. E. Scuseria, Elsevier, Amsterdam, 2005, p. 367; (*c*) M. von Hopffgarten and G. Frenking, *Wiley Interdiscip. Rev.: Comput. Mol. Sci.*, 2012, **2**, 43; (*d*) G. Frenking and F. M. Bickelhaupt, in *The Chemical Bond: Fundamental Aspects of Chemical Bonding*, ed. G. Frenking and S. Shaik, Wiley-VCH, Weinheim, 2014, pp. 121–157.

41 We are using the term tetrele as shortform expression for group-14 atoms C–Pb which has been suggested earlier for elements of the fourth ("tetra") main group.

42 A bonding situation with donor–acceptor bonds between bare group-14 atoms Si and Ge and a diazabutadiene ligand has earlier been discussed for N-heterocyclic silylene and germylene by Arduengo *et al.* who called it "...doubtless an extreme exaggeration of the bonding...": A. J. Arduengo, H. Bock, H. Chen, M. Denk, D. A. Dixon, J. C. Green, W. A. Herrmann, N. L. Jones, M. Wagner and R. West, *J. Am. Chem. Soc.*, 1994, **116**, 6641.

43 (*a*) S. Ishida, T. Iwamoto, C. Kabuto and M. Kira, *Nature*, 2003, **421**, 725; (*b*) T. Iwamoto, H. Masuda, C. Kabuto and M. Kira, *Organometallics*, 2005, **24**, 197.

44 M. Kosa, M. Karni and Y. Apeloig, *J. Chem. Theory Comput.*, 2006, **2**, 956.

45 (*a*) T. Veszprémi, A. Olasz and B. Pintér, *Silicon Chem.*, 2006, **3**, 187; (*b*) T. Veszprémi, K. Petrov and C. T. Nguyen, *Organometallics*, 2006, **25**, 1480; (*c*) K. T. Petrov and T. Veszprémi, *Int. J. Chem. Model.*, 2008, **1**, 1; (*d*) K. T. Petrov and T. Veszprémi, *Int. J. Quantum Chem.*, 2009, **109**, 2526.

46 (*a*) J. S. Binkley, *J. Am. Chem. Soc.*, 1984, **106**, 603; (*b*) J. Kalcher, A. Sax and G. Olbrich, *Int. J. Quantum Chem.*, 1984, **25**, 543; (*c*) H.-J. Köhler and H. Lischka, *Chem. Phys. Lett.*, 1984, **112**, 33; (*d*) D. A. Clabo and H. F. Schaefer, *J. Chem. Phys.*, 1986, **84**, 1664; (*e*) B. S. Thies, R. S. Grev and H. F. Schaefer, *Chem. Phys. Lett.*, 1987, **140**, 355; (*f*) S. Koseki and M. S. Gordon, *J. Phys. Chem.*, 1988, **92**, 364; (*g*) S. Koseki and M. S. Gordon, *J. Phys. Chem.*, 1989, **93**, 118; (*h*) B. T. Colegrove and H. F. Schaefer, *J. Phys. Chem.*, 1990, **94**, 5593; (*i*) B. T. Colegrove and H. F. Schaefer, *J. Am. Chem. Soc.*, 1991, **113**, 1557; (*j*) R. S. Grev and H. F. Schaefer, *J. Chem. Phys.*, 1992, **97**, 7990; (*k*) R. S. Grev, B. J. De Leeuw and H. F. Schaefer, *Chem. Phys. Lett.*, 1990, **165**, 257; (*l*) R. S. Grev, *Adv. Organomet. Chem.*, 1991, **33**, 125; (*m*) Z. Palagyi, H. F. Schaefer and E. Kapuy, *J. Am. Chem. Soc.*, 1993, **115**, 6901; (*n*) Q.-S. Li, R.-H. Lü, Y. Xie and H. F. Schaefer, *J. Comput. Chem.*, 2002, **23**, 1642; (*o*) S. Nagase, K. Kobayashi and N. Takagi, *J. Organomet. Chem.*, 2000, **611**, 264; (*p*) Y.-K. Han, C. Bae, Y. S. Lee and S. Y. Lee, *J. Comput. Chem.*, 1998, **19**, 1526.

47 M. Lein, A. Krapp and G. Frenking, *J. Am. Chem. Soc.*, 2005, **127**, 6290.

48 A. E. Reed, L. A. Curtiss and F. Weinhold, *Chem. Rev.*, 1988, **88**, 899.

49 N. Wiberg, H.-W. Lerner, S.-K. Vasisht, S. Wagner, K. Karaghiosoff, H. Nöth and W. Ponikwar, *Eur. J. Inorg. Chem.*, 1999, 1211.

50 (*a*) N. Takagi, T. Shimizu and G. Frenking, *Chem. – Eur. J.*, 2009, **15**, 3448; (*b*) N. Takagi, T. Shimizu and G. Frenking, *Chem. – Eur. J.*, 2009, **15**, 8593; (*c*) N. Takagi and G. Frenking, *Theor. Chem. Acc.*, 2011, **129**, 615.

51 (*a*) G. Trinquier and J.-P. Malrieu, *J. Am. Chem. Soc.*, 1987, **109**, 5303; (*b*) G. Trinquier and J.-P. Malrieu, *J. Am. Chem. Soc.*, 1989, **111**, 5916; (*c*) E. A. Carter and W. A. Goddard, *J. Phys. Chem.*, 1986, **90**, 998; (*d*) For a discussion of the bonding model see: M. Driess and H. Grützmacher, *Angew. Chem.*, 1996, **108**, 900; M. Driess and H. Grützmacher, *Angew. Chem Int. Ed.*, 1996, **35**, 828.

52 N. Takagi, R. Tonner and G. Frenking, *Chem. – Eur. J.*, 2012, **18**, 1772.

53 T. A. N. Nguyen and G. Frenking, *Chem. – Eur. J.*, 2012, **18**, 12733.

54 (*a*) K. C. Mondal, H. W. Roesky, F. Klinke, M. C. Schwarzer, G. Frenking, B. Niepötter, H. Wolf, R. Herbst-Irmer and D. Stalke, *Angew. Chem.*, 2013, **125**, 3036; K. C. Mondal, H. W. Roesky, F. Klinke, M. C. Schwarzer, G. Frenking, B. Niepötter, H. Wolf, R. Herbst-Irmer and D. Stalke, *Angew. Chem., Int. Ed.*, 2013, **52**, 2963; (*b*) Y. Li, K. C. Mondal, H. W. Roesky, H. Zhu, P. Stollberg, R. Herbst-Irmer, D. Stalke and D. M. Andrade, *J. Am. Chem. Soc.*, 2013, **135**, 12422.

55 (*a*) Y. Xiong, S. Yao, S. Inoue, J. D. Epping and M. Driess, *Angew. Chem.*, 2013, **125**, 7287; Y. Xiong, S. Yao, S. Inoue, J. D. Epping and M. Driess, *Angew. Chem., Int. Ed.*, 2013, **52**, 7147; (*b*) Y. Xiong, S. Yao, S. Inoue, J. D. Epping and M. Driess, *Angew. Chem.*, 2013, **125**, 7287; Y. Xiong, S. Yao, S. Inoue, J. D. Epping and M. Driess, *Angew. Chem., Int. Ed.*, 2013, **52**, 7147.

56 C. Elschenbroich, *Organometallics*, Wiley-VCH, Weinheim, 3rd edn, 2006.

57 E. O. Fischer and A. Maasböl, *Angew. Chem.*, 1964, **76**, 645; E. O. Fischer and A. Maasböl, *Angew. Chem., Int. Ed. Engl.*, 1964, **3**, 580.

58 The first synthesis of a carbene complex is usually associated with the work of Fischer and Maasböl in 1964 (ref. 57). Prior to this work, carbene complexes were already synthesized much earlier by Tschugajeff: (*a*) L. Tschugajeff and M. Skanawy-Grigorjewa, *J. Russ. Chem. Soc.*, 1915, **47**, 776; (*b*) L. Tschugajeff, M. Skanawy-Grigorjewa and A. Posnjak, *Z. Anorg. Chem.*, 1925, **148**, 37. However, the authors did not identify the compounds as carbene complexes which was realized only in 1970: (*c*) A. Burke, A. L. Balch and J. H. Enemark, *J. Am. Chem. Soc.*, 1970, **92**, 2555; (*d*) W. M. Butler and J. H. Enemark, *Inorg. Chem.*, 1971, **10**, 2416; (*e*) W. M. Butler, J. H. Enemark, J. Parks and A. L. Balch, *Inorg. Chem.*, 1973, **12**, 451; (*f*) For a discussion see also: M. Tamm and F. E. Hahn, *Coord. Chem. Rev.*, 1999, **182**, 175.

59 E. O. Fischer, G. Kreis, C. G. Kreiter, J. Müller, G. Huttner and H. Lorenz, *Angew. Chem., Int. Ed.*, 1973, **12**, 564; E. O. Fischer, G. Kreis, C. G. Kreiter, J. Müller, G. Huttner and H. Lorenz, *Angew. Chem.*, 1973, **85**, 618.

60 S. J. McLain, C. D. Wood, L. Messerle, R. R. Schrock, F. J. Hollander, W. J. Youngs and M. R. Churchill, *J. Am. Chem. Soc.*, 1978, **100**, 5962.

61 R. R. Schrock, *J. Am. Chem. Soc.*, 1974, **96**, 6796.

62 (*a*) M. J. S. Dewar, *Bull. Soc. Chim. Fr.*, 1951, **18**, C79; (*b*) J. Chatt and L. A. Duncanson, *J. Chem. Soc.*, 1953, 2929; (*c*) G. Frenking, in *Modern Coordination Chemistry: The Legacy of Joseph Chatt*, ed. G. J. Leigh and N. Winterton, The Royal Society, London, 2002, p. 111.

63 (*a*) G. Frenking, M. Sola and S. F. Vyboishchikov, *J. Organomet. Chem.*, 2005, **690**, 6178; (*b*) G. Frenking and N. Fröhlich, *Chem. Rev.*, 2000, **100**, 717; (*c*) S. F. Vyboishchikov and G. Frenking, *Chem. – Eur. J.*, 1998, **4**, 1428; (*d*) S. F. Vyboishchikov and G. Frenking, *Chem. – Eur. J.*, 1998, **4**, 1439.

64 J. C. Peters, A. L. Odom and C. C. Cummins, *Chem. Commun.*, 1997, 1995.

65 M. I. Bruce and P. J. Low, *Adv. Organomet. Chem.*, 2004, **50**, 179.

66 (*a*) C. E. Laplaza, A. L. Odom, W. M. Davis, C. C. Cummins and J. D. Protasiewicz, *J. Am. Chem. Soc.*, 1995, **117**, 861; (*b*) C. E. Laplaza and C. C. Cummins, *Science*, 1995, **268**, 861.

67 Y. Chen, W. Petz and G. Frenking, *Organometallics*, 2000, **19**, 2698.

68 M. H. Stewart, M. J. A. Johnson and J. W. Kampf, *Organometallics*, 2007, **26**, 5102.

69 S. R. Caskey, M. H. Stewart, J. E. Kivela, J. R. Sootsman, M. J. A. Johnson and J. W. Kampf, *J. Am. Chem. Soc.*, 2005, **127**, 16750.

70 See ref. 68 and 69 and the following: (*a*) P. E. Romero, W. E. Piers and R. McDonald, *Angew. Chem.*, 2004, **116**, 6287; P. E. Romero, W. E. Piers and R. McDonald, *Angew. Chem., Int. Ed.*, 2004, **43**, 6161; (*b*) E. F. van der Eide, P. E. Romero and W. E. Piers, *J. Am. Chem. Soc.*, 2008, **130**, 4485.

71 A. Hejl, T. M. Trnka, M. W. Day and R. H. Grubbs, *Chem. Commun.*, 2002, 2524.

72 S. R. Caskey, M. H. Stewart, M. J. A. Johnson and J. W. Kampf, *Angew. Chem.*, 2006, **118**, 7582; S. R. Caskey, M. H. Stewart, M. J. A. Johnson and J. W. Kampf, *Angew. Chem., Int. Ed.*, 2006, **45**, 7422.

73 W. Beck, W. Knauer and C. Robl, *Angew. Chem.*, 1990, **102**, 331; W. Beck, W. Knauer and C. Robl, *Angew. Chem., Int. Ed.*, 1990, **29**, 318.

74 (*a*) C. Buda, S. R. Caskey, M. J. A. Johnson and B. D. Dunietz, *Organometallics*, 2006, **25**, 4756; (*b*) J. B. Gary, C. Buda, M. J. A. Johnson and B. D. Dunietz, *Organometallics*, 2008, **27**, 814.

75 A. Krapp, K. K. Pandey and G. Frenking, *J. Am. Chem. Soc.*, 2007, **129**, 7596.

76 (*a*) D. Huang, W. E. Streib, J. C. Bollinger, K. G. Caulton, R. F. Winter and T. Scheiring, *J. Am. Chem. Soc.*, 1999, **121**, 8087; (*b*) R. A. Jones, G. Wilkinson, A. M. R. Galas, M. B. Hursthouse and K. M. A. Malik, *J. Chem. Soc., Dalton Trans.*, 1980, 1771; (*c*) J. Huang, K. Hedberg, H. B. Davis and R. K. Pomeroy, *Inorg. Chem.*, 1990, **29**, 3923; (*d*) B. Beagley and D. G. Schmidling, *J. Mol. Struct.*, 1974, **22**, 466; (*e*) D. Braga, F. Grepioni and A. G. Orpen, *Organometallics*, 1993, **12**, 1481.

77 R. Hoffmann, *Angew. Chem.*, 1982, **94**, 725; R. Hoffmann, *Angew. Chem., Int. Ed. Engl.*, 1982, **21**, 711.

78 A. Krapp and G. Frenking, *J. Am. Chem. Soc.*, 2008, **130**, 16646.

79 Reviews: (*a*) R. Waterman, P. G. Hayes and T. D. Tilley, *Acc. Chem. Res.*, 2007, **40**, 712; (*b*) W. Petz, *Chem. Rev.*, 1986, **86**, 1019.

80 J. D. Cotton, P. J. Davidson and M. F. Lappert, *J. Chem. Soc., Dalton Trans.*, 1976, 2275.

81 M. F. Lappert, S. J. Miles and P. P. Power, *J. Chem. Soc., Chem. Commun.*, 1977, 458.

82 Heavy group-14 homologues of carbene complexes have been isolated where the ligand ER_2 is stabilized by a Lewis base. Here we consider only those complexes with unsupported ER_2 groups.

83 D. A. Straus, S. D. Grumbine and T. D. Tilley, *J. Am. Chem. Soc.*, 1990, **112**, 7801.

84 Reviews: (*a*) G. Balázs, L. J. Gregoriades and M. Scheer, *Organometallics*, 2007, **26**, 3058; (*b*) K. K. Pandey, P. Patidar, P. K. Bariya, S. K. Patidar and R. Vishwakarma, *Dalton Trans.*, 2014, DOI: 10.1039/C3DT53632g.

85 R. S. Simons and P. P. Power, *J. Am. Chem. Soc.*, 1996, **118**, 11966.

86 A. C. Filippou, P. Portius, A. I. Philippopoulos and H. Rohde, *Angew. Chem.*, 2003, **115**, 461; A. C. Filippou, P. Portius, A. I. Philippopoulos and H. Rohde, *Angew. Chem., Int. Ed.*, 2003, **42**, 445.

87 A. C. Filippou, H. Rohde and G. Schnakenburg, *Angew. Chem.*, 2004, **116**, 2293; A. C. Filippou, H. Rohde and G. Schnakenburg, *Angew. Chem., Int. Ed.*, 2004, **43**, 2243.

88 A. C. Filippou, O. Chernov, K. W. Stumpf and G. Schnakenburg, *Angew. Chem.*, 2010, **122**, 3368; A. C. Filippou, O. Chernov, K. W. Stumpf and G. Schnakenburg, *Angew. Chem., Int. Ed.*, 2010, **49**, 3296.

89 P. Parameswaran and G. Frenking, *Chem. – Eur. J.*, 2009, **15**, 8807.

90 P. Parameswaran and G. Frenking, *Chem. – Eur. J.*, 2009, **15**, 8817.

91 Examples have been reported in: (*a*) U. Pidun and G. Frenking, *Organometallics*, 1995, **14**, 5325; (*b*) U. Pidun and G. Frenking, *J. Organomet. Chem.*, 1996, **525**, 269; (*c*) R. A. Fischer, M. M. Schulte, J. Weiß, L. Zsolnai, A. Jacobi, G. Huttner, G. Frenking, C. Boehme and S. F. Vyboishchikov, *J. Am. Chem. Soc.*, 1998, **120**, 1237; (*d*) G. Frenking, K. Wichmann, N. Fröhlich, J. Grobe, W. Golla, D. Le Van, B. Krebs and M. Läge, *Organometallics*, 2002, **21**, 2921; (*e*) G. Frenking, K. Wichmann, N. Fröhlich, C. Loschen, M. Lein, J. Frunzke and V. M. Rayón, *Coord. Chem. Rev.*, 2003, **238–239**, 55.

92 A detailed discussion of the strength of the σ and π orbital interactions in $TM(CO)_6$ has been presented in: A. Diefenbach, F. M. Bickelhaupt and G. Frenking, *J. Am. Chem. Soc.*, 2000, **122**, 6449.